EXPERIMENTAL STUDY ON ALKALI ACTIVATED SLAG CONCRETE MIXES BY INCORPORATING PS BALL AS FINE AGGREGATE

Thesis

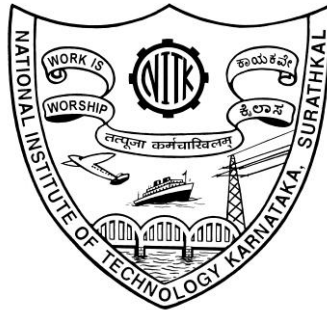submitted in partial fulfilment of the requirements for the degree of

DOCTOR OF PHILOSOPHY

by

AVINASH H TALKERI

(165136CV16F05)

DEPARTMENT OF CIVIL ENGINEERING

NATIONAL INSTITUTE OF TECHNOLOGY KARNATAKA

SURATHKAL, MANGALORE-575025

OCTOBER, 2020

DECLARATION

I hereby *declare* that the Research Thesis entitled "**Experimental Study on Alkali Activated Slag Concrete Mixes by Incorporating PS Ball as Fine Aggregate**" Which is being submitted to the National Institute of Technology Karnataka, Surathkal in partial fulfilment of the requirements for the award of the Degree of Doctor of Philosophy in the Department of Civil Engineering is a bonafide report of the research work carried out by me. The material contained in this Research Thesis has not been submitted to any University or Institution for the award of any degree.

<div align="right">

(**Avinash H Talkeri**)
Registration No. **165136CV16F05**
Department of Civil Engineering

</div>

Place: NITK-Surathkal
Date: 19-10-2020

CERTIFICATE

This is to *certify* that the Research Thesis entitled "**Experimental Study on Alkali Activated Slag Concrete Mixes by Incorporating PS Ball as Fine Aggregate**" submitted by **AVINASH H TALKERI** (Register Number: **165136CV16F05**) as the record of the research work carried out by him/her, is *accepted as the Research Thesis submission* in partial fulfillment of the requirements for the award of degree of **Doctor of Philosophy**.

Research Guide

Chairman - DRPC

DEDICATED TO

MY PARENTS,

FAMILY MEMBERS,

TEACHERS,

FARMERS AND FRIENDS

ACKNOWLEDGEMENT

I am incredibly grateful to my father, Sri. Huchappa, mother Smt. Sharada and my uncle Sri. D. R Ramachandra, my Aunty Mrs. Rekha, for providing me the best available education and encouraged in all my endeavours. I gratefully acknowledge the support and help rendered by my family members during this research work. They have always been a source of inspiration for me. Finally, I am grateful to everybody who helped and encouraged me during this research work.

NITK Surathkal   **AVINASH H TALKERI**
Date: 19-10-2020

ABSTRACT

Improved road connectivity is essential for any country to progress. Well designed and constructed concrete pavements are essential for the development of sustainable highway infrastructure. The increase in infrastructure and urban development activities desire to discover sustainable materials, replacing the natural raw materials required for concrete production. The higher demand for concrete roads and other construction projects has increased Ordinary Portland Cement (OPC) production. However, cement production is associated with environmental issues such as a higher carbon footprint, highly energy-intensive, and exploitation of natural resources. Cement production uses a significant amount of natural resources. Nearly 2tonnes of raw material required to produce 1ton of cement, which emits 850kg of carbon-di-oxide into the atmosphere. The present research community is focusing on developing alternative binders to minimize the production of OPC. Alkali Activated Binders (AABs) such as Alkali Activated Slag (AAS), Alkali Activated Slag Fly Ash (AASF), Geopolymers, etc., can be considered as potential alternatives to OPC. Precious Slag (PS) ball is an industrial by-product obtained from Ecomaister steel beads. PS ball has been identified as an alternative to fine aggregates for concrete production.

In the present study, PS ball was considered fine aggregates to evaluate the performance of in Alkali Activated Slag Concrete (AASC) and Alkali Activated Slag Fly Ash Concrete (AASFC). The AASC and AASFC mixes are designed to attain a minimum strength of M40 grade and compared with conventional concrete. Sodium Silicate (SS) and Sodium Hydroxide (SH) are used as the alkaline activators. The alkaline liquid to binder ratio of 0.35 was kept constant for all the mixes. The influence of SH (i.e., 8, 10, 12, and 14M) and SS to SH ratios (i.e., 1, 1.5, 2, and 2.5) on the properties of fresh and hardened concrete were analyzed. AASC mixes are prepared with 100% GGBFS as a sole binder, while AASFC mixes are prepared by mixing GGBFS and Fly ash (FA) in different proportions, i.e., 90:10, 80:20, 70:30, and 60:40. Preliminary tests were carried out to identify the optimal NaOH concentration and dosage of alkaline activators for AASC and AASFC mixes.

The fresh and hardened properties such as workability, setting time, compressive strength, split tensile strength, modulus of elasticity, flexural strength, and abrasion resistance of different concretes were evaluated as per the standard test procedure. The durability of concrete mixes was evaluated by conducting resistance to sorptivity, hydrochloric acid, sulphuric acid, nitric acid. The water absorption and Volume of Permeable Voids (VPV) were evaluated. The flexural fatigue performance of various concrete mixes was evaluated by carrying out repeated load test on beam specimens. The fatigue life data obtained were represented and analyzed using S-N curves. Probabilistic analysis of fatigue data was carried out using Weibull distribution. Survival probability analysis to predict the fatigue lives of concrete mixes with required probability of failure was carried out.

The laboratory test results indicate that the incorporation of PS ball as fine aggregates in AASC and AASFC mixes improved mechanical strength. The fatigue life improved in AASC and AASFC mixes. The fatigue data of concrete mixes can be modeled by using Weibull distribution. Improved durability performance of AASC and AAFC mixes were observed. The higher water absorption and subsequent increase inVolume of Permeable Voids (VPV) was observed at the low NaOH concentration and silicate content, due to lower hydroxyl ion concentration in the activator solution. It was observed that the activator concentration has a larger influence on the mechanical properties of AASC and AASFC mixes. High sorptivity was reported for the mixes with 8M NaOH with a gradual drop in compressive strength. The permeability property of alkali activated material was dependent on total Na_2O content in the activator solution. The alkali activated mix showed good resistance towards sulphate, nitrate, and chloride attacks. The AASC and AASFC mix with PS ball as fine aggregates proved to be a good concrete for pavement.

Keywords: AASC; AASFC; PS ball; SS/SH ratio; Fatigue analysis.

CONTENTS

GLOSSARY OF TERMS

ACM   ALTERNATIVE CEMENTITOUS MATERIAL

OPC   ORDINARY PORTLAND CEMENT

GGBFS   GROUND GRANULATED BLAST FURNACE SLAG

FA   FLYASH

AAM   ALKALI ACTIVATED MATERIAL

AAS   ALKALI ACTIVATED SLAG

AASC   ALKALI ACTIVATED SLAG CONCRETE

AASFC   ALKALI ACTIVATED SLAG-FLYASH CONCRETE

CASH   CALCIUM ALUMINIUM SILICATE HYDRATE

CSH   CALCIUM SILICATE HYDRATE

NASH   SODIUM ALUMINIUM SILICATE HYDRATE

PS BALL   PRECIOUS SLAG BALL

SCM   SUPPLEMENTARY CEMENTITIOUS MATERIAL

SEM   SCANNING ELECTRON MICROSCOPE

SH   SODIUM HYDROXIDE

SS   SODIUM SILICATE

XRD   X-RAY DIFFRACTION

LIST OF TABLES

LIST OF FIGURES

CHAPTER 1

INTRODUCTION

1.1 GENERAL

India has the second-largest road network in the world, spanning a total length of 5.89 million kilometers (km). This road network transport 64.5% of all goods, and 90% of India's total passenger traffic uses the road network to commute in the country. Road transportation has gradually increased over the years, with improved connectivity between cities, towns, and villages in the country (https://www.ibef.org/industry/roads-india.aspx).

Highways play an integral role in enabling economic productivity and competitiveness by providing the mobility needed to access employment, recreation, and to transport goods between different markets. Road transportation has gradually increased over the years with the improvement in connectivity between cities, towns, and villages. The Government of India has set a target of construction of 10,000 km of national highways in Fiscal Year (FY) 2019. In 2017-18, the total length of roads constructed under Prime Minister Gram Sadak Yojana (PMGSY) was 47,447 km (http://omms.nic.in/).

Rigid concrete pavements are widely used in the construction of long-lasting roads as they enable a better distribution of load over the subgrade and require overall smaller structural depth, compared to flexible pavements. However, pavement slabs are subjected to continuous vehicular traffic and thermal stresses due to temperature variation (Perdikaris et al. 1986, Lee and Barr 2004, Graeff et al. 2012). The initial cost of construction of flexible pavement is much lesser than rigid pavement, but when it comes to the service life, it is un-comparable. The rigid pavement lasts for 30-40 years, whereas the flexible pavement lasts for 10-15 years. As far as the maintenance cost is concerned, the cost of flexible pavement is around 10-15% of the total cost of pavement per year. On

the other hand, the maintenance cost of rigid pavement is around 1-2% per km (http://pmgsy.nic.in/downloads/10janjun06_eng.pdf).

Rigid pavements are preferred over flexible pavement due to low maintenance cost and high service life with minimum distresses. Due to this, a developing country like India gives prime importance to construct rigid pavements (Singh et al. 2017). Portland cement concrete is one material that is widely used to pave highways, airports, parking lots, and other similar types of infrastructure. These pavements typically provide years of service with little or no maintenance needs when properly designed and constructed (Delatte 2009). The concrete industry is currently facing an acute shortage of natural aggregates; this has led to extensive research and the industry to find an alternative material replacing coarse and fine aggregate. By incorporating marginal materials, the environmental impact and construction cost can be reduced (FHWA 2012). The extraction of aggregates from the quarry and mining of the sand from the river creates severe environmental problems. Due to the scarcity of aggregates, the construction cost is escalating enormously (Singh et al. 2017). Consequently, the construction industry exploring more economical and environmentally friendly pavement materials to make the concrete pavements more efficient and long-lasting. The locally available Alternative Cementitious Material (ACM) like Ground Granulated Blast Furnace Slag (GGBFS), Fly Ash (FA), rice husk ash, Red mud, Metakaolin can be used the production of concrete (Duxson et al. 2007). Hence an alkaline activator solution is required to activate the ACM to improve the mechanical properties. The activated source material with an alkali activator solution produces alkali-activated concrete mixtures (Chindaprasirt et al. 2007, Wongpa et al. 2010).

The present investigation aims to develop the concrete with marginal materials by the alkali activation technique. The cement production is associated with environmental issues such as the release of nearly 1-ton CO_2 to the atmosphere for producing 1-ton cement. This contributes to5% of worldwide greenhouse gas emissions (Ding et al. 2016). Nearly 2-tons of raw materials are consumed for producing 1-ton of cement,

resulting in the depletion of natural resources (limestone and shale, etc.),which is extremely energy-intensive that requires 4GJ (Giga Joules) of energy. GGBFS, a byproduct material obtained from the iron and steel industry, can be effectively used as a binder activated under an alkaline medium to produce the concrete. The GGBFS contains a significant amount of constituents like calcium, silicon, and aluminium; it can be activated in an alkaline medium to develop Alkali Activated Slag Concrete (AASC). In recent studies, AASC mixes have also gained more attention to produce sustainable concrete (Wang et al. 1995, Bakharev et al. 2000).

Alkali activated mixtures are developed with less energy consumption along with reduced carbon footprint. GGBFS and FA are the solid precursors in producing the Alkali Activated Materials (AAM) with the aid of an alkaline activator solution (Shi et al. 2006). The decreased outflow of CO_2 has been related to the generation of AASC. The commonly used activator for polymerization of a mix is Sodium Hydroxide (SH) or Potassium Hydroxide (Palomo et al. 1999, Xu and Deventer 2002). These AASC blends have indicated high strength at the early stages of curing and better resistance towards an aggressive environment (Collin and Sanjayan 1999, 2000, Chang 2003, Bakharev 2003, Khale and Chaudhary 2007). Slag and flyash have been progressively considered to be appropriate crude materials for alkali-activated materials because of its availability and the presence of silica and alumina content in it. The past studies on AASC mixtures have shown that physical and mechanical properties of alkali-activated mixtures were significantly affected by binder content, activator concentration, and alkaline liquid to binder ratio (Bernal et al. 2012, Qureshi and Ghosh 2014). The chemical composition of slag, particle size distribution, glass content, and phases of crystalline material have significant contribution on strength development (Wang et al. 2005, Chi 2012, Junaid et al. 2015). The final reaction products in AASC mixtures will be hydrated complexes of calcium alumina-silicate gels (C-A-S-H) with a low ordered Ca/Si ratio, a minimum content of calcium silicate hydrate (C-S-H), and sodium alumina-silicate (N-A-S-H) gel (Puertas et al. 2011, Ismail et al. 2014, Fernandez-Jimenez et al. 2003).

1.2 AN OVERVIEW ON CEMENT

Cement production in the year 2018 was 502 Million Tonnes (MT), and the addition of 20 MT per annum (MTPA) is expected in FY 2019-20. In India, there are 210 cement plants with a capacity of 410MT. The cement industry is an energy-intensive and third-largest coal consumer in the country after the power and steel sectors. It needs both electrical as well as thermal energy for its operation. On average, cement plants are spending around 35-50% of the total manufacturing cost of cement to meet their energy demands, as shown in Fig 1.1 (http://www.indiaenvironmentportal.org.in/files/file/cement.pdf).
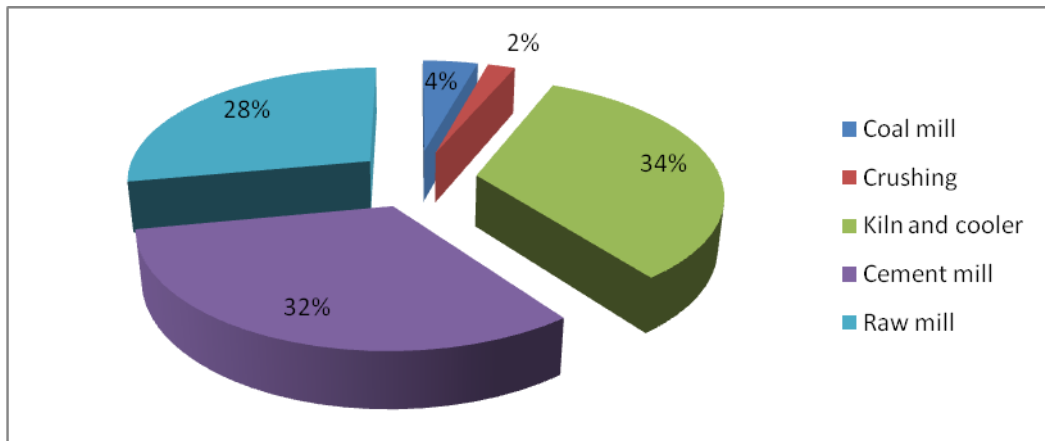
Figure 1.1 Cost breakup in cement manufacturing

(http://www.indiaenvironmentportal.org.in)

1.3 PRECIOUS SLAG (PS) BALL

PS ball is a by-product obtained from molten slag generated from the steelmaking process. It is a solid spherical ball obtained by Slag Atomizing Technology (SAT).In the Electric Arc Furnace (EAF) of high efficiency, the molten slag was formed into small droplets. There is no free CaO present in the product. The surface of the PS ball is shiny having stable spinel structure with a combination of $CaO\text{-}Fe_2O_3$, $CaO\text{-}SiO_2$. SAT is the process of changing the liquid slag (1500°C-1550°C) into small balls with a diameter ranging from 0.1 mm to 4.5mm. In the process, a high-speed wind system with a catalyst

and water were used to convert the liquid slag into balls of different sizes. The surface of the PS ball formed by the oxide compound does not allow easy movement of ions or electrons. Due to this, the ion or electron movement from the PS ball required for the chemical reaction to take place becomes difficult, and therefore it can be considered as stable material that offers very strong resistance to chemical and physical weathering. It is an Eco-friendly material since it is pollution-free and non-toxic as it does not contain free silica. When this material is compared to sand, it exhibits superior characteristics, showing higher crushing strength (35%), hardness (43), and anti-weathering properties.

The slag byproducts are used for various applications ranging from agriculture, landfills, cement making, paver blocks, and construction of roads to railway ballast. In India, the current production of steel slag is around 12 million tonnes per annum. While only a little quantity of the steel slag generated in India is recycled, a large portion of the steel slag generated is disposed in stockpiles or dump yards. This causes problem due to the paucity of land, dumping costs, and other environmental aspects. However, the production of PS ball by SAT eliminated the problem of landfills or dumping. The utilization of PS ball in concrete can lower the environmental impacts along with a reduction in valuable landfill space and protection of natural aggregates for the future. The use of PS ball as fine aggregates in the construction industry will solve the sand mining problem. The awareness of the utilization of PS ball as road material is limited in India. However, before promoting such a material, there is a need for extensive research to be carried out to check its suitability in road applications.

1.4   NEED AND SIGNIFICANCE OF PRESENT INVESTIGATION

The growth of vehicular traffic has led to the construction of new highways. Improved road connectivity is essential for any country's development. The roads need to be durable and sustainable. The high demand of concrete for roads and other construction purposes has resulted in the augmented production of OPC.

The development of eco-friendly and sustainable construction materials has gained major attention from the construction industry. With the augmented emissions of greenhouse gases, high energy consumption, and environmental hazards from the increased OPC production, the researchers focus on developing possible alternatives to OPC. Alkali activated binders can be looked upon as an alternative to conventional OPC binders, which have the capabilities to be used in the construction industry, causing a significant reduction in OPC production (Rashad 2013). Alkali activated binders include clinker-free binders, such as AAS, AASF, Geopolymers, etc., which include the use of a strong alkaline activator along with calcium or silicate rich precursor material such as GGBFS, FA, etc., to form a final product, having properties equivalent or better than OPC. The energy required for the production of alkali-activated binders is less than that required for OPC concrete and are further associated with low CO_2 emissions.

Over the years, the natural aggregates have been used as the filler material in concrete. The present-day research has been concentrated on seeking alternative materials as a replacement for natural fine aggregates in concrete. PS ball, which is generally considered as an industrial by-product from the iron and steel industry, can be viewed as a potential replacement for natural fine aggregates. The utilization of PS ball in concrete mixes will have several advantages such as elimination of cost of dumping, minimization of environmental problems related to disposal of unused slag, conservation of natural aggregates, etc. Despite of satisfactory performance of PS ball as fine aggregates in both normal and high-performance OPC concrete, there is limited research available regarding the incorporation of PS ball as fine aggregates to produce AAB based concrete mixes.

The present experimental study focuses on the possible utilization of industrial waste materials such as GGBFS, FA, and PS ball in the production of sustainable concrete. The aim of the study is not just to protect the natural raw materials, but to recycle the disposal wastes generated from the industries. Since the kind of curing adopted in the present research is air curing, this type of concrete will be of great advantage in arid and desert regions, where there is an acute shortage of water. Presently in India, there limited field

application of AAB based concrete in pavements or any other structures, mainly due to limited research, non-acceptability of new materials, lack of expertise and confidence, etc. The scenario can be changed by conducting proper research and communicating the performance of AAB concrete for different applications.

1.5   SCOPE OF WORK

The IRC:58 (2015) recommends a minimum grade of M40 with a minimum flexural strength of 4.5 MPa for concrete roads. As per the requirements, AASC and AASFC mixes were designed to attain a minimum strength of M40 and compared with a control mix. AASC mixes were prepared with 100% GGBFS as a sole binder, while AASFC mixes were prepared by mixing GGBFS and FA in different proportions, i.e., 90:10, 80:20, 70:30, and 60:40. Preliminary tests were carried out to identify the optimal NaOH concentration and dosage of alkaline activators for each AASC and AASFC mixes. PS ball as fine aggregates were incorporated in the AASC and AASFC mixes by replacing the natural fine aggregates by volume replacement method at 100% replacement level. The fresh and hardened properties such as workability, setting time, compressive strength, split tensile strength, modulus of elasticity, flexural strength, and abrasion resistance of different concrete mixes was evaluated as per standard test procedures. The durability of concrete mixes in terms of resistance to sulphuric acid, hydrochloric acid, nitric acid were investigated. The water absorption and volume of permeable voids are also evaluated. Flexural fatigue performance of various concrete mixes was determined by carrying out repeated load tests on beam specimens. The fatigue life data obtained were represented and analyzed using S-N curves. Probabilistic analysis of fatigue data was carried out using two-parameter Weibull distribution method. Survival probability analysis to predict the fatigue lives of concrete mixes was carried out.

1.6   OBJECTIVES

It is observed that attempts have already been made by researchers to understand the mechanism of Alkali Activated Slag Concrete (AASC) and Alkali Activated Slag-Fly Ash Concrete (AASFC). However, there is limited research on the incorporation of PS ball as fine aggregates to produce AASC and AASFC mixes. The aim of the proposed study is to focus on a detailed experimental investigation to address the suitability and performance of air-cured AASC and AASFC mixes by incorporating PS ball as fine aggregate.

- Evaluate the workability and engineering properties of AASC and AASFC mixes developed using PS ball.
- Study the flexure, fatigue behavior of the AASC, and AASFC mixes.
- Evaluates the durability performance of AASC and AASFC mixes
- Selection of mixes for concrete pavement.

1.7   THESIS OUTLINE

The research work is reported in 7 chapters. The first chapter is an introduction to the topic; other chapters are organized as follows:

Chapter-1 introduces the topic.

In Chapter-2, the literature related to Alkali-Activated Slag Concrete, including the definition of the materials and the properties of concrete, SH and SS as activator solutions including the reaction process involved and solubility of silicates are discussed.

Chapter-3 presents the materials, experimental design, mix proportions, and research methodology adopted.

Chapter-4 deals with the engineering properties of AASC, including compressive strength, splitting tensile strength, modulus of elasticity, abrasion resistance, flexural strength and fatigue behavior of different mixes and influencing factors.

Chapter-5 deals with the effect of alkaline concentration on the fresh and hardened properties of AASFC.

Chapter-6 covers the durability properties of alkali-activated mixtures.

The main conclusions and recommendations for future work are discussed in Chapter-7. The list of references is presented at the end of the thesis.

CHAPTER 2

LITERATURE REVIEW

In this chapter, available literature on alkali-activated concrete along with various factors influencing the development of alkali-activated concrete and its implications are discussed.

2.1   ALKALI ACTIVATION OF CONCRETE

Several attempts have been made in discovering alternatives to Portland cement by considering environmental effects and higher energy-intensive production procedures of cement. The material used as alternatives to cement should be pozzolanic in nature. Pozzolana is a material of ash type, essentially consisting of silica and alumina as major components in the glassy structural phase of the source material. On reaction with hydroxides of calcium in the presence of water at room temperature, hydrated products of Calcium Silicate Hydrate (CSH) compound having cementitious properties are formed. The pozzolanic materials such as slag, FA, silica fume, rice husk ash, etc., are industrial by-products that can be used as Supplementary Cementitious Material (SCM).

Slag is the by-product of the iron and steel industry. The main chemical constituent includes calcium, magnesium, aluminium, and silicate with 95% glass content. The composition of slag differs with crude materials and the manufacturing process. The cooling procedure and composition are the two factors that essentially impact the structure and properties of slag. Specifically, Blast Furnace Slag (BFS) refers to the slag delivered from the pig iron manufacturing process. If the molten slag is quenched sufficiently, it forms a material called granulated blast furnace slag quickly. Slag has latent hydraulic properties. If slag comes in contact with water alone, it dissolves to a smaller extent; however, a defensive film insufficient in Calcium (Ca^{2+}) is immediately formed, which suppresses the further reaction process involved. The reaction proceeds if the pH is adequately high.

The pore structure of cement, which is basically one of the alkaline hydroxides, is an appropriate medium. The contribution of Potassium (K^+) and Sodium (Na^+) particles is constrained; however, these ions are partially utilized for hydration products, and the occurrence of strong calcium hydroxide guarantees the supply of OH^- in hydrated phases. The slag can also be activated by OH^- particles provided in different ways; for example, the inclusion of SH or SS (Taylor 1997). The major component of slag includes calcium oxide, silicon dioxide, aluminium trioxide, magnesium oxide, etc. The alkali-activation of slag results in the formation of amorphous CSH compounds with a significant amount of alumina content (Pacheco et al. 2007). This shows that slag can be activated by Ordinary Portland Cement (OPC), which is the most common procedure and furthermore with alkali solution in alkali activated mixtures. The alkali solution can be alkaline hydroxide (MOH), non-silica salts of weak acids (M_2CO_3, M_2S, MF), and silica salts of $M_2O(n)SiO_2$ type or combination of blends of these, where M represents an alkaline metal such as Na, K, Lithium (Li). Of all these alkaline solutions, SS (Na_2SiO_3) is the best activator solution (Wang et al. 1995).

2.2   FACTORS AFFECTING ACTIVATION OF SLAG

The factors affecting slag activation can be summarized as:

a)   Type of slag

Slag chemical composition plays a vital role in the hydraulic activity of binder particles. Thus, the micro-structural and hardened concrete properties are produced. The high alumina content brings about high early strength where a significant amount of slag reacts and hardens quickly. Subsequently, the Al_2O_3/SiO_2 proportion is viewed as a quality modulus, and slag with 12-15% of Al_2O_3 is preferred. Minor constituents of Phosphorous, Fluoride, Sulphur, Manganese, and Titanium regularly have a significant influence on strength development. The excess Fe_2O_3 content diminishes the slag reactivity (Wang et al. 1994). The mineralogical composition of slag has a greater influence on reactivity; the crystalline mixes found to be less reactive compared to the amorphous type, determined by XRD technique.

b) Fineness of slag

Slag reactivity depends on the fineness, grain size distribution, and the specific surface area. It is well known that increasing the fineness of slag enhances the strength with a decreased setting time of slag blends. The fineness of slag for alkali-activated slag ranges between 450-500 m^2/kg by Blaine's permeability (Wang et al. 1994).

c) Type of Activator

Activators used include Potassium Hydroxide (KOH), SH, Sodium Sulphate (Na$_2$SO$_4$), Sodium Carbonate (Na$_2$CO$_3$), and SS, which is the best activator according to several researchers (Wang et al. 1994).

d) Method of Adding Activator

Alkaline activator solution is added to the binder system in three ways: solution, solid precursor, and in the solid-state where the alkali activator is added separately as one of the mix constituents. The addition of alkali in the solid-state represents lower strengths compared to the solution form but also produces fluctuation in the test results, which can be attributed to lower solubility and lesser dissociation of alkalis. Due to the hydrophilic nature of solid alkalis, it might absorb moisture during storage, which inhibits the activation process. Anhydrous sodium meta-silicate/sodium silicate (containing chemically bound water) in the solid form produces very low strength under a normal curing regime. But, when the same alkali is added in solution form, a similar type activation mechanism can be achieved with sodium silicate solution. A combination of sodium hydroxide with sodium silicate has been found to provide the best strength performance for the activation of alkali-activated binders (Rashad 2013). When Na$_2$CO$_3$ is added in solid alkali form with ground Na$_2$CO$_3$, slag gives high strength. Due to higher solubility, SH pellets and solution can act as a good activator solution (Wang et al. 1994). In general, the alkali solution shows better performance in strength development with loss in workability and reduced setting time.

e) Activator Dosage

Several authors have made an attempt to optimize the alkaline dosage with inconsistency in test results. Alkali-activated mixtures can be developed with SH (by binder weight) range between 1-10%. A variation in SH dosage (3-11%) shows a remarkable loss in strength. Alkali dosage can also be expressed in terms of Na_2O content; high Na_2O content tends to increase strength. However, Na_2O content beyond the threshold limit (the type of slag, the concentration of activator solution and curing regime) decreases the strength of the activated mixture. This tends to produce detrimental properties like an increase in efflorescence and brittleness due to the availability of free alkaline ions. The Na_2O content from 3-5.5% with sodium SS can be used as an activator solution (Wang et al. 1994). Alkali-activated mixtures developed using different alkali solutions such as SH, Na_2CO_3, SS, and Na_2SO_4 or a combination of these solutions can be used as activator solutions. The best results are obtained for the mixes with silica modulus 0.75 and 5% Na_2O content. The strength properties of alkali-activated slag mixture were influenced by the activator solution, alkaline dosage, and the observed optimum dosage of Na_2O was in the range between 3-5% (Fernandez-Jimenez et al. 1999). The high strength concrete can be developed using a slag-cement blend activated by SS with a modulus of 1.6-1.5 (Krizan and Zivanovic 2002). The strength of alkali-activated fly ash mixes activated with SH variation in Na_2O content between 5-15% is influenced by alkaline liquid/binder (a/b) ratio (Fernandez and Palomo 2005).

f) Silica Modulus

Silica modulus (M_s) refers to the molar ratio of SiO_2/Na_2O. These main reactive components are primarily responsible for the hydration reaction and strength development. Alkali-activation of slag particles converts amorphous silica (SiO_2) forms to silica-gel. For constant Na_2O content, high strength can be achieved with an increase in silica mineral. But limiting the solid content in the activator solution has to be considered for solubility. Therefore, high silica modulus utilizes more solid content to achieve high Na_2O content. The strength of AABs is governed by the type of alkaline activator,

activator modulus, and dosage of alkaline activator (Fernandez-Jimenez et al. 1999). The M_s is a ratio of the mass of SiO_2/Na_2O components present in the alkaline activator, while the dosage (usually referred to as $Na_2O\%$) is the total sum of the mass of Na_2O present in the alkaline activator (mass of Na_2O present in sodium silicate + mass of Na_2O equivalent in SH if the combination of SS and SH is used as an alkaline activator). Also, SS with high modulus results in a quick setting of alkali-activated slag mixtures, which necessitates optimizing the silica modulus. Good test results were obtained for the alkali-activated mixtures with silica modulus range between 1 to 2.

Wang et al. (1994) reported that mechanical strength and other properties of AAS mortars were influenced by the nature of the alkaline activators. The dosage and the activator modulus have significant effects on the properties of alkali activated binders. They have provided a range of activator modulus depending on the GGBFS type within which the maximum compressive strength may be obtained. The type of slag includes Acid slag having a basicity coefficient range between 0.75 – 1.25, Neutral slag having a coefficient range between 0.90 – 1.3 and Basic slag having a coefficient range between 1.0 – 1.5.
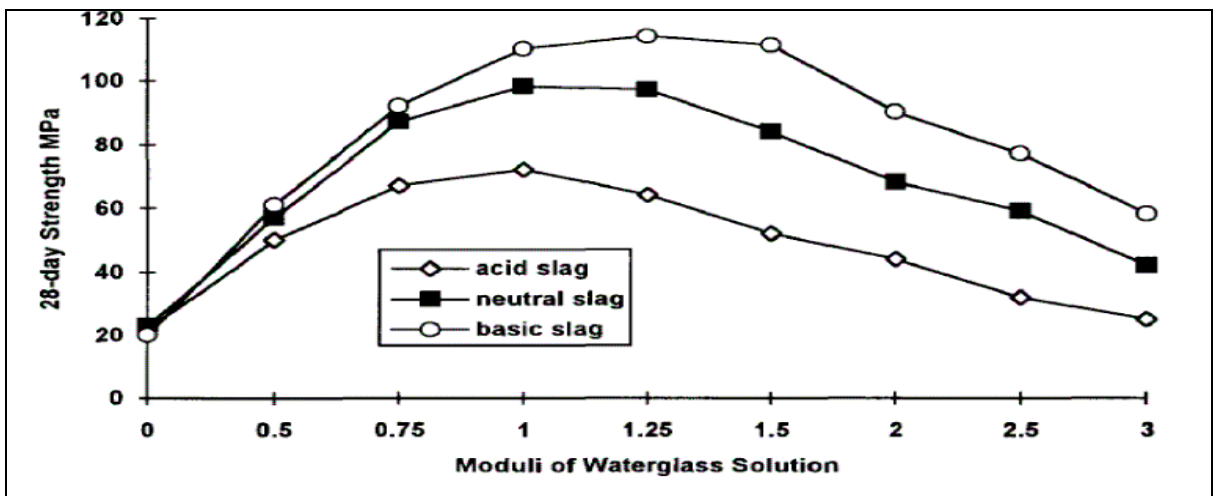
Figure 2.1 Moduli of sodium silicate solution (Wang et al. 1994)

g) Curing regime

The hydration reaction of alkali activated mixtures with slag is dependent on the curing temperature. The high-temperature curing leads to the formation of crystalline products, whereas ambient cured mixes result in the formation of amorphous products (Wang et al. 1994). Past studies on alkali activated mixtures have been studied at different curing conditions such as heat curing, steam curing, normal room temperature curing (air curing), water curing, etc. Altan and Erdogan (2012) studied AAS mortar mixes activated using a combination of sodium silicate and sodium hydroxide at room and elevated temperatures. They observed that heat-cured samples gained strength rapidly; however, samples cured at room temperature gained strength gradually. It is also reported that the heat liberated in alkali activated mixtures during the hydration process was lesser compared to hydration in OPC.

Bilim et al. (2015) investigated the AAS mixes with Na_2O dosages of 4% and 6% by mass of slag. The test results reported that the curing conditions affected the mechanical behavior of AAS mixes as compared to OPC mixes. The AAS mixes attained high early strength at elevated temperatures when compared to OPC mixes. For example, an alkali-activated mixture of phosphorus-based slag (neutral or acid type) had strength of 30 MPa when air-cured, 62 MPa on heat curing, and 71-76 MPa on autoclave curing. Whereas, an alkali-activated slag (basic) attained the strength of 80 MPa on air curing and 85-95 MPa on autoclave curing. The autoclave curing of sodium hydroxide activated alkali activated mixtures reported an increase in compressive strength compared to the conventional curing.

Aydin and Baradan (2012) reported that high strength mortars with strengths upto 70 MPa can be produced with alkaline activators with alkali content of 2% (by mass of binder) under autoclave curing. In the case of heat curing, the curing time and temperature are the critical factors in determining the strength of alkali-activated mixes (Shekhovtsova et al. 2014). Qureshi and Ghosh (2014) studied the effect of curing regime on the strength behavior of AAS pastes under different curing conditions such as water

curing at 27^0C, heat curing at 50^0C and controlled curing with relative humidity 50%, 70% and 90 % at 27^0C respectively and reported that maximum strength was obtained under water curing condition. They concluded that the mechanical behavior of AAS paste was significantly affected by the curing conditions.

Activation of slag (GGBFS), the reaction begins with the attack of alkalis on slag particles, thus breaking the outer layer and then continued by poly-condensation of reaction products. Although the initial reaction products are formed due to the process of dissolution and precipitation, at later stages, a solid-state mechanism is followed where the reaction occurs on the surface of formed particles dominated by slow diffusion of the ionic species into the un-reacted core (Wang et al. 1994). In the initial stages of hydration, alkali cation (R^+) behaves like as mere catalyst cat-ion exchange with the Ca^{2+} ions for the reaction, as shown in the following equations 2.1, 2.2, and 2.3 (Glukhovsky 1994,Krivenko 1994).

$$Si\text{-}O\text{-} + R^+ = Si\text{-}O\text{-}R \qquad\qquad ...\,(2.1)$$

$$Si\text{-}O\text{-}R + OH^- = Si\text{-}O\text{-}R\text{-}OH^- \qquad\qquad ...\,(2.2)$$

$$Si\text{-}O\text{-}R\text{-}OH\text{-} + Ca^{2+} = Si\text{-}O\text{-}Ca\text{-}OH + R^+ \qquad\qquad ...\,(2.3)$$
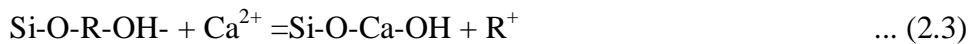
While the alkaline cation act as structure creators, the nature of anion in the solution plays a significant role in activation, especially during the early stages, particularly concerning paste setting (Fernández-Jiménez and Puertas 2001). A descriptive model showing the reaction mechanism is presented in Figure 2.2.

Final hydration products in case of activation of slag are similar to the products of OPC hydration i.e. Calcium-Silicate-Hydrate (C-S-H), but with a low Ca/Si ratio. However, the rate and intensity of activation of slag differ majorly as compared to that hydration of OPC. It is reported that the alkalis are not freely available in the pore solution since they are bound to the reaction products, thereby negating the potential for alkali-silica reactivity; however, this depends on the concentration of alkali used.
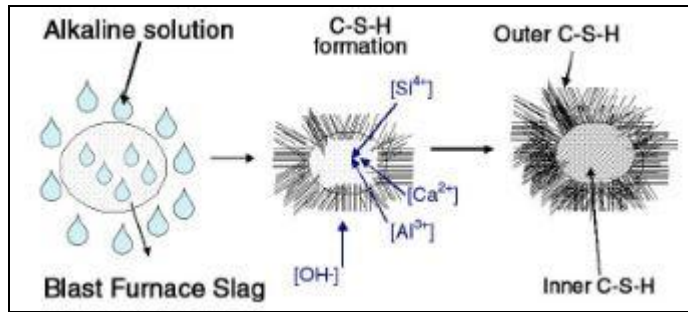
Figure 2.2 Reaction mechanism of alkali-activated slag (Palomo et al. 2014)

The hydration mechanism of Alkali Activated Slag-Fly Ash (AASF) is very similar to that of AAS; however, they slightly differ in the rate of hydration. There have been certain contradictions on the reaction products in the hydration of AASF. Studies carried out by researchers (Puertas et al. 2000) claim the main product formed in AASF to be C-S-H with no existence of A-S-H, while others (Chi and Huang 2013) have reported the presence of both. Chi and Huang (2013) reported that amorphous alkaline alumina-silicate and C-S-H gel, to be the products of hydration of AASF. Idawati et al. (2013) found the C-A-S-H phase and hybrid C-(N)-A-S-H phases in smaller quantities. The dissolution of calcium present in slag affects both early and later age properties significantly, and the availability of free calcium prolongs the FA dissolution and enhances geopolymer gel formation. They proposed that the hardening process was initiated with the precipitation of C-S-H/C-A-S-H, while rapid hardening continues due to accelerated geopolymerization. It was also reported AASF display a basic network formation due to the formation of alumina-silicate geopolymer at a very early age, and that product formation was observed on both slag as well as FA spheres.

The polymerization process is an exothermic polycondensation reaction which involves alkali activation by cation, thus leading to the formation of a polysialic geopolymer (Davidovits1999).A chemical reaction occurs between alumino-silicate oxides (Si_2O_5, Al_2O_2) and alkali polysiliates forming polymeric Si – O – Al bonds. Equation 2.4 shows an example of polycondensation by alkali into poly (sialate).

$$(Si_2O_5, Al_2O_2)n + nSiO_2 + nH_2O \xrightarrow{\text{NaOH, KOH}} n(OH)_3 \; \overset{(-)}{-Si-O-Al-O-Si-(OH)_3}$$

$$(OH)_2$$

$$n(OH)_3 \; \overset{(-)}{-Si-O-Al-O-Si-(OH)_3} \xrightarrow{\text{NaOH, KOH}} (Na,K)^{(+)} -(-Si-O-\overset{(-)}{Al}-O-Si-O-) + nH_2O$$

$$(OH)_2$$

$$\text{...} (2.4)$$

From the above equation, it may be seen that cat-ion which is introduced as KOH or NaOH, is used to activate the reaction. The main reaction product formed is amorphous alkali alumina-silicate-hydrate (A-S-H), which has a similar structure to that of zeolitic precursors. A descriptive model showing the activation mechanism of fly ash is presented in Figure 2.3.

Figure 2.3 Mechanism of gel formations in alkali-activated fly ash binder (Jimenez et al. 2005)

A higher early strength development with high sodium hydroxide concentration can be attributed to the faster reaction at an early stage of polymerization initiates with a high temperature curing regime (Rattansak and Chindaprasirt 2009, Ryu et al. 2008). The

past studies on the synthesis of geopolymer analyzed the compatibility of CSH or NASH compound for greater depth shows the stable form of the NASH compound is highly dependent on the P^H of the activator solution (Hodeiro et al. 2011). A geopolymer developed under room temperature has a similar strength development trend as that of conventional concrete, i.e., with an increase in curing period, strength properties increases, due to the polymerization reaction silica and alumina mineral under an alkaline environment (Somna et al. 2011).An investigation by Puertas et al. (2000) guarantees the primary reaction product to be C-S-H in AASF with the absence of ASH compound, while others have detailed the presence of both. Idawati et al. (2013) discovered the C-A-S-H compound and partially C-(N)-A-S-H compound in minor proportion. The increased FA content in the AASF binder has decreased strength with increased workability (Rashad 2013).

AASF mixes containing 50% FA (weight of binder) develops adequate strength under ambient curing; however, the compressive strength development reduces with higher FA content (Bakharevet al. 1999). For example, the heat released during the hydration process is to lower than conventional concrete, the mechanical properties of AAM are generally higher than conventional concrete, particularly the early strength development (Bakharevet al. 1999), good durability properties because of the refined pore structure, higher fire resistance (Rashad 2013), high chloride resistance (Roy 2000), improved interface transition zones in concrete matrix (Shi and Xie 1998). These AAM possess good mechanical and durability properties compared to conventional concrete, which should increase the probability of these binders being the substitutes for binders in conventional concrete. In general, AAM has shown a greater potential to be environmentally friendly than cement with comparable or even better performances. In this manner, it is promising to apply AAM to replace the cement-based materials for different applications.

Bernal et al. (2011) demonstrated the comparative study on the AASC and conventional concrete. The AASC mixes developed for the binder content ranging

between 300-500 kg/m^3. Irrespective of the binder content in the AASC mix, the AASC mixes developed high compressive strength than conventional mixes. It was concluded that, by controlling the mix design parameters, it is possible to develop the AASC mixes with greater mechanical strength and durability properties compared to the conventional mixes.

The performance of fly ash-based geopolymer blend has been reported for the acid-resistance test (Bakharev 2005, Song et al. 2005), sulphate attack (Bakharev 2005), and chloride attack (Miranda et al. 2005). Metakaolin based alkali-activated material remains unaffected by the various acid solutions such as Sea-water, Deionized water, sodium sulphate, and sulphuric acid (Palomo et al. 1999). Satisfactory performance of alkali-activated fly ash material was observed on sulphate attack and sea-water. When exposed to sulphates, a negligible amount of sodium sulphate is formed as a deterioration product. In sea-water, the sodium (Na$^+$) ions are interchanged by Magnesium (Mg$^+$) ions results in the formation of more porous products affecting the microstructure. Low-calcium fly ash-based geopolymer tends to degenerate aluminium particles under highly acidic conditions results in substantial mass loss with a decrease in strength (Fernández - Jimenez et al. 2007). Fly ash-based geopolymer exposed to 5% sodium sulphate for 52-weeks reported no-sign of sulphate attack or deterioration. However, the samples exposed to 2% sulphuric acid significantly reduce compressive strength (Wallah and Rangan 2005).

Fly ash (low calcium) based alkali-activated material on alkali-silica reaction as per ASTM C 1260-84. (Fernández -Jimenez et al. 2007). The long-term properties of fly ash (low calcium) based geopolymer found to be a low creep and dry shrinkage properties on heat curing. After 52-week dry shrinkage strain was approximately 100x10^{-6}, and creep factor varies between 0.44-0.63 with compressive of 60 MPa (Wallah and Rangan 2005). Fly ash (low calcium) based geopolymer shows better resistance towards acidic attack; the fly ash mortar contains a substantial amount of Mesopore size pores (Kong et al. 2007, Sindhunata 2006).

Pore structure development of activated material is considerably lower than cement mortar, which prolongs the curing period. The increased silica and alkali concentration have a relative influence on pore structure and porosity (Ma et al. 2013). Lower water absorption and sorptivity exhibited by fly ash-based geopolymer on heat-curing. An alkaline liquid/ binder ratio, aggregate content, and alkaline concentration are the major parameters influencing the permeability properties (Olivia et al. 2008). The past studies have shown heat-cured geopolymer concrete has great potential to be an alternative for conventional concrete. However, the durability of these mixtures has to be established, particularly air-cured alkali-activated material. The experimental study present in this chapter utilizes ambient curing to the alkali-activated mixtures for durability properties.

2.3   EFFECT OF SODIUM HYDROXIDE

Alkali-activator solution has a prime role in dissolving the silica and alumina minerals to produce a geopolymer solid precursor with alumina-silica complexes as final reaction products. SH and KOH are commonly used for activator solutions (Davidovits 1999, Palomo et al. 1999, Fernandez et al. 1999, Swanepoel and Strydom 2002, Xue et al. 2002). The alkaline solution prime role in the alkali-activated system is similar to the addition of water to cement blended with slag/fly ash. Suppose the water is added directly to the slag mix, the hydration reaction is interrupted by the passive layer/coat formation on slag particle. An alkaline solution of a strong base such as NaOH and KOH is necessary to breakdown the passive layer for enhancing the polymerization (Taylor 1997).

Three different types of slag (acidic, basic, and neutral) with sodium silicate have an activator solution with different activator modulus. The test results indicate that the optimum activator modulus was found to be 0.75-1.25 (acidic), 0.9-1 (neutral), and 1-1.5 (basic). At a lower P^H (>11), the solubility of silica mineral is very low, which is a major constituent of slag. The P^H of the activator solution is expected to have a significant effect on the final reaction products (Song and Jennings 1999). The activator solution with high

SH concentration is directly related to the dissolution of alumina-silica mineral. Since the dissolubility of silica mineral enhances with the P^H of activator solution with the greater dissolution of silica-alumina mineral complex (>4M SH) (Moruf et al. 2014).The increase in SH concentration beyond 10M does not contribute to strength development due to the lower rate of polymerization. This prompted the increase in strength properties at a high concentration of sodium hydroxide; thus, CASH formed as the final reaction product (Zuhua et al. 2009). The excess hydroxyl ion produced with high SH concentration prompts ionic blockage that may prevent oligomeric polymerization, i.e., $Al(OH)_4$ and $Si(OH)_4$ exchanges, which restrains the formation of CASH. This could decrease the strength properties, observed for the mixes with 12M and 16M SH.

Activator solution with a high concentration of SH enhances the dissolution process; it suppresses ettringite mineral and calcium hydroxide phases during the formation of reaction products (Khale and Chaudary2007). It was observed that geopolymer mixes activated with SH develops a greater crystalline compound, which enhances the durability properties (Criado et al. 2007). Fly ash-based alkali-activated concrete with sodium hydroxide (8M-12M) as an alkali-activator solution; oven cured for 24-hours at 85^0C produces the concrete having a compressive strength range between 35-40 MPa. This attains the strength of 90 MPa (SiO_2/Na_2O =1.23) (Palomo et al. 1999). The high molarity of SH used as an activator solution enhances the strength properties with a substantial effect on early strength (Ryu et al. 2013).

Increased SH concentrations from 8M-18M positively affect setting time (Hanjitsuwan et al. 2014).The lower Na/Al ratio represents the lower SH concentration and vice-versa. A Na/Al ratio of 1 and 2 have the lower dissolution of fly ash particles due to lower SH content results in the lower polymerization. Hence, the rapid setting of a geopolymer is achieved (Siyal et al. 2016). An increase in Na/Al ratio of 1.4 leads to the greater dissolution of the FA particle produces more silica, and alumina with low calcium content enhances the polymerization reaction. The early stage of polymerization requires

more time for a complete reaction, which was greatly influenced by the setting time of geopolymer paste (Chindaprasirt et al. 2012, Alonso and Palomo 2001).

Alkali-activated fly ash concrete developed with 6M SH at SS/SH ratio=1; the setting time was significantly high compared to the mixes of SS/SH ratio 0.5 and 1.5. The faster setting time was reported for the mixes with 4M and 6M SH at the SS/SH ratio of 1.5. However, the setting time was greatly influenced by the interaction between the aqueous phase of SS and SH (Lee and Lee 2013). The addition of gypsum to the alkali-activated slag matrix shows a significant reduction in the setting time with an increase in compressive strength. Meanwhile, the addition of phosphoric acid enhanced the setting time affecting the early strength of concrete (Rashad 2013).

A Phosphoric and Malic acid is used as a retarder in alkali-activated slag material and sodium silicate-based mixtures to enhance the setting time (Brough et al. 2000). Palacios and Puertas (2005) investigated the different types of superplasticizers (Melamine, poly-carboxylates, naphthalene and based polymers) and shrinkage reducing agents (poly-propylene glycerol and its derivatives) admixtures affecting the fresh and hardened concrete properties of alkali-activated material. This study showed naphthalene-based admixtures along with sodium hydroxide, reported high strength compared to the alkali-activated slag mixes without admixture. Hardjito et al. (2015) asserted the effect of SH concentration on the strength properties of FA blended geopolymer mixes. The test result's activator concentration is directly related to the strength development of geopolymer mixes. They also claim the strength development of geopolymer mixes were dependent on the SH concentration.

Synthesis of metakolinite based geopolymer mixes with a higher concentration of SH enhances the dissolving ability of metakaolinite mineral and produces a more reactive form of monomer units, with an increase in intermolecular bond strength. They also claimed the mechanical properties of geopolymer concrete of metakaolin based activated by SH and SS solution were primarily dependent on the SH concentration (Wang et al. 2018). A lower concentration of SH results in the lower dissolution of the source

material. This tends to use the high concentration of sodium hydroxide to improve the P^H of activator solution and speed up the dissolution of the source material. The lower heat evolution attributes to the passive layer formation on the un-reacted binder particles formed due to reaction products derived from the source material (Wang et al. 2018). The essential polymerization of a geopolymer is highly dependent on the SH concentration and type of source material.

NaOH concentration up to 8M has a reasonable variation in setting time. However, the sodium hydroxide concentration of 14M significantly delayed the setting time (Yasser et al. 2019). An increase in SH concentration geopolymer matrixes, the setting time of the geopolymer blend reduces so as to surge the solid content of sodium hydroxide. The test results claim higher cohesion of geopolymer composites observed at the lower solution/ powder ratio. The setting time of geopolymer mixes with 5M and 10M sodium hydroxide concentration is within EN-193guidelines except for the mixes with 1M (Tekin2016). The aqueous phase of SH in the alkaline medium initiates the dissolution process in geopolymeric system with a significant effect on final reaction products. FA on contact with SH enables leaching of calcium, silica, alumina and other traces of minerals from source material.

The leaching effect is predominantly dependent on the SH concentration and duration of leaching (Rattanasak and Chindaprasirt 2009). The increase in SH concentration from 4.5M-9.5M increase the compressive strength of geopolymer paste, marginal improvement in strength was reported for the mixes with 9-14M (Somna et al. 2011). The compressive strength increases with an increase in SH concentration, due to leaching of silica and alumina minerals from the source material with high SH concentration (Chindaprasirt et al. 2009).

Geopolymer mixes with SH concentration varying from 9.5-14M reported a high compressive strength range between 23-25MPa. However, 16M SH shows a reduction in strength. The excess hydroxyl ion concentration accelerates the dissolution of FA particles hindering the polymerization reaction (Zaharieva et al. 2009). An increase in

alkali-activator concentration enhances the strength development of geopolymer mixes, but excess hydroxyl ion leads to the precipitation of alumina-silica gel during the early stages of polymerization, results in low strength geopolymer matrixes (Lee and Van 2002). FA based geopolymer concrete activated by sodium hydroxide cured under room temperature produces remarkable strength. The strength properties and microstructure formation of polymeric material depended on SH content (Somna et al. 2011).

Mustafa et al. (2012) reported an effect of sodium hydroxide (6M, 8M, 10M, 12M, 14M, and 16M) on FA based geopolymer mortar. The test results reported the geopolymer mixes with 12M SH concentration produced the high strength at 70^0C for 24 hours curing regime. Wang et al. (2018) investigated an effect of SH concentration on the rheological properties, microstructure and geometrical property of geopolymer paste. They claim fluidic properties of geopolymer mixes were influenced by the sodium hydroxide content. Lower activator concentration has the zeta potential of fresh geopolymer paste of less than 3 mV due to the lower rate of dissolution of silica and alumina minerals from the source material.

2.4   EFFECT OF SODIUM SILICATE

Reaction capability and solubility of the pozzolanic silicates were affected by P^H of the activator solution. A final reaction product was dependent on the activator concentration and binder type; the calcium-silicate-hydrate (CSH) may be the main hydrated product with small traces of alumina content (Pacheco et al. 2007). Sodium silicate cannot be used as an independent activator unit in an alkaline-activator solution. Since it does not contain a significant amount of hydroxyl ion to initiate the series of polymerization. Generally, the SS is mixed with SH solution as a catalytic substance to enable alkalinity of the activator solution for strength development (Kong et al. 2007). An effect of activator modulus and fineness of slag have a significant contribution towards the strength development of alkali-activated material.

Douglas et al. (1991) activated the slag with SH, SS, and Calcium Hydroxide as activating reagents. The test result shows SS can be efficiently used as an activator solution for desired workability and strength. Wang et al. (1995) reported the fineness of slag, activator modulus (Na_2O/ SiO_2), and water/solid ratio are the most influencing parameters affecting the fresh and hardened concrete properties of alkali-phosphorous slag cement. The anions from sodium silicate react with Ca^{2+} ions, dissolves the surface layer of slag granules, results in the formation of CSH at the early stages of reaction. The main reaction products formed are CASH with a low ca/si ratio (Wang et al. 1995).

Bakharev et al. (1999) developed AASC concrete with NaOH, Na_2CO_3, Na_2SiO_3, and Na_2SO_4 as an activator solution. The test results reported the compressive strength range between 20-40 MPa with SS as the most effective form of activator solution. The liquid SS decreases the saturation of alkali metal ions in hydrated phases of the pore solution and enhances the inter-molecular bonding properties (Feng et al. 2004). A polymeric blend of series-A (40% activator solution) and series-B (35% activator solution) exhibited low workability with an increase in slag content and decreased by SS/SH ratio. The basic polymeric blend with an alkaline solution of 35% showed a remarkable loss in workability compared to the series-A mix without extra water (Deb et al. 2014).

The concentration of activator solution plays a vital role in the formation of a successful geopolymeric system with improved strength properties compared to conventional concrete. An increase in alkaline concentration enhances the rate of reaction; lower porosity and high strength of FA blended geopolymer concrete (Chareerat et al. 2016). The AASC mixes with high alkali-activator concentration and silica modulus above 1.2, enhances the setting time (Atis et al. 2009, Bakharev et al. 1999). The past studies on alkali-activated materials reported a remarkable loss in the strength for the mixes with silica modulus greater than 1(Wang et al. 1994).

For flyash based geopolymer, the optimum SiO_2/Al_2O_3 ratio of 1.6 is sufficient to produce the high strength geopolymer mixtures (Song-Piriyakij et al. 2010). An increase in Si/Al ratio has silica in larger content with an increase in sodium oxide content

enhances the polymerization reaction. It requires less time to complete the dissolution process before the setting of mixes leads to the rapid setting of geopolymer mixes with a reduction in setting time (Allahverdi et al. 2011). Chindaprasirt et al. (2012) investigated an effect of SiO_2 and Al_2O_3 on fly ash-based geopolymers with high calcium content and observed the increase in SiO_2 and Al_2O_3 content reduced the setting time. An increase in SiO_2/Al_2O_3 ratio from 2-5 improved the setting time for metakaolin based geopolymer (Silva et al. 2007). The workability of alkali-activated concrete produced with slag and fly ash as solid precursor material decrease with the increase in the SS/SH ratio, which was in good agreement with the past studies (Deb et al. 2014, Nath and Sarkar 2014). Since a sodium silicate is the most viscous solution in the activator solution, with an increase in SS/SH ratio 1.5-2.5, the viscosity of alkali-activated concrete tends to increase, results in the lower workability (Fang et al. 2018).

The setting time of alkali-activated material was significantly affected by the SS/SH ratio. The setting time of the alkali-activated flyash-slag blend decrease from 2-2.5. The variation in the effect of SS/SH ratio on setting time may attribute to the strong interaction between SS and SH. A high compressive strength AASC can be produced using SS with a silica modulus range between 0.6-1.5 (Gao et al. 2016, Krizan and Zivanovic 2002).

The higher silica content has a significant effect on the formation of a geopolymer matrix; due to quick stiffening of the geopolymer paste decreases the synthesis of geopolymer paste (Siyal et al. 2016). The consistency of FA based geopolymer mixtures were primarily affected by the variation in the SS/SH ratio. Since SS is more viscous than SH, the viscosity of the activator solution tends to increase with SS/SH ratio. This shows the relative influence of an activator solution on the physical properties of geopolymer mixes. An SS/SH ratio increases, the amount of reactive silica increases in the mixtures. This accelerates the polymerization reaction to a smaller extent. Hence, reduction in setting was observed for the mixtures with a high ratio of SS/SH observed for SS/SH ratios 1.5, 2, and 2.5 have an activator modulus of 0.99, 1.13, and 1.9, respectively (Nath

and Sarker 2014). The dissolution of silica mineral increased with an SS/SH ratio of 2-2.5, thus reducing setting time. A substantial increase in silica content accelerates the alkali-activation system and hinders the dissolution reaction. As a result, a reduction in setting time was observed (Fang et al. 2018). An increase in alkaline liquid concentration and silica modulus accelerates the rate of hydration with reduced setting time. The alkaline concentration (6.5%) and silica modulus (0.85) reported high compressive strength. The AASC mixes with higher strength development were observed for the mixes with high silica modulus (Hamed et al. 2016).

2.5 OTHER MATERIALS USED AS FINE AGGREGATE

Wang et al. (2005) reported that superfine slag exhibits a much higher activity at early ages and middle ages, but it exhibits a lower activity at later ages; the concrete containing steel slag shows lower compressive strength with high porosity and permeability. Bakharev et al. (2000) reported that the strength of geopolymer concrete is increased with an increase in the percentage of M.Sand in various percentages; for E-waste, 20% maximum is the replacement. An increase in the amount of E-waste proportion in geopolymer requires a higher dosage of superplasticizer to get good workability. Albitar et al. (2015) reported that utilization of granulated lead smelter slag as fine aggregate results in significant improvement in compressive strength when flyash acting as a binder reduced by 50%, also granulated lead smelter slag may act as a supplementary binder when there is insufficient flyash to complete polymerization reaction. Joy and Mini Mathew (2015) reported that workability decrease with an increase in the foundry sand since foundry sand is hydrophilic in nature, and it attracts water to its surface, and there is no significant increase in compressive strength on 7 days curing. Singh et al. (2017) reported that the addition of granite cutting waste fines ensures effective packing of cement aggregate matrix (micro filler action), leading to a reduction in space for free water and large dispersion of cement particles resulting in a better-hydrated condition and increased bonding components of concrete. Mithun et al. (2016) reported that AASC mixes with copper slag, as a replacement of sand up to 100% by

volume, show no marked loss in strength characteristics. AASC mix with either sand and copper slag possess similar modulus of elasticity, lower porosity, less water absorption, and reduced chloride ion penetration as compared to ordinary Portland cement concrete mixes. Priyadarshini et al. (2017) reported that the molarity of NaOH is a significant factor that affects all the properties of geopolymer mortar with different fine aggregate, workability reduced with increasing NaOH concentration, also higher curing temperature helps in Geopolymerization makes matrix dense and stiff, resulting in better mortar properties.

2.6 PAST STUDIES ON PS BALL AS FINE AGGREGATE

Concrete produced with 100% PS ball as fine aggregate results in an increase of compaction factor by 40% compared to the conventional mix. This fact is attributed to low water absorption, and it possesses a round shape, which helps in increasing the workability of concrete with increasing content of PS Ball as fine aggregates. With PS balls content more than 40% of fine aggregates, even though the density of the concrete increased with an increase in substitution for sand with PS balls, the compressive strength decreased. This decrease in strength may be attributed to the smooth surface of the PS ball (Sharath et al. 2019). Uses of steel slag in the form of PS Ball enhance the mechanical properties of concrete, such as compressive strength and flexural strength of concrete (Tan 2015). The PS Ball incorporated mortar exhibited 10% lower strength at 28-day age; it showed stronger and less porous aggregate- matrix interface between (from particle surface up to 35 μm width) as compared to that of normal mortar containing sand, which is justifiable by the chemical composition of PS Ball attributed to the potential chemical binding (Hyeongi et al. 2020). The effects of replacing sand by different percentages of PS Balls (9, 12, 15, 18, 27 and 36%) by weight of used fine aggregate were analyzed for fresh and hardened concrete properties. Test results indicate a better performance of mixtures containing PS Balls compared with reference concrete in terms of mechanical properties and durability cement reference concrete in mechanical

properties and durability aspects (Jagadish et al. 2020). Two replacement materials, namely slag aggregate and recycled coarse aggregate, were used to replace the natural aggregate in M40-grade concrete by proportions of 0%, 15%, 25%, 35%, and 45% by weight, and the performance of the resulting mixes was compared against that of the original M40-grade concrete. The test results showed by introducing SS into the concrete containing RCA caused an increment in the mechanical properties. Also, the best result was produced with a mix consisting of 25% steel slag and 15% recycled concrete aggregate (Amjad 2019). However, there is limited research available on the effect of PS ball as fine aggregates on the properties of alkali activated binder concrete mixes.

SUMMARY

It was observed that the strength and durability of alkali activated concrete mixes are affected by many factors such as type of binder, the chemical composition of the binder, water-to-binder ratio, percentage of sodium oxide dosage (Na_2O), type of alkali activator, modulus of alkali activator, water content, type of curing, etc. Alkali Activated Slag Concrete (AASC) and Alkali Activated Slag-Flyash concrete (AASFC) mixes, if designed properly, may obtain higher strength and better durability as compared to conventional concrete. Alkali activated mixes containing higher quantities of GGBFS can attain sufficient strength if subjected to air curing. The inclusion of higher amounts of flyash in AASFC concrete mixes increases the strength properties; however, the workability decreases. The activation energy required for alkali-activated mixes containing large proportions of flyash is higher, and hence the replacement of GGBFS with FA beyond 50% in AASFC mixes require a higher dosage of the alkaline activator solution. A proper combination of sodium hydroxide and liquid sodium silicate gives the best activator combination for these materials. The strength and durability properties of alkali activated concrete mixes are significantly influenced by the sodium oxide dosage (Na_2O) and silicate content of the alkaline solution. There exist optimal sodium hydroxides to sodium silicate ratio at which the maximum strength of mixes can be

attained. The optimal sodium hydroxide dosage varies between 10M and 12M, SS/SH ratio 1.5-2, whereas higher dosages may lead to uneconomical mixtures and efflorescence problems. Alkaline liquid to binder ratio, sodium hydroxide (Molarity), SS/SH ratio (silicate content), etc., needs to be controlled in order to obtain mixes of the required strength and workability. PS ball, an industrial byproduct that can be considered as a potential replacement for traditional fine aggregates in concrete. Improved or satisfactory performance of PS ball aggregates has been reported by few researchers when used in conventional OPC concrete. The use of PS ball as fine aggregates in concrete does not lead to volume expansion and reaction with binder particles. The PS ball is a treated material, and it does not require any weathering process before using it as an aggregate for concrete production. However, limited research is available on the strength, durability, and fatigue performance of alkali activated concrete mixes incorporating PS ball as fine aggregate. The present research focuses on studying the properties of sustainable air-cured AASC and AASFC mixes with PS ball as fine aggregate. The methodology adopted in developing alkali activated slag and slag-flyash concrete using PS ball as fine aggregate is discussed in Chapter-3.

CHAPTER 3

METHODOLOGY

3.1 DESCRIPTION OF MATERIALS

In this chapter, a brief description of the mix-design procedure adopted for the alkali-activated slag and slag-fly ash mixtures was provided. The materials such as GGBFS, FA, aggregate (coarse and fine), PS ball, SH, and SS are used to prepare concrete. The tests to be conducted to investigate the physical properties such as setting time (initial and final), workability, and mechanical properties like compressive strength, split tensile strength, modulus of elasticity, flexural strength, abrasion resistance, and fatigue are explained in detail.

3.1.1 Fly Ash (FA)

FA used in this study was procured from UPCL, Udupi, India, confirms to IS: 3812- 2003. The chemical composition of FA was obtained from X-Ray Fluorescence (XRF) analysis, and the results are tabulated in Table 3.1. The physical and chemical properties of FA vary depending on the source and type of coal used for combustion.

Table 3.1 Chemical and Physical Properties of Fly Ash (Class F)

Chemical Constituent	Oxide Content (% by weight)	Requirement as per IS 3812(Part II) -2003
CaO	0.86	5% max
Al_2O_3	32.08	SiO_2+ Al_2O_3+ Fe_2O_3 combined 70% min
Fe_2O_3	3.73	
SiO_2	57.23	35% min
SO_3	0.78	2.75% max
Na_2O	0.51	Total alkalis, 5% max
K_2O	1.52	
Loss on Ignition	0.04	12% max
Insoluble Residue	2.26	
MgO	0.99	

The calcium oxide (CaO) content in the FA is less than 10%, and silicon dioxide is 57%. Based on the chemical analysis, the FA is classified as Class F (low calcium type) as per ASTM C 618. Figure 3.1 shows the microscopic image of the FA particle.
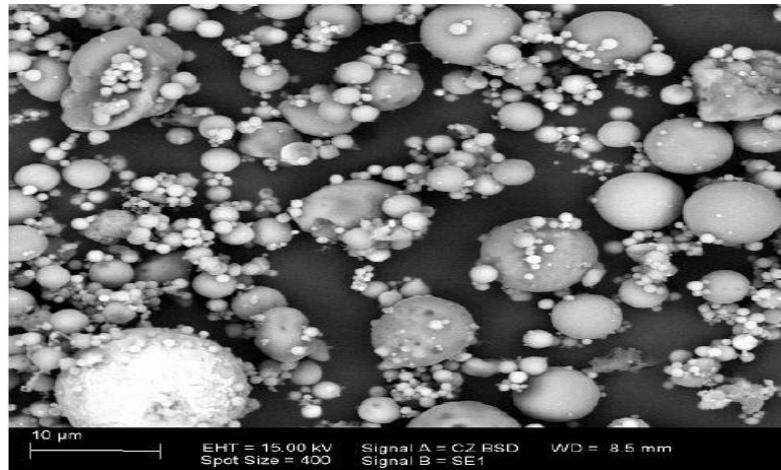
Figure 3.1 Microstructural image of FA particle

3.1.2   Ground Granulated Blast Furnace Slag (GGBFS)

In the present investigation, the slag is procured from M/s, Jindal Steel Works, Bellary, India, confirming to IS 12089-1999. The chemical composition and physical properties of slag are tabulated in Table 3.2. Fig 3.2 shows the microstructural images of slag particles.
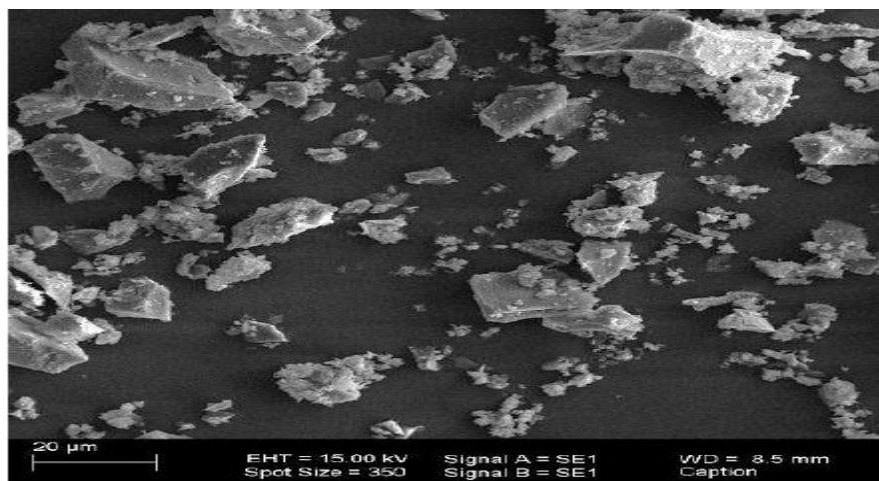
Figure 3.2 Microstructural images of slag particle

34

Table 3.2 Chemical and Physical properties of Slag

Chemical Constituent	Slag (%)
CaO	37.34
Al_2O_3	14.42
Fe_2O_3	1.11
SiO_2	37.73
MgO	8.71
MnO	0.02
Sulphur	0.39
Loss on Ignition	1.41
Insoluble Residue	1.59
Glass content	92
Chemical module: 1. $\dfrac{CaO+Mgo+1/3\ Al_2O_3}{SiO_2+2/3\ Al_2O_3}$	1.07
Loss of Ignition	1.59
Blaine's Fineness (m^2/kg)	375
Specific gravity	2.91
Particles retained on 45 microns	8%

3.1.3 Alkali- activators

To activate the slag and slag-fly ash mixtures, a combination of SH and SS solution were used. The industrial-grade SH flakes with 97% purity were used to prepare the varying molar concentration, and the potable water was used for the preparing activator solution preparation. The SH solution was prepared by dissolving the flakes in water. The mass of NaOH solids varies depending on the concentration of the NaOH solution, expressed as molarity. NaOH solids per litre of activator solution for desired NaOH concentration can be obtained by multiplying the NaOH molecular weight (40g) with desired molarity. For example, 10M NaOH solution, 10x40=400 grams (NaOH flakes) were dissolve in water and made it to 1 litre. The chemical composition of SS is presented in Table 3.3. The alkaline activator solution was prepared one day prior to mixing, to dissociate the ions, reduce the heat liberated during exothermic reaction, and to prevent the quick setting of fresh concrete during mixing.

Table 3.3 Chemical and Physical properties of Sodium Silicate

Chemical constituent	Na$_2$O (%)	SiO$_2$ (%)	H$_2$O (%)	SiO$_2$/ Na$_2$O	Specific gravity	Density (kg/m^3)
Sodium silicate	14.7	32.8	52.5	2.23	1.45	1570

3.1.4 Coarse Aggregates

In this study, crushed granite aggregates of size 20mm down are used as coarse aggregate conforming to IS 383-1970. The sieve analysis and physical properties of coarse aggregates were evaluated as per IS 2386 (Part I-IV)-1963, and the test results are tabulated in Tables 3.4.

Table 3.4 Physical Characteristics of aggregates

Sl. No	Test	Crushed granite aggregates	Method of Test
1	Specific Gravity	2.67	IS 2386 (P-III) -1963
2	Bulk Density a) Dry loose	1492 kg/m^3	
	b) Dry compact	1643 kg/m^3	
3	Aggregate Crushing Value	22%	IS 2386 (PIV)-1963
4	Los Angeles Abrasion value	20%	
5	Aggregate Impact value	23%	
6	Water Absorption	0.5%	

3.1.5 Fine Aggregates

Locally available river sand conforming to Zone II of IS: 383-1970 was used. The physical properties and sieve analysis of river sand were tested according to IS: 2386 (Part I-IV)-1963, and the test results are tabulated in Tables 3.5 and 3.7.

3.1.6 Precious Slag (PS) ball

PS ball procured from Ecomaister Beads Hospet, Bellary, India. The PS ball was black in color, having a spherical shape, free from CaO and Fe$_2$O$_3$, making it non-reactive

material. The material passing through 4.75 mm sieve was considered as fine aggregate in the present study. The image of the PS ball is depicted in Fig. 3.3. The physical and chemical properties of PS ball are as tabulated in Tables 3.5 and 3.6. Gradation of PS ball falls in zone-1 as per IS: 383-1970, and the results are tabulated in Table 3.

Fig. 3.3 Precious Slag (PS) ball

Table3.5 shows the physical characteristics of the river sand and PS ball. Chemical composition of PS ball is tabulated in Table 3.6. Gradation of PS ball in depicted in Fig. 3.4. The PS Ball satisfies zone-1 gradation specified for the fine aggregates (IS 383-2002).

Table 3.5 Physical Properties of fine aggregates

Sl. No	Test	River sand	PS ball	Method of Test
1	Specific Gravity	2.62	3.45	IS 2386 (P-III) -1963
2	<u>Bulk Density</u> a) Dry loose	1472 kg/m^3	2219 kg/m^3	IS 2386 (P-III) -1963
	b) Dry compact	1541 kg/m^3	2376 kg/m^3	
3	Water Absorption	0.78%	0.03%	IS 2386 (PIV)-1963

Table 3.6 Chemical composition of PS Ball

Chemical constituent	Percentage (%)
CaO	29.99
Al_2O_3	11.24
Fe_2O_3	32.95
SiO_2	18.32
MgO	6.13
SO_3	0.058
Na_2O	0.29
K_2O	0.16

Table 3.7 Gradation of coarse and fine aggregates

Fine aggregates				Coarse aggregates			
Sieve No (mm)	IS:383-1970 requirement	River sand (%)	PS ball (%)	Sieve No (mm)	IS:383-1970 requirement	Passing (%)	
						Crushed granite	Steel slag
10	100	100	100	20	95-100	98	96
4.75	90–100	98.5	99.3	10	25-55	40	42
2.36	75–100	95.4	87.4	4.75	0-10	5	2
1.18	55–90	71.5	50.5				
0.6	35–59	47	17.5				
0.3	8–30	12	2.7				
0.15	0–10	3.1	0.2				
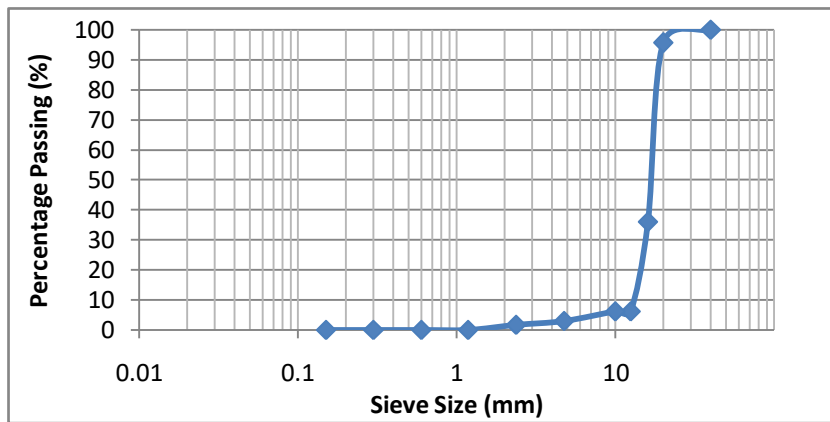
Figure 3.4 Gradation of PS ball

38

The details of the experiments conducted along with the test sequence are depicted in a flow chart (Figure 3.5).
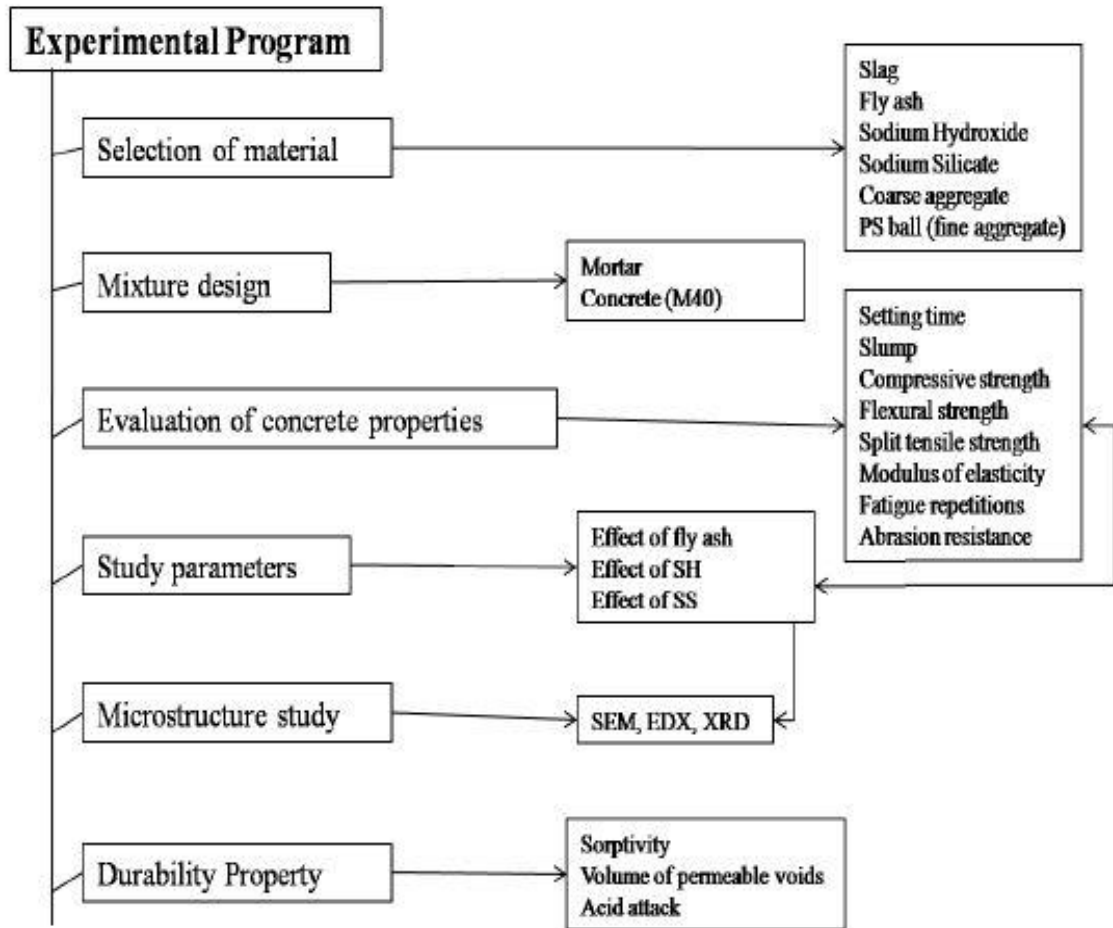
Figure 3.5 Flowchart of the experimental program

3.2   TEST METHODS

After proper mixing of the ingredients, the specimens are prepared to test the hardened and durability properties of concrete. All the tests were conducted as per the relevant standard codes. The mixtures were tested for the modulus of elasticity, abrasion resistance, flexural strength, and fatigue.

Fig. 3.6 Alkali activated samples kept for air curing.

Fig. 3.7 Concrete cubes after casting and demoulding

3.2.1 Flexural Strength Test

The flexural strength was conducted on test prism of dimension 100mm x 100mm x 500mm over an effective span of 400mm under two symmetrical load points spaced at 1/3rd of the span. The rate of loading was kept at 0.8-1.2 MPa/min. The test was carried out as per IS 516:1959 (ASTM C 78-94, BS 1881 Part 118: 1983) guidelines. The theoretical maximum tensile stress reached the bottom-most fiber of the test beam is known as flexural strength or modulus of rupture. Fig. 3.8 depicts the experimental setup

of the flexure test. If the fracture occurs within the central one-third portion of the beam, the modulus of rupture is calculated on the basis of an elastic theory of bending and is equal to

$$f_r = \frac{PL}{bd^2} \qquad \text{--- (3.1)}$$

Where f_r =modulus of rupture in N/mm^2, P = Maximum load on the beam in Newton, L = Span in mm, b = Width of a beam in mm, d = Depth of beam in mm.

If a fracture occurs outside the load points at a distance 'a' from nearest support, the modulus of rupture is given by

$$f_r = \frac{3Pa}{bd^2} \qquad \text{--- (3.2)}$$

Where 'a' = distance of fracture point from nearest support in mm

Figure 3.8 Flexure test set up

3.2.2 Modulus of Elasticity

The modulus of elasticity of material under compression or tension is given by the slope of the stress-strain relationship of concrete under uniaxial loading. The cylindrical specimen of 150mm in diameter and 300mm height was tested. Young's modulus (E) describes tensile elasticity, or the tendency of an object to deform along an axis when opposing forces are applied along that axis. It is the ratio of tensile stress to tensile strain. The test for Modulus of Elasticity was conducted as per IS 516:1959. Fig. 3.9 shows the experimental setup of the Modulus of elasticity test.

Figure 3.9 Modulus of elasticity test set up

3.2.3 Abrasion resistance

The abrasion resistance test was performed as per IS 9284:1979 on a cube specimen of 10 cm size using a pneumatic sandblasting machine with the operating condition of air pressure of 0.14 N/mm^2, 4000g of the abrasive charge passing 10mm and retained on 0.5mm IS sieve. The revolving disk type abrasion resistance test set up is depicted in Figure 3.10. The test is repeated on the other three surfaces after the sample is made to rotate by 180^0 in the horizontal plane till two impressions are made on the surface. Then the sample is removed by cleaning its surface and weighed.

Figure 3.10 Revolving disk abrasion test set up

3.2.4 Flexural Fatigue Test

Flexural fatigue tests on alkali-activated concrete samples were carried out on beam specimens of dimensions 100x100x500 mm using MTS servo-controlled hydraulic repeated load testing machine having a capacity of 5 tonnes. The equipment used in this study was manufactured by M/s Spranktronics, Bangalore, India. The loading system includes a double-acting hydraulic cylinder with suitable mounting flanges. It is associated with a power pack unit consisting of a pump coupled with a motor (1 HP, 3-phase, 1440 rpm), valves and filters, a heat exchanger (cooling system), servo valve, pressure gauge, etc. A load sensor device was used to sense the applied load to the specimen during testing. The load cell used for testing was of capacity 50 kN (5000 kg). The loading is generally with half sinusoidal waveform (zero -maximum load-zero). The application frequency can be between 1-5 Hz with or without a rest period. The servo

amplifier system is used to link the function generator and the servo valve. The Control Unit is used to monitor the load and the repetitions. It is connected to the PC with an ADD ON card to acquire or log the data.

The flexural test of all samples was carried out before starting this test. The flexural load corresponding to flexural strength to 4.5MPa is kept constant for the study (i.e., the minimum value selected from the lot). The fatigue tests were conducted on alkali-activated mixtures containing 100% PS ball as fine aggregates. Three specimens were tested for each mix at each stress level.

The beam specimen was loaded at the same span (i.e., 400 mm) as it was loaded in case of static flexural tests. The specimens were subjected to loading using constant amplitude half sinusoidal waveform at a frequency of 3Hz without any rest period until the failure of specimen. In this study, the stress ratios were limited to 0.65, 0.75, 0.80, and 0.85 to obtain a relationship between different stress ratios (S) and the number of cycles (N). The Fatigue life (N) of the samples was recorded (i.e., the number of cycles up to failure).

Figure 3.11 Repeated load testing set up

3.3   SYNTHESIS OF ALKALI-ACTIVATED MIXTURE

The concentration of sodium hydroxide and SS/SH ratio has a significant influence on the strength properties of the alkali activated binders. For each type of binder, there exists an optimal NaOH concentration for which the mix attains the highest strength activated at constant sodium silicate content. Hence, it is necessary to identify the optimal activator modulus based on the strength requirement. Preliminary studies were carried out to determine the strength of AASC, and AASFC mixes at different NaOH concentrations (Molarity) and silicate content. Based on the results, the optimal NaOH concentration for different mixes was identified, and later these mixes were further optimized to identify the silicate content dosages to obtain the required strength. According to the Indian standard code IRC: 58:2002, Pavement Quality Concrete (PQC) should have a minimum compressive strength of M40 and a slump value in the range 25-50 mm.

Preliminary mix design was carried out for AASC, and AASFC mixes to identify the optimal NaOH concentration to achieve the desired strength grade of M40 with slump value in the range 25-50 mm. The AASC and AASFC mixes were prepared using binder content of 443 kg/m³with alkaline liquid to binder ratio (al/b) of 0.35. In the case of AASC, 100% GGBFS was used as a binder, while in case of AASFC, GGBFS: FA in the ratios 90:10, 80:20, 70:30 and 60:40. The mixes were activated at sodium hydroxide (molarity) dosages of 8M, 10M, 12M, and 14M, and the SS/SH ratio was varied between 1 to 2. The NaOH concentration for which the mix attained the maximum compressive strength was considered for further optimization for determining the sodium silicate dosage as per the desired strength. Cube specimens of size 100 mm were prepared and tested for compressive strength after 28 days of air curing. The workability tests, i.e., the ease of compaction, was also determined using the slump tests, as it would help to carry out water content correction based on the required slump and the strength of the mixes.

3.4   Mixture design

The mixture proportion involves various factors influencing the mix design. A conventional mix design procedure is not applicable to alkali-activated material, and no standard mix design is available. The reactivity and chemical composition of the source material and alkaline-activator type are the two major contributors to the properties of alkali-activated materials. Apart from effective reaction kinetics between binder particle and activator solution is primarily dependent on the curing regime (temperature, curing period, and relative humidity).

However, it is very difficult to generalize the concept of mix design for alkali-activated concrete, considering the alumina-silicate source, activator concentration, and its chemical composition. Hence, by trial and error method, the final mix will be obtained. The detailed procedure is explained in Appendix-1. The mix proportions adopted for various combinations of mixes are tabulated in Tables 3.8 and 3.9.

Table 3.8 Details of Mix Proportions of AASC mixes (kg/m^3)

Mix ID	SS/SH ratio	Molar	Slag	SH	SS	PS ball	Sand	Coarse aggregate
M-8	1	8	443	66.5	66.5	657	--	1167
M-10	1	10	443	66.5	66.5	657	--	1167
M-12	1	12	443	66.5	66.5	657	--	1167
M-14	1	14	443	66.5	66.5	657	--	1167
N-8	1.5	8	443	53	80	657	--	1167
N-10	1.5	10	443	53	80	657	--	1167
N-12	1.5	12	443	53	80	657	--	1167
N-14	1.5	14	443	53	80	657	--	1167
P-8	2	8	443	44	89	657	--	1167
P-10	2	10	443	44	89	657	--	1167
P-12	2	12	443	44	89	657	--	1167
P-14	2	14	443	44	89	657	--	1167
C-8	1	8	443	66.5	66.5	--	657	1167
C-10	1	10	443	66.5	66.5	--	657	1167

Where SS- Sodium Silicate, SH- Sodium Hydroxide and PS ball- Precious Slag ball

Table 3.9 Details of mix proportions of AASFC mixes

Mix ID	Slag/fly ash	SS/SH ratio	Molar	Al/B ratio	Slag	Fly ash	SH	SS	PS ball	Sand	Coarse aggregate
A-8	90/10	1	8	0.35	399	44	66.5	66.5	657	--	1167
A-10	90/10	1	10	0.35	399	44	66.5	66.5	657	--	1167
A-12	90/10	1.5	12	0.35	399	44	53	80	657	--	1167
A-14	90/10	1.5	8	0.35	399	44	53	80	657	--	1167
A-16	90/10	1.5	10	0.35	399	44	53	80	657	--	1167
B-8	80/20	1	8	0.35	354	89	66.5	66.5	657	--	1167
B-10	80/20	1	10	0.35	354	89	66.5	66.5	657	--	1167
B-14	80/20	1.5	8	0.35	354	89	53	80	657	--	1167
C-8	70/30	1	8	0.35	310	133	66.5	66.5	657	--	1167
C-10	70/30	1.5	10	0.35	310	133	53	80	657	--	1167
C-14	70/30	2	8	0.35	310	133	44	89	657	--	1167
D-8	60/40	1	8	0.35	266	177	66.5	66.5	657	--	1167
D-10	60/40	2	10	0.35	266	177	44	89	657	--	1167
D-14	60/40	2	8	0.35	266	177	44	89	657	--	1167
M-8	90/10	1	8	0.35	399	44	66.5	66.5	--	657	1167
M-10	80/20	1	10	0.35	354	89	66.5	66.5	--	657	1167

Where SS- Sodium Silicate, SH- Sodium Hydroxide, Al/b ratio- Alkaline liquid/ binder ratio and PS ball- Precious Slag ball

3.4.1 Preparation of aggregates

Initially, the coarse aggregates are soaked in water for 24 hours and later air-dried. The soaking of fine aggregate is avoided to retain finer particles. The sand was air-dried before usage as per ASTM C 128-7.

3.4.2 Preparation of the alkaline activator solution

SH solution was prepared one day prior to mixing and allowed to cool to room temperature and then stored in an air-tight container. For the alkali solution, both SH and SS solution were mixed together. An exothermic reaction is evolved during mixing, liberating heat; hence, it is allowed to cool before adding to dry ingredients. The final alkali-activator solution was prepared at least 30-60 minutes before to final mixing with the dry ingredients.

3.4.3 Final mixing of concrete

The mixing was done in a 120-liters capacity ribbon type concrete mixer. The concrete mix was done in accordance with IS 10262:2009.

The steps adopted are as follows:

- The concrete mixer should be cleaned thoroughly before using it. The inner surface of the pan was moistened slightly to minimize the interaction of water from the mixture.
- First, the coarse aggregate was loaded to the mixing pan then followed by sand; and mixed thoroughly for 2-3 minutes.
- Then binders (slag and slag-fly ash blend) were added and thoroughly mixed for about 2-3 minutes before the addition of alkali-activator solution.
- Premixed activator solution was added gradually, while the mixing of raw material was in progress. Mixing was continued for another 3-5 minutes to get a homogenous mixture.

3.4.4 Casting and curing of samples

Before casting, all concrete moulds were checked for the presence of any foreign materials. The inner surfaces of moulds were cleaned and oil-greased. Test samples were cast soon after mixing. The moulds for compression, abrasion resistance

(150x150x150mm), and flexure tests (100x100x150mm) were filled in two-layers, whereas for split tensile and modulus of elasticity tests (cylinder of 150mm diameter 300mm height) were filled in three-layers. After pouring the concrete, it is compacted using a vibratory table. The compaction effort was continued until the voids are expelled out, aggregates were submerged in a mortar, and the top surface was leveled with a trowel. The concrete moulds were stored at 22-25^{0}C with a relative humidity of 55± 10%.

SUMMARY

Preliminary investigations are carried out to arrive at the optimized mix design. The dosage of sodium hydroxide, optimal silicate content and water content for different binder types was identified as per the strength (M40) and workability (slump value of 25-50 mm) requirements. The AASC and AASFC mixes were prepared using binder content of 443 kg/m^3 with alkaline liquid to binder ratio (al/b) of 0.35. In case of AASC, 100% GGBFS was used as the binder; while in case of AASFC, GGBFS: FA in the ratios 90:10, 80:20, 70:30 and 60:40 were used as binders. The preparation of the concrete specimen, properties investigated, the test methodologies followed for testing specimens are also explained in detail here. The results and discussion will be elaborated in chapter-4.

CHAPTER 4

ALKALI ACTIVATED SLAG CONCRETE

4.0   INTRODUCTION

In this chapter, the test results of AASC mixes by complete replacement of river sand with PS ball, both in the fresh and hardened state, are discussed. The workability and setting time, compressive strength, split tensile strength, modulus of elasticity, flexural strength, fatigue behavior, and abrasion resistance were discussed in detail. Weibull distribution and analysis is carried out to determine the fatigue response of AASC mixes.

4.1   WORKABILITY

A slump of around 25 ± 15mm was aimed. The workability results of AASC mixes are depicted in **Fig. 4.1**. The workability of mixes decreased with the increased molar concentration of NaOH. The workability of 8M specimen is found to be higher when compared to the 10, 12, and 14M. The decrease is due to increased viscosity of the activator solution. For M-series 8M, 10M, 12M, 14M, the workability was reduced gradually by 55, 49, 43, 38mm, respectively. For N-series, slump value decreases by52, 45.5, 39.5, 34.5mm for N-8, N-10, N-12, and N-14, respectively, as compared to the M-8 of 55mm. In P-series, the slump decreases by 48, 41.5, 35, 30mm for P-8, P-10, P-12, and P-14, respectively, as compared to N-8 of 52mm.

The effect of molar concentration of sodium hydroxide is most obvious with high silicate. The workability of AASC mixes decreased with the increase of the SS/SH ratio, where the viscosity of AASC mixes tends to increase, results in lower workability. Conversely, the increased molar of NaOH enhanced the viscosity by draining the silica and alumina mineral from the source material, which decreases the workability; a similar trend was observed by Rattanasak and Chindaprasirt (2009). For the mix with lower

NaOH content SS/SH=1.5 and 2, the workability was influenced by the soluble silicate concentration.
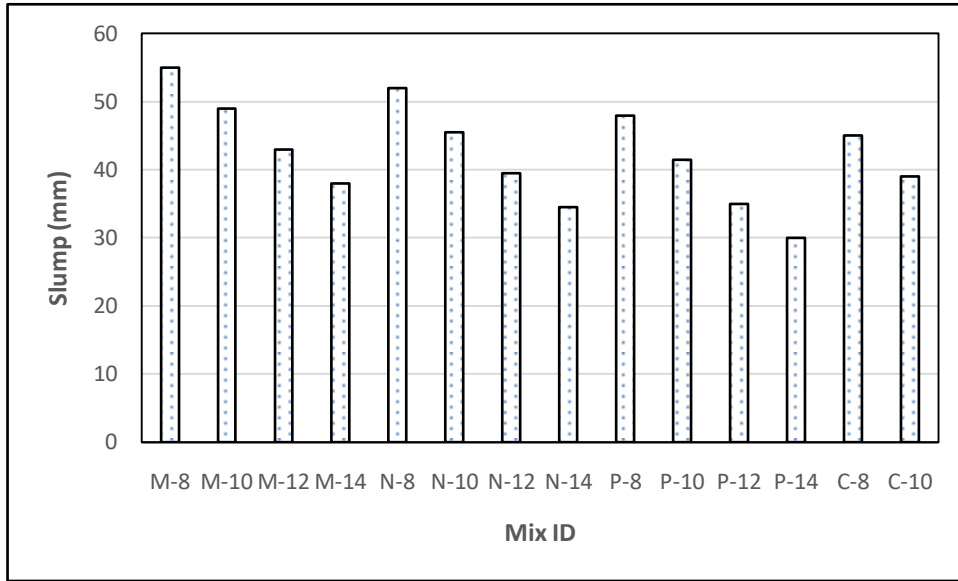

Figure 4.1 Workability of AASC mixes

4.2 SETTING TIME

Setting time was affected by the increased concentration of NaOH, the reaction mechanism controlled by the polymerization and the calcium mineral present in the binder governs the setting time; a similar trend was observed by Fernández-Jiménez et al. (2003). Fig. 4.2 depicts the variation of setting time with variation in NaOH concentration. M-series had an initial setting time of 54, 59, and 62, 49 minutes, final setting time of 103, 112, 117, 92 minutes for M-8, M-10, M-12, and M-14, respectively. While N-series had an initial setting time of 47, 52, 58, 43minutes, final setting time of 89, 99, 110, 82minutes for N-8, N-10, N-12, N-14, respectively. The P-series had an initial setting time of 49, 47, 55, and 40minutes and final setting time of 83, 89, 94, 75minutes for P-8, P-10, P-12, P-14, respectively. An increase in SS/SH ratio from 1 (M-series), 1.5 (N-series), and 2 (P-series) indicates that the dissolute silica content was increased with the increase of SS/SH ratio. Higher content of dissolute silica would

enhance the alkali activation process and reduce the time to complete the dissolution reaction resulting in the decrease of setting time.

Initial setting time of 54, 47, 49 minutes, final setting time of 103, 89, 83 minutes for M-8, N-8, P-8, respectively, were observed. Whereas, for 10M, the initial setting time of 59, 52, 47 minutes, final setting time of 112, 99, 89minutes for M-10, N-10, P-10 respectively were observed. The 12M specimens had a relatively higher initial setting time of 62, 58, 55minutes, the final setting time of 117, 110, 94 minutes for M-12, N-12, P-12, respectively, was observed.
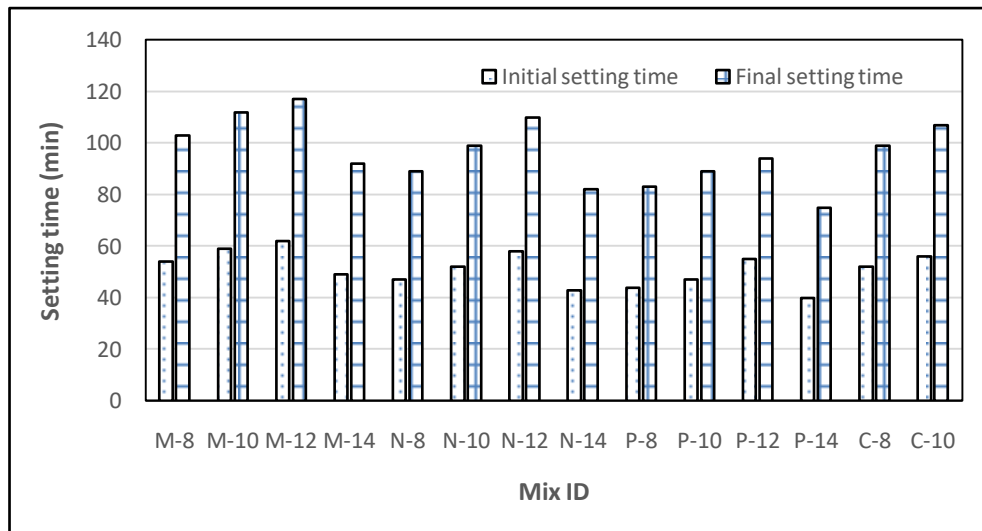

Figure 4.2 Setting time of AASC mixes

4.3   COMPRESSIVE STRENGTH

The compressive strength test was conducted in accordance with IS 516:1999. The test results are depicted in Fig. 4.3. The increase in NaOH concentration enhances the strength of AASC blends. At a higher concentration of NaOH greater dissolution of the solid precursor material in the binders restrains the polymerization reaction; subsequently, there was an improvement in strength. The reason is being the silica and alumina having a more significant dissolution from the solid precursor minerals by the binders in the aqueous phase from 8M-12M. The reaction process is more effective in the

amorphous phase of binder molecules, which enhances the polymerization. Further, the increased NaOH beyond 12M results in excess hydroxyl ion concentration, which hinders the polymerization process. An increase in hydroxyl ion concentration that accelerates the dissolution of raw materials. It means that increasing the SH molarity would also affect the silica modulus (molar ratio of SiO_2/Na_2O) of the alkaline liquid, which would influence the alkaline process. Thus, a decrease in strength is observed for 14M mixes.
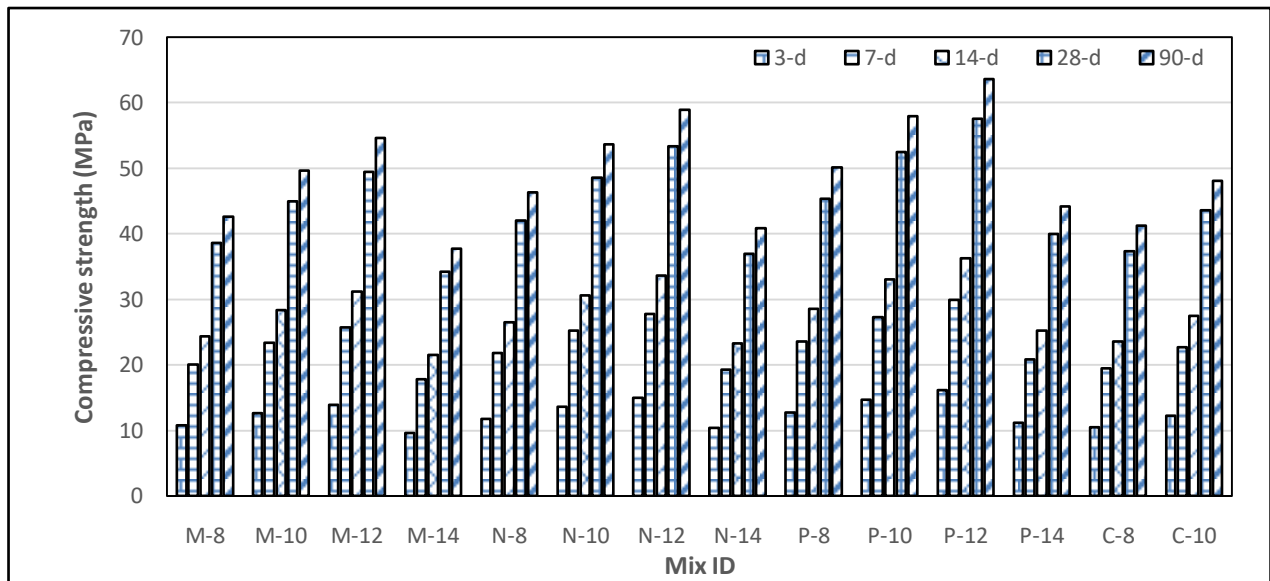

Figure 4.3 Compressive strength of AASC mixes

4.3.1 Effect of Sodium Hydroxide

It can be noted that an increase in the NaOH concentration from 8M-12M, the compressive strength gradually increased. Fig. 4.4 shows the effect of NaOH concentration on the compressive strength of AASC mixes. The 28-days compressive strength of AASC mixes with 8M NaOH increased by 3.11%, 1.95%, 17.62% for M-8, N-8, P-8, respectively, when compared to the control mix of C-8.Similarly, for 10M compressive strength was increased by 3.11%, 10.3%, 16.95% for M-10, N-10, P-10,respectively, compared to the control mix of C-10. For 12M NaOH, strength was increased by 7.3%, 14.1%, for N-12, P-12, respectively, when compared to the M-12 mix.The14M results in a gradual drop in the compressive strength due to excess hydroxyl

ion concentration. This affected the polymerization reaction and hence decreased in strength was observed by 11.4% for M-14 compared to M-8, 11.92% for N-14 compared to N-8, and 11.89% for D-14 compared to P-8. By an increase in the molarity of NaOH from 8M-12M, the compressive strength gradually increases, which is due to the internal reaction of Ca, Al, and Si minerals causing the increased breakage of T-O-T bond into Ca-O and Si-O bonds in slag. At the higher NaOH concentrations, the leaching of alumina and silica was enhanced, which increased polymerization, leading to strength.
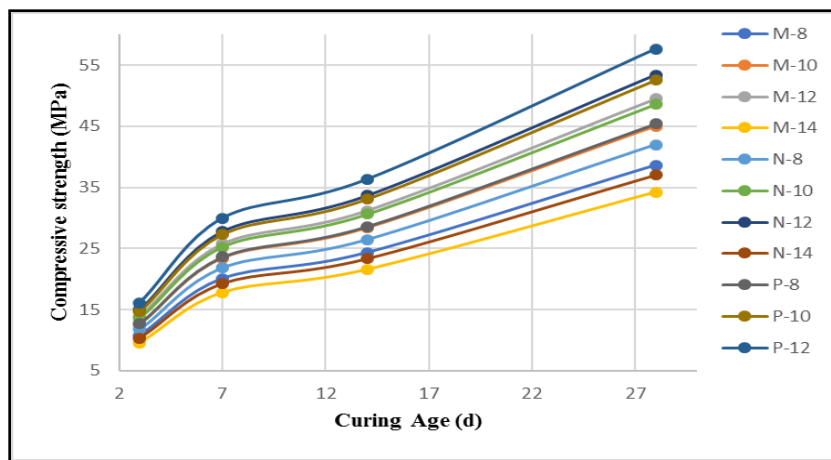

Figure 4.4 Compressive strength of AASC mixes with different NaOH concentration

4.3.2 Effect of Sodium Silicate

At SS/SH=1, the compressive was slightly higher than that of mixes with SS/SH=1.5 and 2 at 28-days of curing. The reduction in strength is due to the increased soluble silicate concentration in the activator solution influencing the polymerization reaction (Gao et al. 2014, Nath and Sarker 2014). Fig. 4.5 shows the compressive strength of AASC mixes with different SS/SH ratios of 1 (M-8, M-10, M-12, and M-14), 1.5 (N-8, N-10, N-12, and N-14), and 2 (P-8, P-10, P-12, and P-14). The 3 day compressive strength of AASC mixes with lower SS/SH ratio was slightly higher than that of specimens with a higher SS/SH ratio at later ages of curing (Lee and Van Deventer 2002).
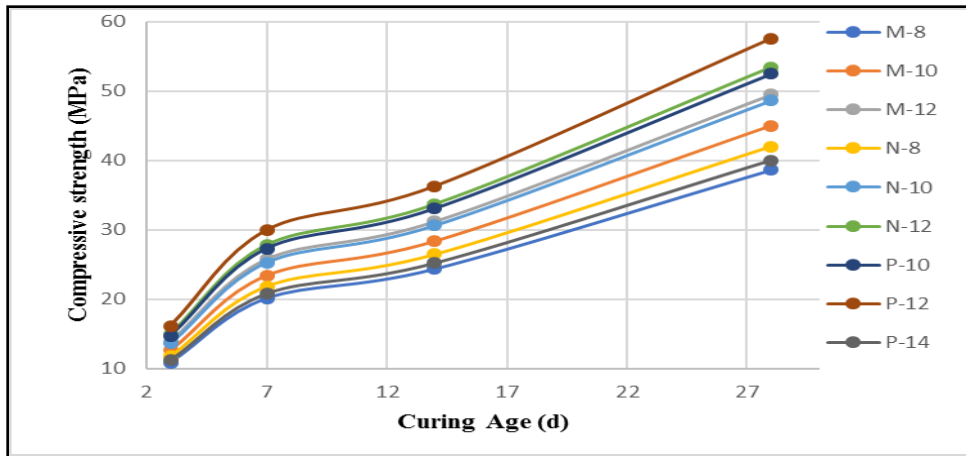
Figure 4.5 Compressive strength of AASC mixes with different SS/SH ratio

4.4   SPLIT TENSILE AND YOUNG'S MODULUS

It is evident that the split tensile strength of 28-days cured specimens with SS/SH=1 was lower than that of a series with the SS/SH=1.5 and 2. The split tensile tests were performed according to IS 5816-1999, and the results are shown in Fig. 4.6 for the various mixes at 28-days curing period. The geopolymer concrete produced with the higher hydroxyl ion content and silicate solution tends to have higher Interfacial Transition Zone (ITZ) strength due to lower porosity in the geopolymer mortar and the similar trend was observed by Lee and Van Deventer 2002.The availability of higher calcium compound in the AASC mix developed more CSH products by filling the void present in the alumina-silica complex resulting in increased strength; a similar trend was observed by Hanjitsuwan et al. (2014).

However, it is strongly affected by various influential parameters such as the chemical composition of alkaline liquid and source material, the molar concentration of NaOH and SS/SH ratio, alkaline liquid to binder ratio. When the NaOH concentration was increased from 8M to 12M, the split tensile strength increases by 14.22% and 22.1% for M-10 and M-14, respectively, decreases by 11% for M-14 compared to the M-8, similarly the split tensile strength increases by 13.58% and 21.35% for N-10 and N-12 respectively, decreases by 11.9% for M-14 compared to the N-8 and for P-10 and P-12

the increase in split tensile strength by 13.52% and 21.18% respectively, decreases by 11.9% for P-14 compared to the P-8. The split tensile strength increases from SS/SH=1 (M-8, M-10, M-12, and M-14) to SS/SH=2 (P-8, P-10, P12, and P14). The influence of NaOH concentration on the split tensile, compressive strength was found to be similar. Hardjito et al. (2015) and Diaz Loya et al. (2011) proposed the following equations 4.1 and 4.2 to determine the young`s modulus values.

$$Ec= 4834 \, f_t +5300 \quad …(4.1)$$

$$Ec = 4834 f_t \quad …(4.2)$$

Where,

E_c= Young's Modulus (MPa),

f_t= Splitting tensile strength (Predicted),

$f_t = 0.56\sqrt{f_c}$ (as per ACI 318R-92)

AASC mixes produced with a higher concentration of sodium hydroxide, and sodium silicate tends to have higher Interfacial Transition Zone (ITZ) strength due to lower porosity in the concrete mixture. A similar trend was observed by Lee and Van Deventer (2002). Availability of high calcium content from source material developed more CASH product by filling the void present in alumina-silica complex resulting in increased strength observed for the mixes of 8M, 10M, and 12M.

AASC mixes were tested for modulus of elasticity according to IS 516:1959 after 28-days cured samples, and the results are shown in Fig. 4.7. The static elastic modulus of AASC mixes steadily increases with an increase in molar concentration of NaOH increased from 8M to 12M.
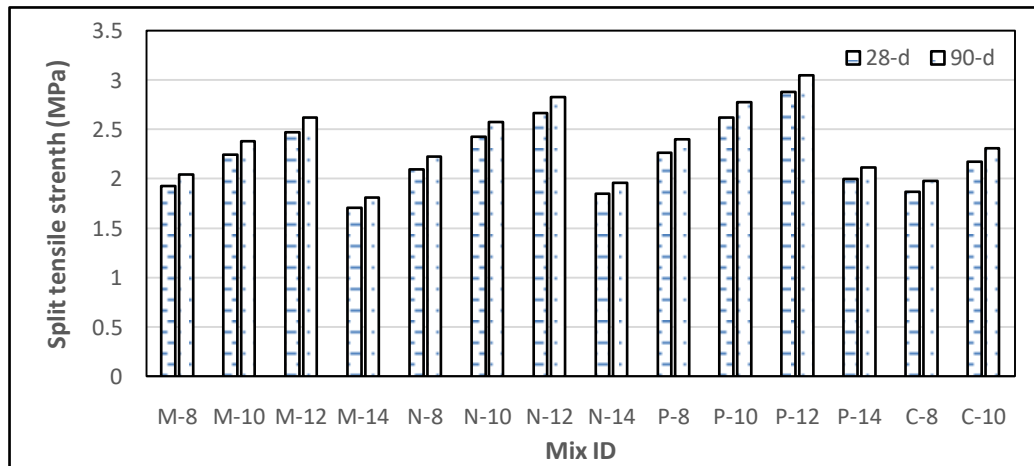
Figure 4.6 Split tensile strength of AASC mixes.

Figure 4.7 Modulus of elasticity of AASC mix.

4.5   FLEXURAL STRENGTH

The flexural strength was determined as per IS 516:1959. The static type flexural strength tests were conducted for 28-days of cured samples, and the results are depicted in Fig. 4.8. It is observed that the higher alkaline concentration in AASC mixes increases the flexural strength at 28-days curing; only M-12, N-10, N-12, P-10, and P-12 mixes

achieved the minimum strength requirement of 4.5 MPa. It can be noted that by increasing the molarity of sodium hydroxide from 8M to 12M, the flexural strength increases and sh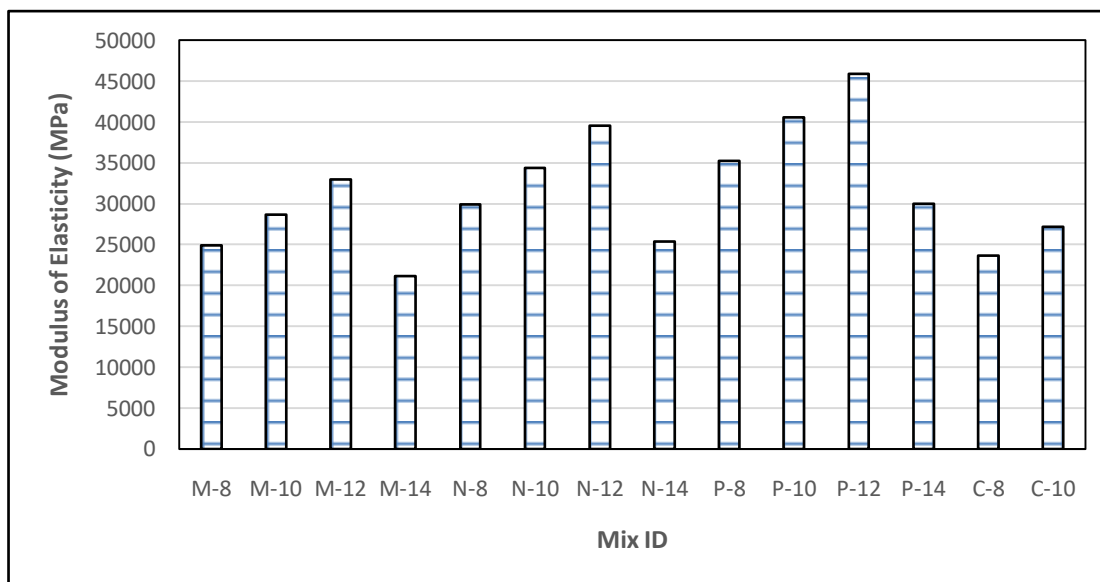ows the same phenomena observed in compressive strength. The molar concentration beyond 12M results in weaker ITZ due to excess hydroxyl ion concentration; hence decrease in strength is observed.

The flexural strength of AASC mixes increased by 14.22% and 22.02% for M-10 and M-12 respectively, and decreases by 11.4% for M-14 compared to the M-8 mix. Similarly, for N-10 and N-12 mixes, the flexural strength of AASC mixes increase by 13.6% and 21.35%, respectively, and decreased by 11.9% for N-14 compared to the mix N-8. The mix for P-10 and P-12, the flexural strength increased by 13.5% and 21.1%, respectively, and decreased by 11.88% for P-14 when compared to the mix P-8. The effect of the SS/SH ratio on flexural strength was more pronounced, and it was observed for M-P-series in Fig 4.8.
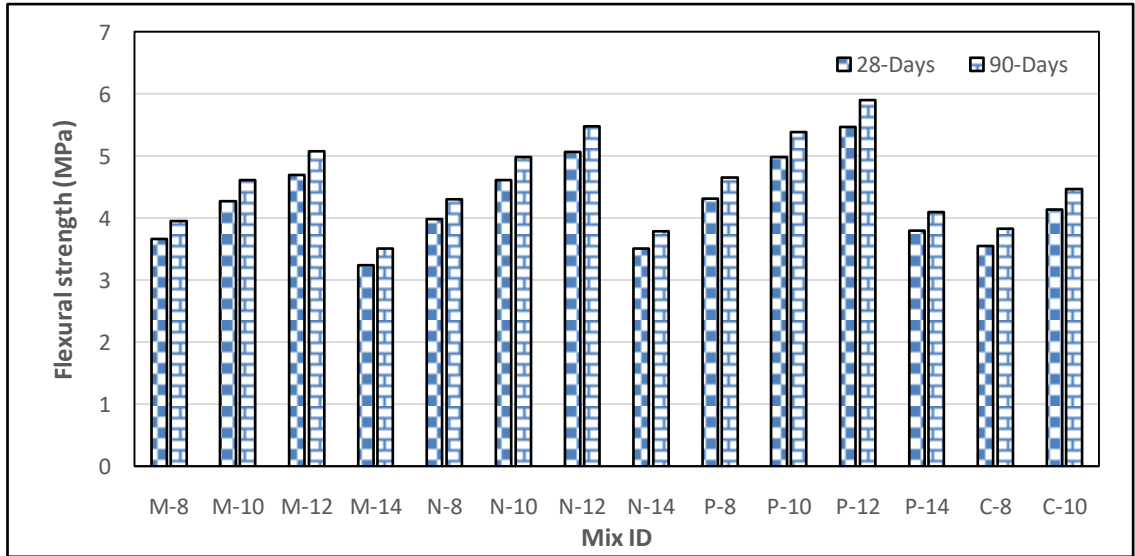

Figure 4.8 Flexural strength of AASC mixes.

4.6   FATIGUE BEHAVIOR

In the present study, the flexural fatigue performance of AASC and AASFC mixes incorporating 100% (by volume) PS ball as fine aggregate was investigated. The specimens were subjected to different stress ratios (0.60, 0.75, 0.80, and 0.85) and the number of cycles for failure of the specimen at each stress ratio was determined. A probabilistic analysis of fatigue test data was carried out to ascertain the fatigue life of the material.

The fatigue life of AASC mixes represented by the S-N curve, where the Stress ratio (S) versus No. of cycles (N) plots for fatigue life analysis is shown in Figs. 4.9-4.11. The statistical equation obtained from the S-N curve may be applied for predicting the fatigue life cycle at the required stress level. The specimens which have passed minimum flexural strength were selected for the fatigue life analysis, i.e. (M-12, N-10, N-12, P-10, and P-12). The AASC mixes SS/SH= 2, indicating a strong bond of ITZ between the mortar and aggregate matrix, preventing the early crack initiation and its propagation towards the inner structure of concrete compared to the mixes with SS/SH=1. The AASC mixes reported a reasonably good fatigue life cycle compared to the control mixes as shown in Figs. 4.9-4.11.

As the fatigue test data of concrete shows a considerable scatter and is random in nature, a probabilistic approach can be introduced for analyzing the fatigue data and evaluating the probability of unfavorable performance. The fatigue life data at a given stress level were arranged in ascending order of cycles to failure. The empirical survivorship function $L_N(n)$ for each fatigue life data ranked in the order of number of cycles to failure; at a given stress level is calculated using mean rank. The fatigue life (N), i.e., the number of cycles up to failure for AASC mixes with PS ball slag aggregates are shown in Figs. 4.9 to 4.11. The equations obtained from the S-N curves can be utilized for the estimation of fatigue cycles at any stress level. The statistical correlation ranging from 0.978- 0.991 for AASC mixes, indicating good correlation together with significant of fatigue life.

From Table 4.1 it can be noticed that the AASC mixes with 100% PS ball display higher resistance to fatigue failure as compared to natural aggregates, irrespective of the applied stress level. This may be due to the highly dense interfacial transition zone between the paste and the aggregate in alkali activated binders. The fatigue life of AASC mixes decreased with the lower concentration of NaOH and silicate content in the activator solution. This may occur due to a weak aggregate-paste interface (insufficient polymerization) that may lead to higher and faster propagation of the crack leading to earlier failure. It was observed that specimens exhibit lower fatigue life when subjected to higher stress ratios, while at lower stress ratios, specimens exhibited higher fatigue lives. The fatigue lives of all the concrete mixes satisfied the minimum fatigue cycles as recommended by IRC 58:2002. The failures of the specimens were visually examined and were found to have failed within the middle one third spans.

Table 4.1 Fatigue life of AASC mixes

Mix ID	Specimen no	Stress Ratio			
		0.85	**0.80**	**0.75**	**0.60**
		No of cycles to failure			
M-8	1	198	291	462	33567
	2	225	369	570	34647
	3	276	402	624	35187
M-10	1	237	330	555	33606
	2	264	408	609	34686
	3	315	441	663	35226
M-12	1	243	336	561	34152
	2	285	414	615	34692
	3	321	447	669	35232
N-8	1	267	360	531	34176
	2	294	438	639	34716
	3	345	471	693	35256
N-10	1	378	516	696	34617
	2	405	549	750	35256
	3	456	582	804	34497
N-12	1	483	621	747	33852
	2	510	654	855	34932
	3	561	687	909	35898
P-8	1	588	681	852	34497
	2	615	759	960	35577
	3	666	792	1014	35918
P-10	1	693	786	957	34602

	2	720	864	1065	35682
	3	771	892	1119	36023
P-12	1	834	927	1107	34680
	2	861	1077	1251	35874
	3	914	1257	1395	36128
C-10	1	132	225	396	33501
	2	159	270	504	34581
	3	210	336	558	35226

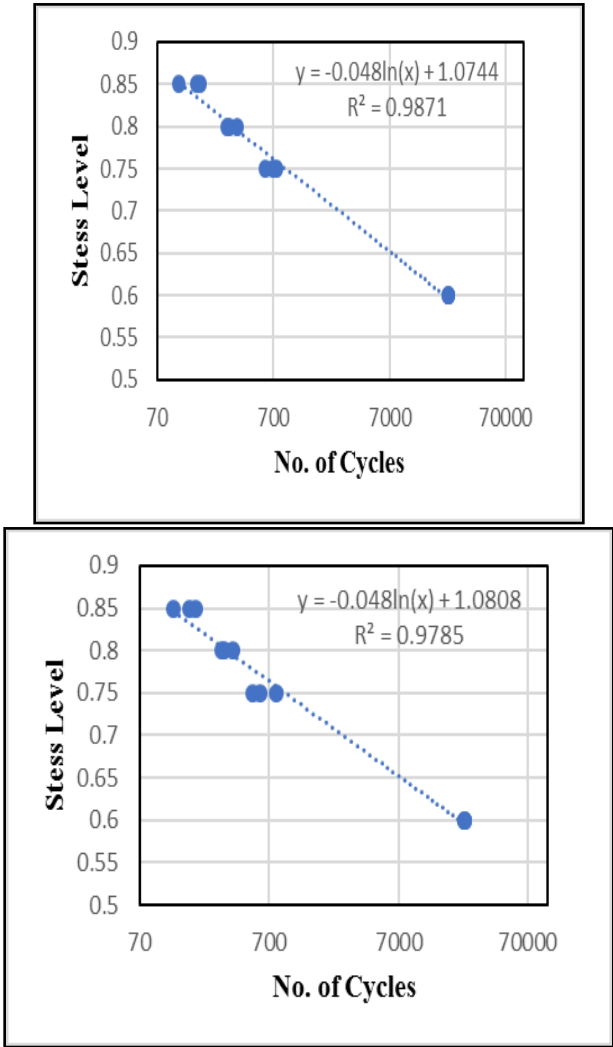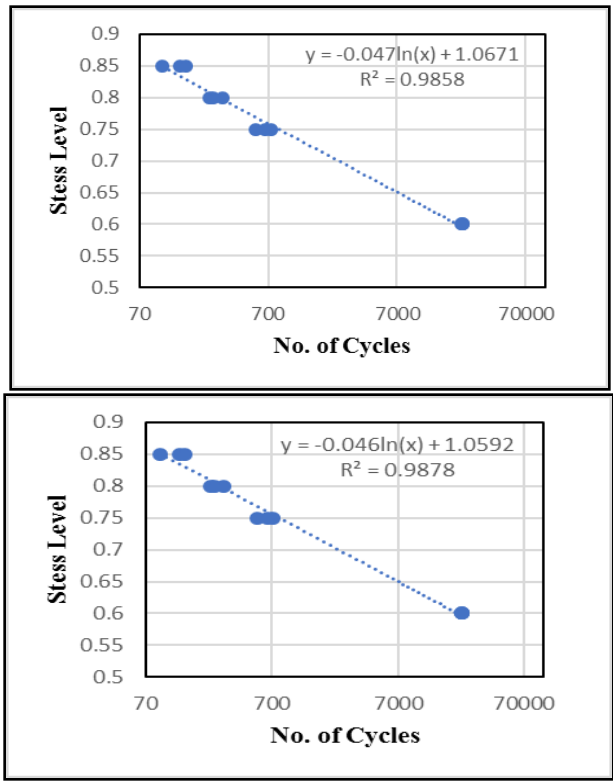**Figure 4.9** Fatigue life of AASC mixes, M-12 and N-10

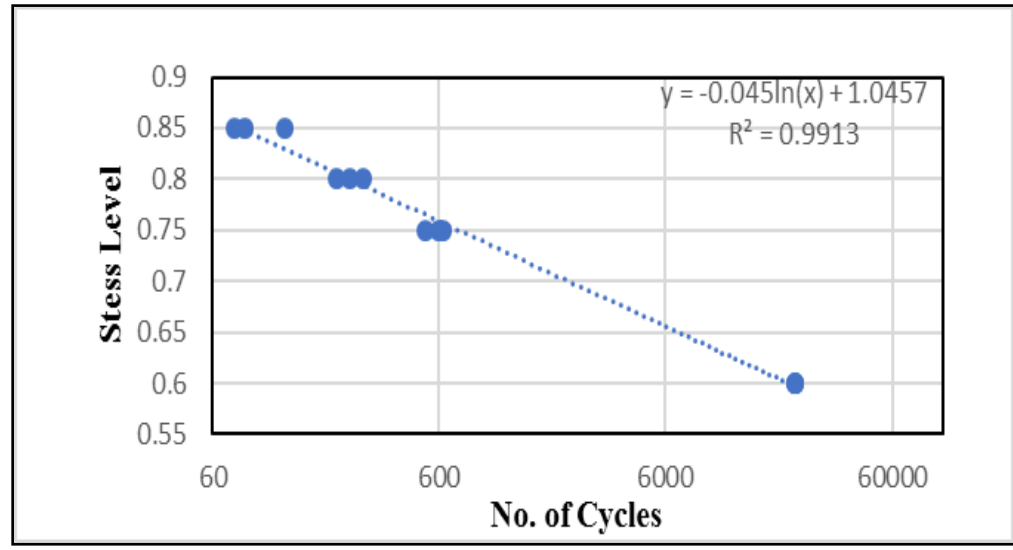**Figure 4.10** Fatigue repetitions of AASC mixes, N-12 and P-10

Figure 4.11 Fatigue life of AASC mix P-12

4.7 ABRASION RESISTANCE

The abrasion resistance test was performed as per IS 9284:1979, the influence of the sodium hydroxide and sodium silicate concentration on the abrasion resistance was analyzed for the series M, N, and P along with NaOH concentration of 8, 10, 12, and 14M. It can be observed from Fig. 4.12 that the increase in mass loss in the case of SS/SH=1.5 and 2 is very low when compared to the mixes with SS/SH=1. The decrease in weight loss observed with SS/SH=1.5-2, along with an increase NaOH concentration from 8M-12M when compared to the other mixes.

AASC mixes developed with 14M results in the excess hydroxyl ion concentration, hindering the polymerization process, which accelerates the dissolution of raw materials. An increase in the SH molarity would also affect the silica modulus (molar ratio of SiO_2/Na_2O) of the alkaline liquid, influencing the alkaline process. Thus, a decrease in abrasion resistance is observed for all 14M mixes. Variation of SS/SH ratio on strength may be attributed to the interaction between SS and SH. The increase in soluble silicate concentration leads to the formation of $Ca(OH)_2$ at the early stages of polymerization and by enhancing the C-A-S-H gel formation, which condenses the microstructure of concrete, results in decreased abrasion.

Abrasive weight loss of AASC specimen decreased by 5.35%, 17.85% for M-10, M-12, respectively, and increases by 12.5% for M-14 when compared to the M-8 mix. Similarly, for the N-10, N-12 abrasive weight loss decreases by 10.14%, 20.28%, respectively, and increases by 4.82% for N-14 when compared to the N-8 mix. The abrasive weight loss for P-10, P-12 mix decreases by 9.09%, 18.18%, respectively, and increase by 3.26% for P-14 when compared to the P-8 mix.
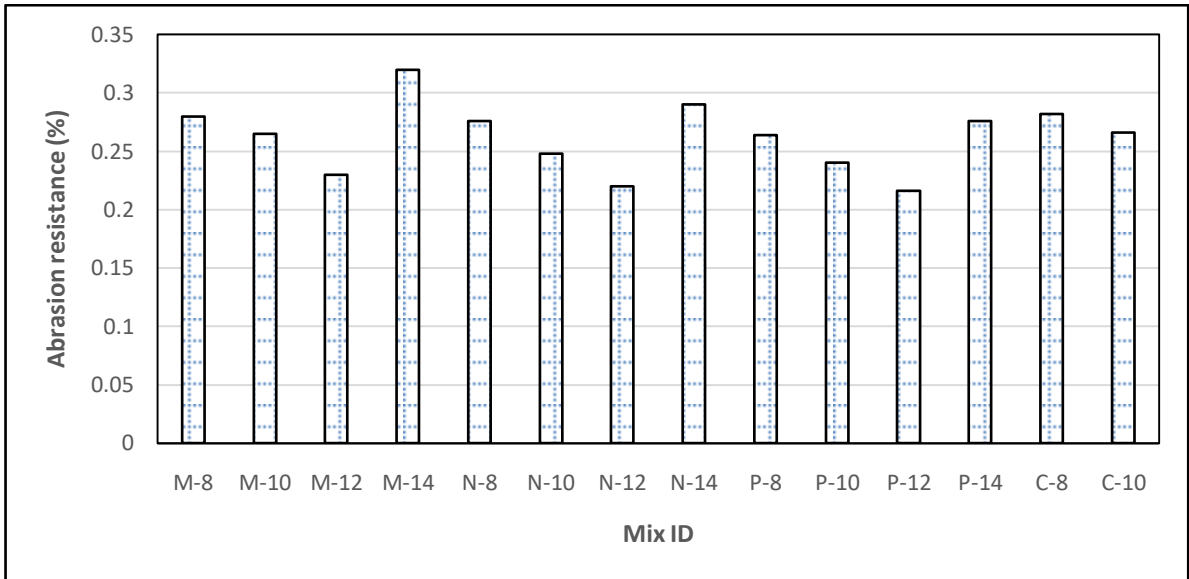
Figure 4.12 Abrasive resistance of AASC mixes

4.8 GRAPHICAL METHOD OF TWO-PARAMETER WEIBULL DISTRIBUTION

As the fatigue test data of concrete show considerable scatter and are random, a probabilistic approach can be introduced for analyzing the fatigue data. ASTM guidelines for fatigue testing and statistical analysis suggest that fatigue life follows a lognormal distribution. Further, experimental studies based on valid assumptions have shown that the distribution of fatigue life of concrete under given stress follows the Weibull distribution and is commonly employed in assessing the reliability of composite structures. A Weibull distribution is characterized by three parameters: 1) shape parameter (α), which describes the shape of the distribution, and 2) characteristic life or scale parameter (η). The probability density function F(t) and the cumulative distribution function f (t) may be expressed in the following terms, as given below.

$$F (t) = Q (t) = 1 - e^{\wedge}(-[t/\eta]\beta) \qquad \text{.......(4.3)}$$

After simplifying the above equation, we get,

$$\ln (\ln (1/ (1- Q (t))) = \beta \ln (t) - \beta ln(\eta) \quad …(4.4)$$

Where β=shape parameter and η= Characteristic life

Benards approximation used for calculating median rank by the following equation

$$f (t) = f (t) = \frac{(j-0.3)}{(n+0.4)} \qquad …(4.5)$$

Where j= failure order, n= sample size

Two-parameter Weibull distribution was employed in assessing the reliability to describe fatigue data. When the location parameter is said to zero (n_0=0), it reduces to two-parameter Weibull distribution. To estimate the parameters of the graphical distribution method was employed, and the results were depicted in Figs. 4.13 and 4.14. The value of the shape parameter was found to be more than 1 for the mixes, which indicates the progressive degradation of material strength after every repetition. Hence, the fatigue life of AASC mixes can be suitably described by two-parameter Weibull distribution.

Weibull parameter estimated was used to obtain the fatigue cycle of different series for various stress levels at survival probability of 5%, 50%, and 95%. Weibull Parameters of fatigue life at different stress levels is tabulated in Table 4.2, and calculated fatigue repetitions are depicted in Fig 4.15. It indicates that fatigue life is high at higher survival probability and fatigue life decreases as the survival ship decreases (or as the failure probabilities increase).

Figs. 4.13 and 4.14 shows the Graphical analysis of fatigue life for M-12 mixes under different stress level with statistical correlation coefficient value ranging from 0.815-0.993.This indicates that the two-parameter Weibull distribution is suitable for the statistical distribution of fatigue life at various stress levels for AASC mixes.
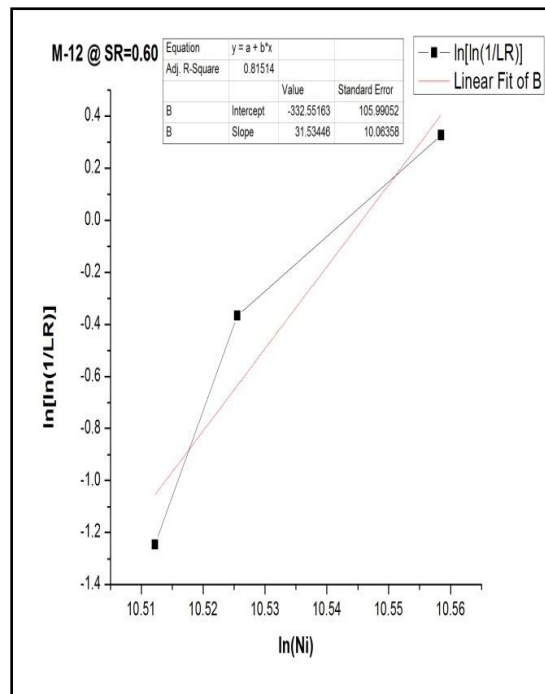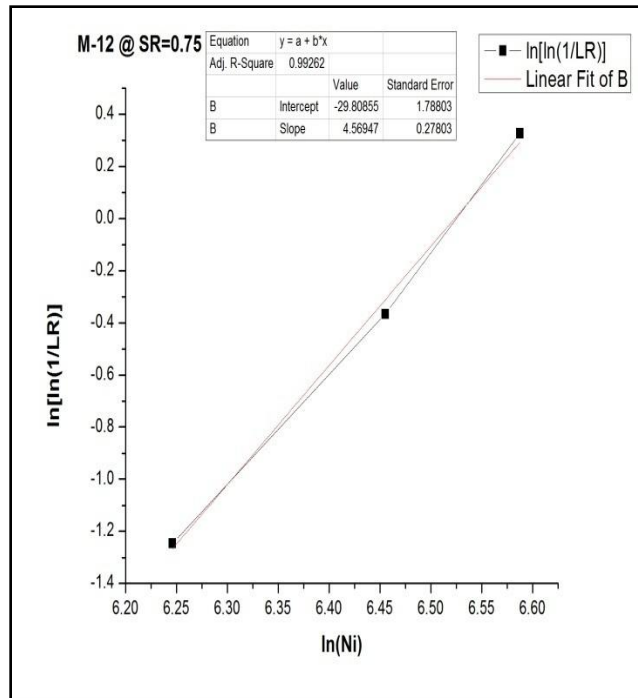
Figure 4.13 Graphical analysis of fatigue life for M-12 mixes at SR=0.60 and 0.75
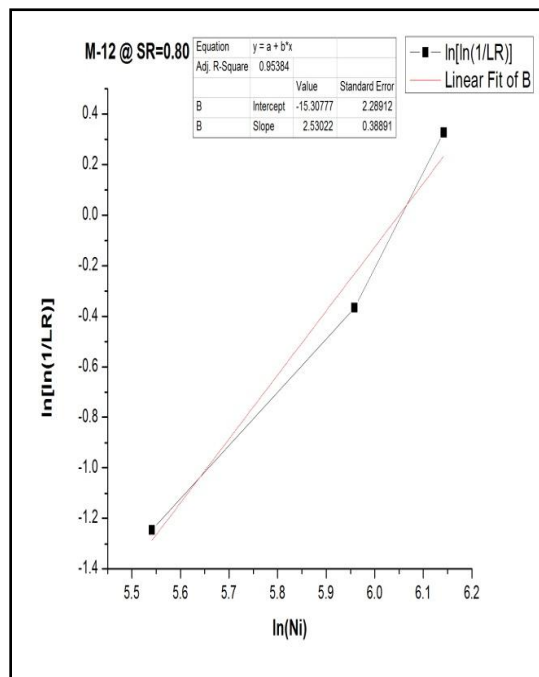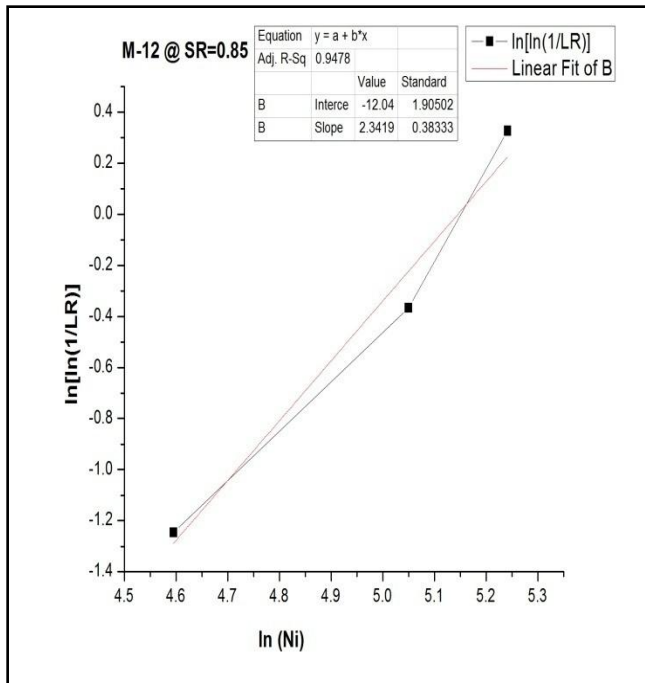
Figure 4.14 Graphical analysis of fatigue life for M-12 mixes at SR=0.80 and 0.85

Table 4.2 Weibull Parameters at different stress levels

Mix ID	Stress level	α	μ	R^2
M-12	0.6	31.534	38015.91	0.815
	0.75	4.57	680.6008	0.993
	0.8	2.53	424.7002	0.954
	0.85	2.34	171.6228	0.948
N-10	0.6	31.76	37916.29	0.82
	0.75	4.88	648.9852	0.993
	0.8	2.55	403.4288	0.953
	0.85	2.42	159.2138	0.951
N-12	0.6	31.96	38203.73	0.818
	0.75	5.33	704.3133	0.994
	0.8	3.1	434.499	0.96
	0.85	2.84	178.8629	0.957
P-10	0.6	32.116	38315.82	0.82
	0.75	5.7	732.5204	0.995
	0.8	3.36	499.8388	0.962
	0.85	3.13	195.3437	0.961
P-12	0.6	32.32	38538.23	0.82
	0.75	6.134	799.5556	0.995
	0.8	3.87	563.0302	0.966
	0.85	3.54	216.7037	0.964

Table 4.3 Calculated fatigue life lives corresponding to different failure probabilities (P_f= 5%, 50%, and 95%)

Mix ID	Survival Probability, L_n= (1- P_f)	Stress Level			
		0.85	0.80	0.75	0.60
M-12	0.95	250	620	813	39429
	0.5	137	349	602	37481
	0.05	47	126	353	34530
N-10	0.95	263	619	865	39538
	0.5	157	386	658	37768
	0.05	63	167	404	34813
N-12	0.95	274	655	865	39362
	0.5	146	367	628	37577
	0.05	48	131	355	34599
P-10	0.95	277	692	887	39646
	0.5	173	447	686	37880
	0.05	75	206	435	34930
P-12	0.95	294	747	955	39869
	0.5	195	512	753	38103
	0.05	93	261	492	35154

4.9 SEM ANALYSIS

Approximately 10-12gm of AASC specimen was collected after carrying out the compressive strength test for the cube specimen. The collected pieces of the concrete sample after compressive strength test were analyzed for microstructure analysis for M-12, N-10, N-12, P-10, and P-12 mixes. Figs. 4.15-4.16 distinctly show that activation of the slag particles has initiated more effectively at the higher alkalinity of the activator solution, i.e., at 10M and 12M mixes.

It can be observed from micrograms that the mixes at different stages of hydration having GGBFS shows small traces of gradually developing C-A-S-H products in stratified layers with a minimal number of un-hydrated particles. But the micro-cracks can be observed. The final dense microstructures developed in almost all of the mixes due to the complete activation of most slag particles in the presence of hydroxyl ions available from the activator solution. In some AASC mixes, products of alkali activation forming the dense clusters. The fully developed denser microstructures, preferably without accompanying micro-cracks/voids, are responsible for higher strengths of AASC mixes prepared at 12M.The magnification on a lower scale shows a denser microstructure; further magnification reveals the activation of the micro-slag particle with a negligible amount of un-reacted slag particles in the mix with the dark spots. The complete reaction of slag particles in Fig. 4.15 representing the white patches at different magnification levels.

However, a small irregular dark spot is distinctly visible in the lower magnification indicating the un-reacted slag particles. The final dense microstructures developed in almost all of the mixes that may be due to the complete activation of most of the slag particles. The increased molar concentration of NaOH along with silicate from activator solution and the silica available in source material condenses the microstructure of the AASC mix.
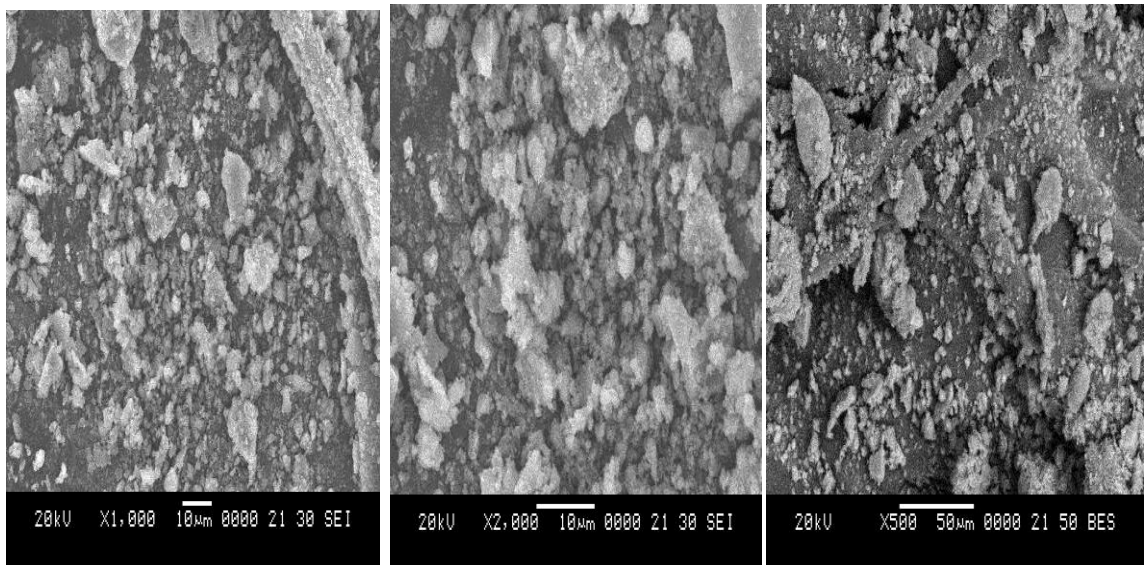
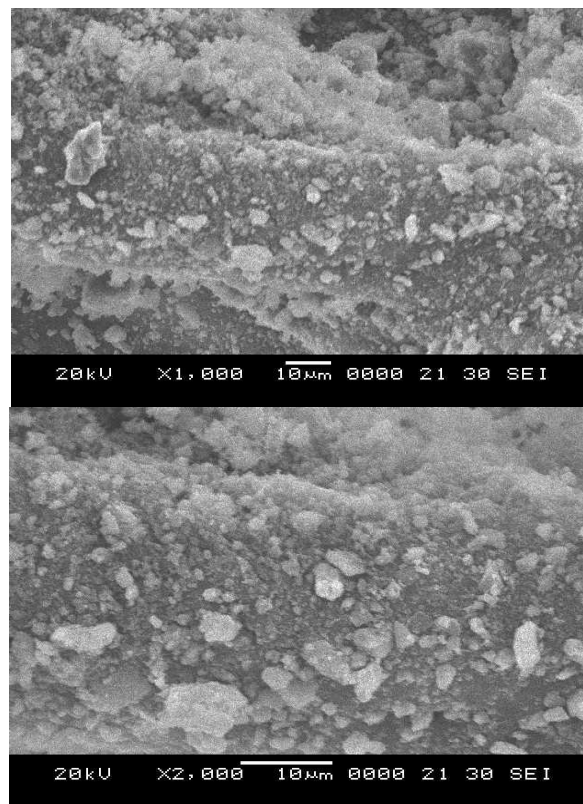**Figure 4.15** SEM Micrograms of Mixes, M-12, N-10 and N-12

Figure 4.16 SEM Micrograms of Mixes, P-10 and P-12

From Figs. 4.15 and 4.16, it is apparent that in a given sample, reacted slag particles are more in quantity as the molar concentration of NaOH and SS/SH ratio increases from 10M-12M and 1-2, respectively. The excess hydroxyl ion concentration due to increased molarity and soluble silica concentration from alkaline liquid enhances the polymerization reaction, a similar observation made by Nath and Sarker (2014). The increased NaOH concentration leads to adequate solubilization and accelerates the formation of CASH gel. Thus, an increase in strength is observed, since larger particles (>20 μm) do not react chemically, but become physically embedded in the glassy matrix.

4.10 XRD Analysis

Approximately 10-12gm of AASC specimen was collected after the compressive strength test from the specimen. The XRD patterns were obtained by scanning at a rate of two degrees per minute from 10^0-80^0 (2θ). A single letter was assigned to each phase to facilitate easier representation. Typical EDX-plots obtained for the AASC mixes M-10, M-12, N-10, N-12, P-10, and P-12 are shown in Fig. 4.17 and 4.18. In each of these plots, peaks that correspond to various elements like SiO_2, CASH, Calcite, and Hydrotalcite are seen, suggesting the presence of O_2, Ca, Si, Na, and Al elements in the mixes. The details of average atomic percentages measured over a small region in the microgram of the corresponding mix are obtained from the analyzer. Generally, the range of values of the three elemental atomic ratios – Ca/Si, Na/Si, and Al/Si governs the mechanical properties of the AASC mixes. Here, in the present set of high strength mixes, these ratios are predominantly in the narrow ranges, 0.67–0.75, 0.4–0.55, and 0.3– 0.4 respectively, for 12M mixes. While the corresponding low values of the three ratios (amongst the fifteen mixes) are 0.42, 0.29, and 0.22, respectively, for 10M mixes. Thus all the AASC mixes, the elemental order occur with mass-wise, in the order Si > Ca > Na > Al, which possibly as constitutes the formation of C-A-S-H gels.

Sharpening peak in the calcite region revealed a Quartz mineral, which indicates a continuous chain reaction of polymerization involved. Due to a more reactive form of the amorphous phase, there is an increase in the mechanical strength, which cannot be

determined by X-ray diffraction. It was observed that change in phases of the Quartz mineral due to its reaction with the hydroxyl ion indicating higher concentrations of NaOH enhances the reaction kinetics of the process, the sharp diffraction peak in the region 20^0-40^0, represents the occurrence of alumina-silicate glass complex with low ordered crystalline structure as the main reaction product, which is more reactive form with water compared to the glassy structure of silica compound and forming the compound of CASH, resulting in increased strength of the hardened concrete matrix.
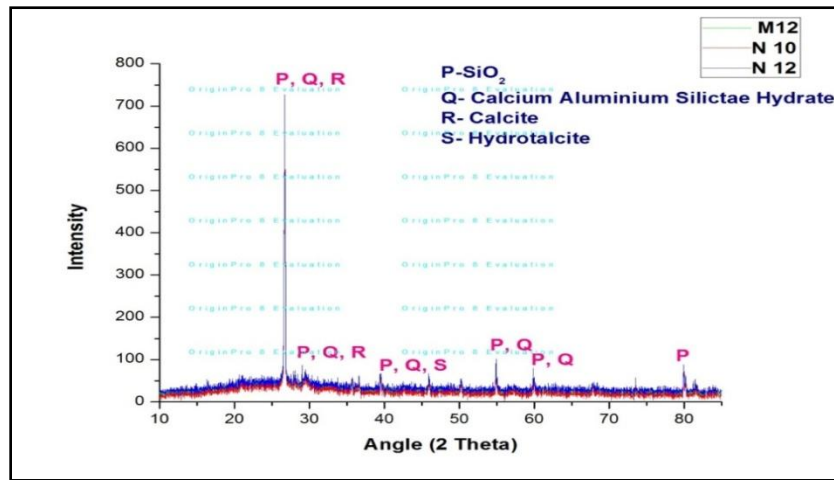

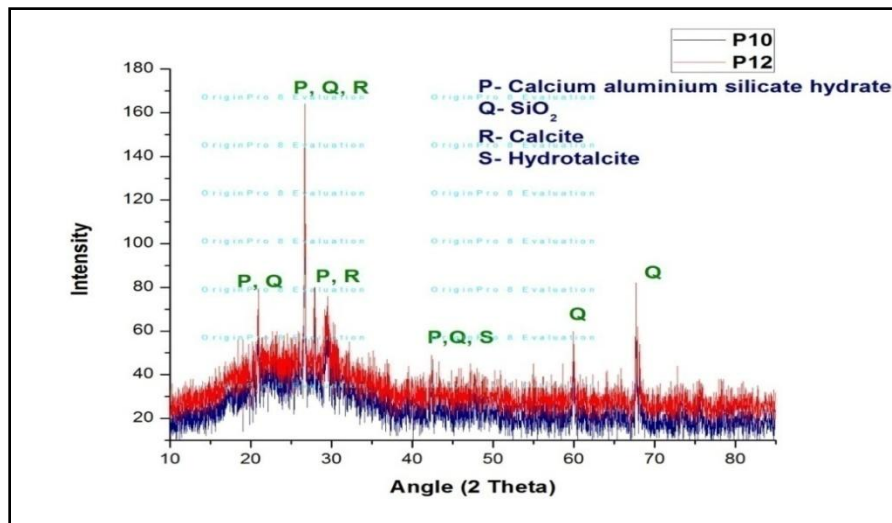**Figure 4.17** XRD peak analysis for M-10, N-10 and N-12 sample

Figure 4.18XRD peak analysis of P-10 and P-12 sample

Summary

In this chapter, the effect of sodium hydroxide and sodium silicate on the physical and mechanical properties of alkali-activated slag concrete was discussed. AASC using PS ball as fine aggregate cured under ambient temperature was investigated in terms of workability, setting time, compressive, split tensile, and flexure strength. AASC mixes can be developed with PS ball as fine aggregate since it satisfies the physical and mechanical properties. An increased NaOH concentration varying between 8M-12M with binder content of 443 kg/m^3 has proved to be quite effective for developing the AASC. The graphical method used for estimating the Weibull distribution parameter yield results with a statistical correlation coefficient range from 0.815-0.995. Based on laboratory results, the PS ball can be used as a fine aggregate in AASC mixes. In the next chapter-5, the mixes with the slag-fly ash blends are discussed in detail with the relevant test.

CHAPTER 5

ALKALI-ACTIVATED SLAG-FLYASH CONCRETE

5.0   INTRODUCTION

In this chapter, the physical and mechanical properties of the Alkali Activated Slag Flyash concrete (AASFC) mixes by complete replacement of river sand with PS ball, both in the fresh and hardened state, are discussed. The properties of fresh concrete, such as workability, setting time, and the properties of hardened concrete like compressive strength, split tensile strength, modulus of elasticity, flexural strength, fatigue behavior, and abrasion resistance, were analyzed. Weibull distribution is used to analyze the laboratory results.

5.1   WORKABILITY

AASFC mixes are characterized by lower workability due to the presence of silica mineral from the source material, attributed to viscous mix in the alkali-activated slag concrete. For the relatively low slump mix, the vibrating table is used for compaction for AASFC mixes. The addition of flyash to the sole binder adversely affected the workability also the setting time of the AASFC mixes, and hence Trisodium phosphate was used as a retarder. No additional water was added to any mixtures. The workability of AASFC mixes for different percentages of flyash is represented in Fig. 5.1.

AASFC mix with series A indicates slag/fly ash combination 90/10, series B 80/20, series C 70/30, and series D 60/40. The slump values decreased with the increase of FA content in the AASFC mixes, which is due to the acceleration of reaction kinetics of calcium minerals and the angular shape of slag particles. The slump of A-8, B-8, C-8, D-8, A-16 are 57mm, 53mm, 49mm, 45mm respectively, when compared to M-8 and M-10, these values are higher. For series A, the slump value for A-10, A-12, A-14, A-16 are 49, 52, 44, 47.5mm, respectively, and these values are less when compared to the A-8 mix of 57mm.For series B, the slump value for B-10, B-14,is 49.5mm, 50mm, respectively, and

these values are less when compared to the B-8 mix of 53mm. For series C, the slump value forC-10, C-14, is 40.5, 44.5mm, respectively, and these values are less when compared to the C-8mix of 49mm. For series D, the slump value of mix D-10, D-14, is 38mm, 41.5mm, respectively, and these values are less when compared to the D-8 mix of 45mm. Conversely, the increase in NaOH concentration enhanced the viscosity by draining the silica and alumina mineral from the FA, which decreased the workability.
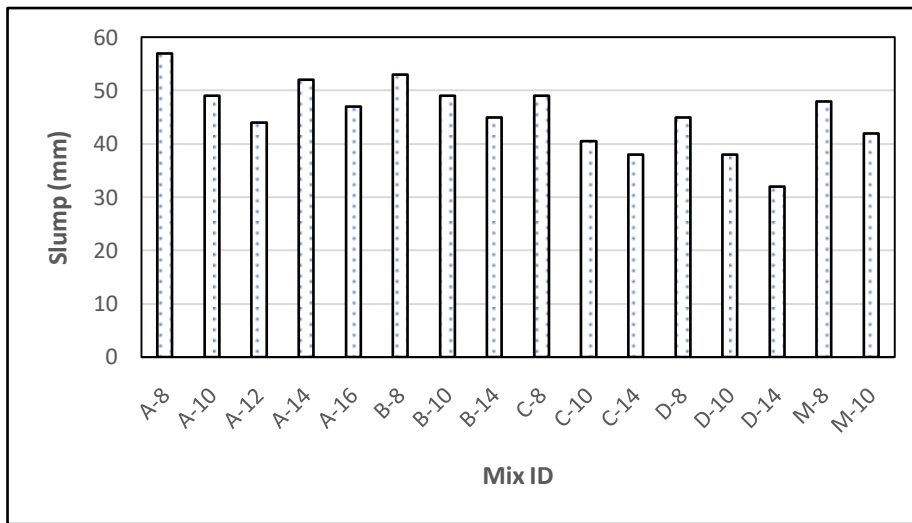

Figure 5.1 Slump values of Various AASFC mixes

5.2   SETTING TIME

The setting time of the AASFC blend was influenced by the flyash content, NaOH concentration, and SS/SH proportion. Fig. 5.2 shows the variation of the setting of AASFC mixes with different FA content. The higher initial and final setting time of AASFC mix with 10% FA is observed, further increase of FA content setting time decreases. The initial and final setting time of A-8, B-8, C-8, D-8 are 55, 54, 49, 42, 115, 103, 95, 86 minutes, respectively, and these values are higher when compared to M-8 and M-10 mix. The effect of SS/SH ratio on setting time may be attributed to the interaction between SS and SH, which indicates that the dissolute silica content was increased with the increase of SS/SH ratio from 1.0 to 2.

76

Thus, the decrease of setting time with the increase of SS/SH ratio from 1.0 to 2 may be related to the dissolute silica content. Higher content of dissolute silica would enhance the alkali activation process and reduce the time to complete the dissolution reaction resulting in the decrease of setting time. The 8M mix with 10% FA had an initial setting time 65min and final setting time of 115minutes, and these values are higher when compared to the 10M mix. A similar trend is observed for the mixes with 20%FA. As SS/SH ratio increases, the dissolution of silica component takes place and thus decreases the setting time.
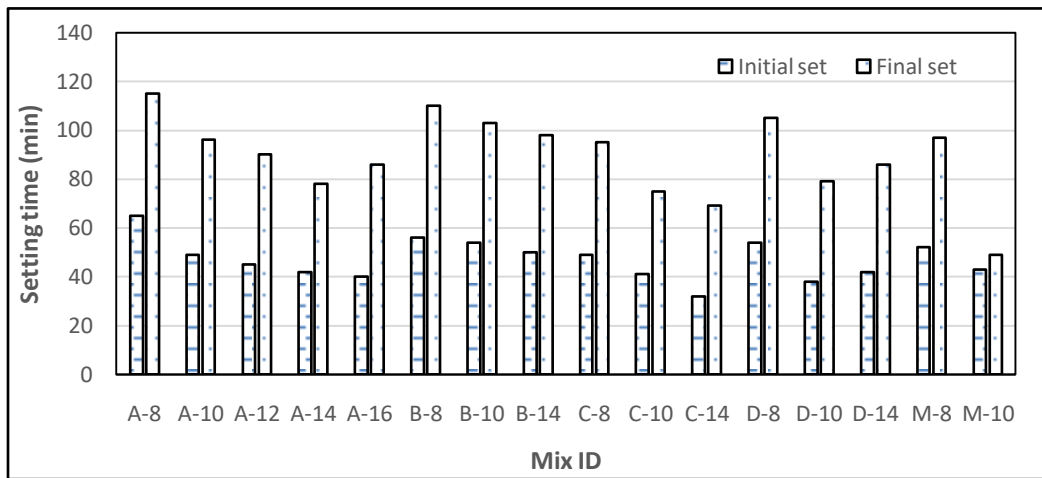
Figure 5.2 Setting time of AASFC mixes

5.3   COMPRESSIVE STRENGTH

The compressive strength test was conducted in accordance with IS 516:1999. The test results are depicted in Fig. 5.3. The addition of FA to the sole binder increased the compressive strength along with increased NaOH concentration. For the AASFC blends, the increment of FA from 10% to 40% increases the strength compared to the control mixes, whereas the increased SS/SH ratio enhances the lubricating effect in the mix and due to this segregation of the PS ball from mixture, take place and hence decrease in the strength.

77
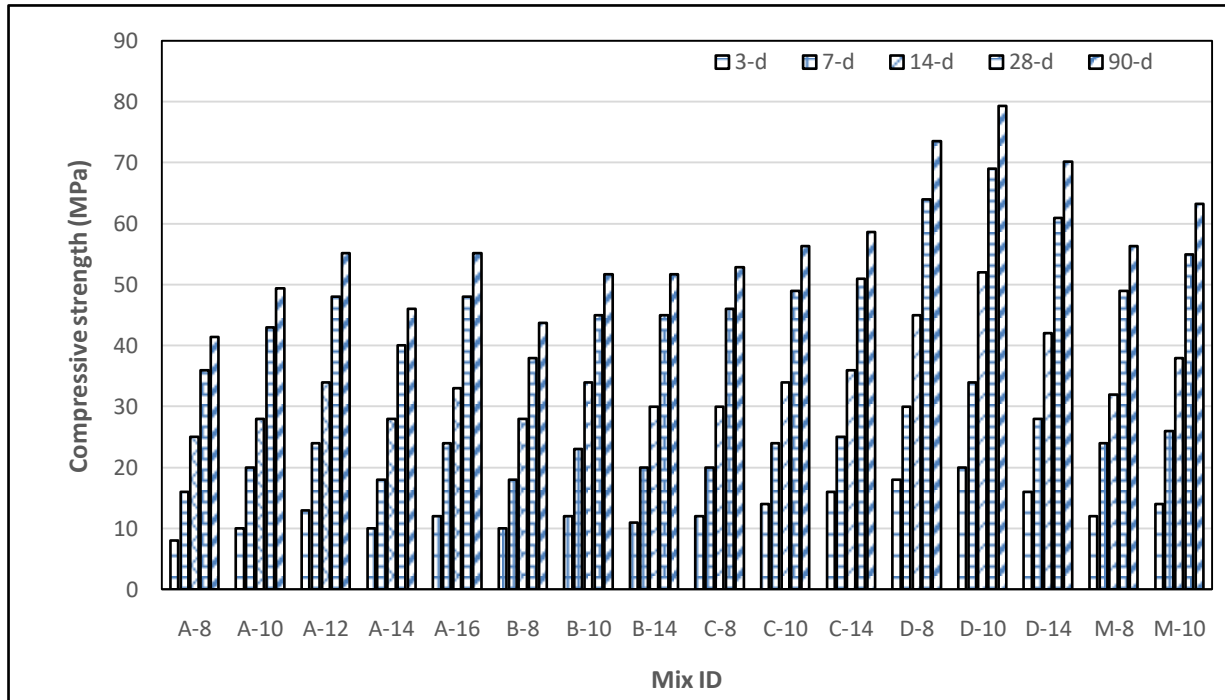
Figure 5.3 Compressive strength of AASFC mixes

5.3.1 Effect of flyash

Fig. 5.4 shows the compressive strength of AASFC mixes with different FA replacement level. The compressive strength of AASFC mixes increases from 3-days to 28-days curing period, and after that, the increase in strength is marginal. As FA content increases, compressive strength tends to increase. For instance, when the FA content increased from 10% to 40%, the compressive strength at 28-days curing was increased from 36MPa to 74MPa.

Figure 5.4 Compressive strength of AASFC mixes with different FA content

5.3.2 Effect of Sodium Hydroxide (SH)

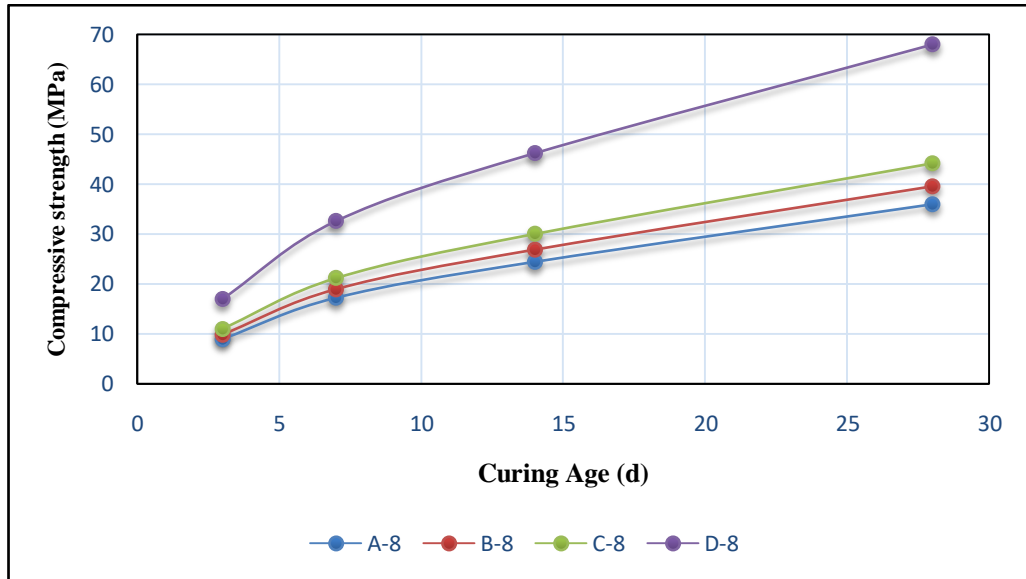The effect of the molar concentration of NaOH on the compressive strength of AASFC mixes is depicted in Fig. 5.5.
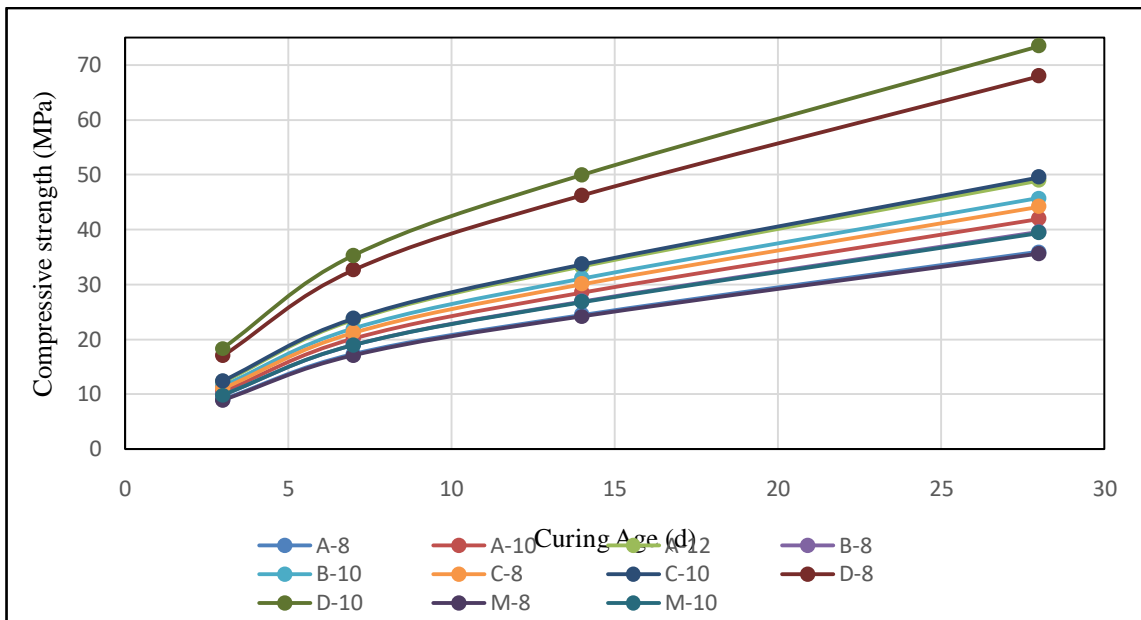

Figure 5.5 Compressive strength of AASFC mixes with different NaOH concentration

From the figure, it is evident that by increasing the molarity, the compressive strength increases. The 28-days compressive strength AASFC mixes were increased by 14% from A-8 to A-10 and 26.53% from A-8 to A-12 when compared to the mix M-8 and M-10.Further increase of FA content enhances the compressive strength. At the higher NaOH concentrations, the leaching of alumina and silica occurs and enhances the polymerization resulting in high compressive strength.

5.3.3   Effect of Sodium Silicate (SS)

The compressive strength of 28 days cured AASFC mixes with different SS/SH ratios are depicted in Fig. 5.6. The 28 days compressive strength of the AASC mix with SS/SH=1 was slightly higher than the remaining mixes with SS/SH=1.5 and 2. The reduction in the strength from SS/SH ratio more than one is due to increased soluble silicate concentration in the activator solution influencing the polymerization reaction.
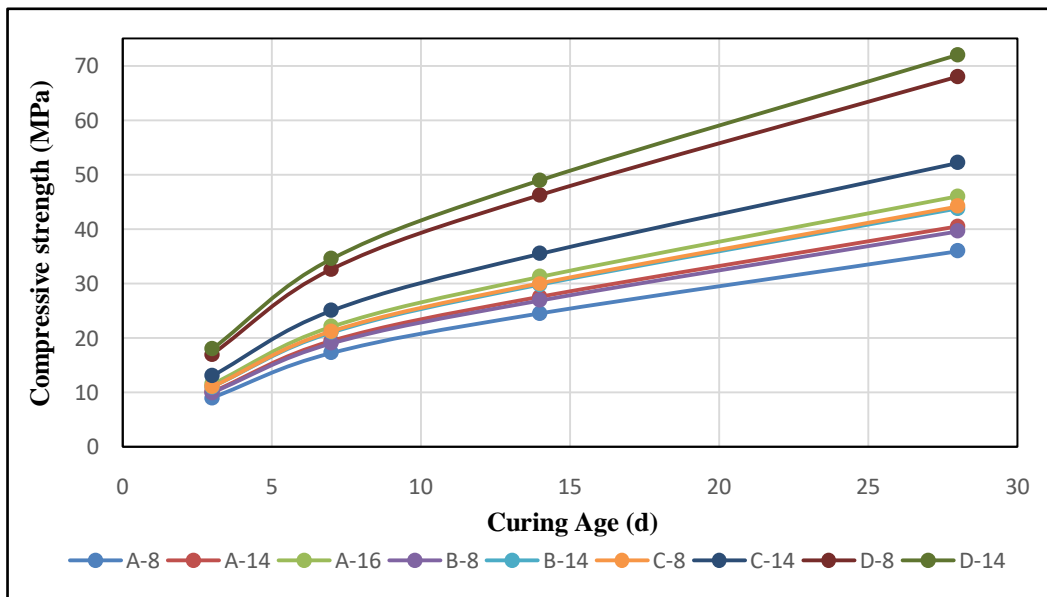

Figure 5.6 Compressive strength of AASFC mixes with different SS/SH ratio

5.4   SPLIT TENSILE AND YOUNG'S MODULUS

The split tensile tests were performed according to IS 5816-1999 for 28 days cured specimen, and the results are shown in Fig. 5.7. The split tensile strength for SS/SH=1 is higher when compared to other ratios of 1.5 and 2 due to increased soluble silicate concentration in the activator solution influencing the polymerization reaction. For the conventional concrete, the ACI 318-05 and Eurocode are commonly used for predicting the split tensile strength. The equations developed and presented by ACI 318-05 and Eurocode are given in equations 5.1 and 5.2.

$$\text{Fct} = 0.56\sqrt{\text{Fck}} \qquad \qquad \text{...(5.1)}$$

$$\text{Fct} = \frac{1}{3}\,\text{Fck}^{2/3} \quad \text{for } F_{ck} < 50 \text{ MPa} \quad \text{...(5.2)}$$

Where

F_{ct} is Split tensile strength (MPa) and

F_{ck} is average compressive strength (MPa)

For the AASFC mixes, it was found that most of the experimental results of split tensile strength were lower than those predicted with a linear relationship between F_{ct} and $\sqrt{F_{ck}}$ with constant 0.48 and 0.45, respectively (Sofi 2007, Lee and Lee 2013). The addition of flyash to the sole binder increased the compressive strength along with increased NaOH concentration. For the AASFC blends, the increment of FA from 10% to 40% increases the strength compared to the AASC mixes. At the higher NaOH concentrations, leaching of alumina and silica takes place, enhancing the polymerization resulting in high strength of AASFC mixtures. However, it is strongly affected by various influential parameters such as the chemical composition of alkaline liquid and source material, the molar concentration of NaOH and SS/SH ratio, alkaline liquid to binder ratio.
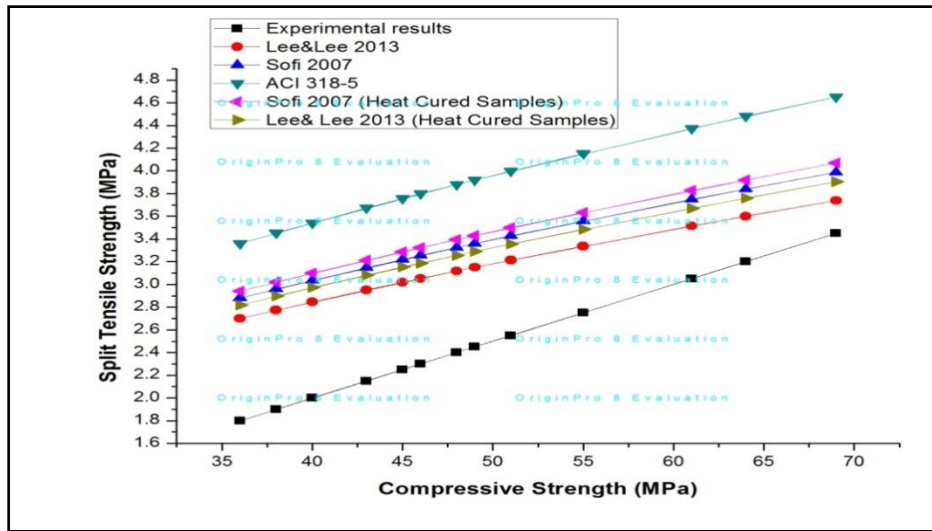
Figure 5.7 Comparison of experimental and predicted split tensile strength of AASFC mixes.
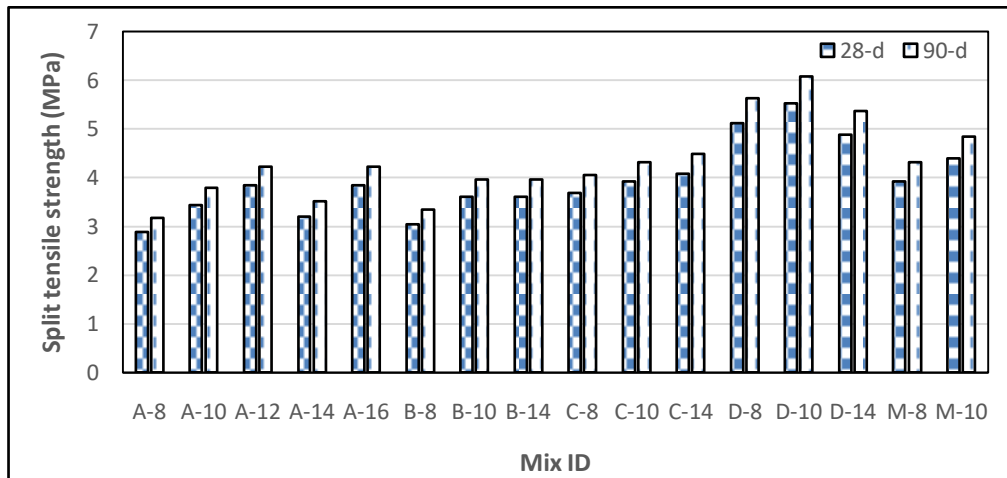
Figure 5.8 Split tensile strength of AASFC mixes.

The AASFC mixes of 28 days cured samples were tested for modulus of elasticity according to IS 516:1959, and the results are shown in Fig. 5.8. The static elastic modulus of concrete as per to IS 456- 2007, ACI-318, Eurocode and BS 8100-2 are given below in Equations 5.3, 5.4, 5.5 and 5.6, respectively.

$$E = 5000\sqrt{Fck} \;\ldots(5.3)$$

$$E = 4700\sqrt{Fck} \;\ldots(5.4)$$

$$E = 9100fc^{0.3} \;\ldots (5.5)$$

$$E = 9800fc^{0.3} \ldots (5.6)$$

Where

E is elastic modulus (MPa),

f_c and F_{ck} is average compressive strength (MPa).

The experimental values and the values obtained from the above equations are plotted in Fig. 5.10, which shows that the E values obtained from experimental results are higher than the values obtained from Equations 5.3 to 5.6. The experimental versus conventional equations graph is plotted and is depicted in Fig. 5.10. It is evident from Fig. 5.10 as static elastic modulus increases with an increase in SS/SH ratio. These equations are not derived for the AASC. To check the validity, the above-mentioned equations are used, though it is not very appropriate.
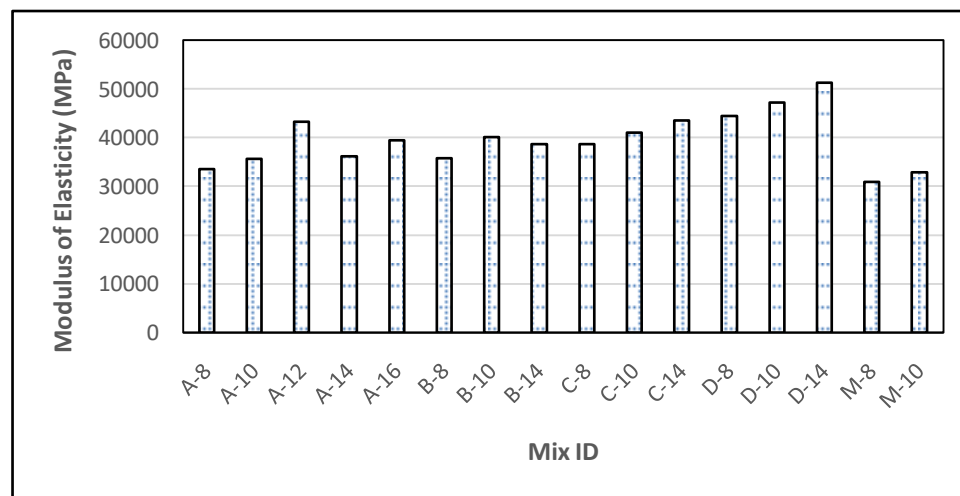
Figure 5.9 Modulus of elasticity of AASFC mixes.
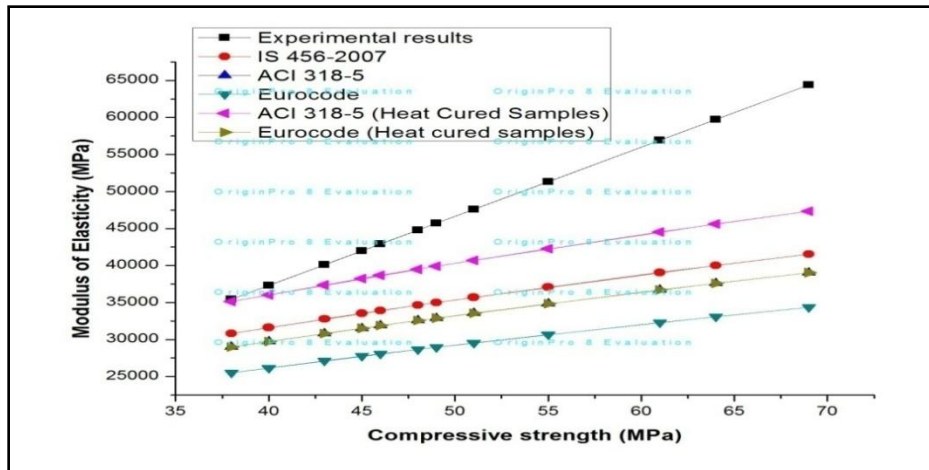
Figure 5.10 Comparison of experimental and static elastic modulus of AASFC mixes

5.5   FLEXURAL STRENGTH OF AASFC MIXES

The flexural strength of 28 days cured AASFC mixes was determined as per IS 516:1959. The static type flexural strength tests were conducted, and the results are depicted in Figs. 5.11 and 5.12.   The flexural strength of OPC concrete commonly predicted using the ACI 318-05 as given in equation 5.7. Similarly, some equations were proposed to predict the flexural strength of alkali activated flyash slag concrete. The relationship between flexural strength and compressive strength of activated mixes developed by Diaz-Loya et al. (2011) and Nath and Sarker (2014) are given in equation 5.8 and 5.9, respectively.

$$fct = 0.62\sqrt{fck}   \ldots (5.7)$$

$$fct = 0.93\sqrt{fck}   \ldots (5.8)$$

$$fct = 0.69\sqrt{fck}   \ldots (5.9)$$

Where

f_{ct} is flexural strength, and

f_{ck} is the average compressive strength

The values obtained from above mentioned equations and experimental results are plotted in Fig. 5.11. The flexural strength predicted using IS code is closer to the experimental results. It can be seen from Fig. 5.12 the flexural strength of AASFC mixes increases with FA content and NaOH concentration. The flexural strength of AASFC mixes with 10% FA for mixes A-10, A-12, A-14, A-16 are 6.2, 6.8, 5.8, 6.5 MPa respectively. These values are higher than the A-8 mix. As the FA content increases, the flexural strength increases, and it is evident from Fig. 5.12

Figure 5.11 Flexural strength of AASFC mixes.
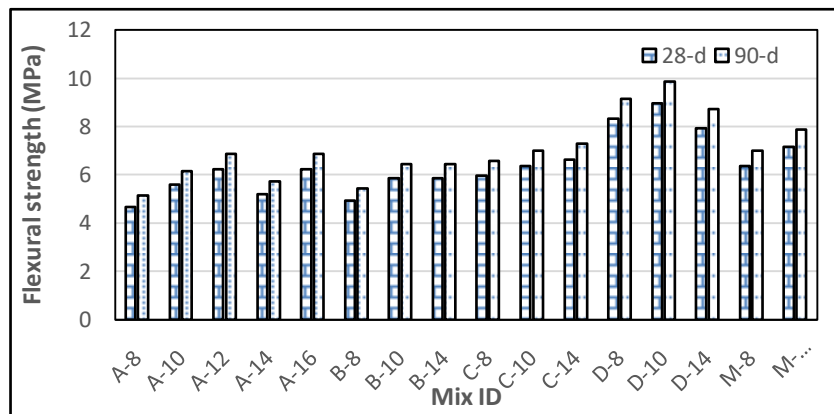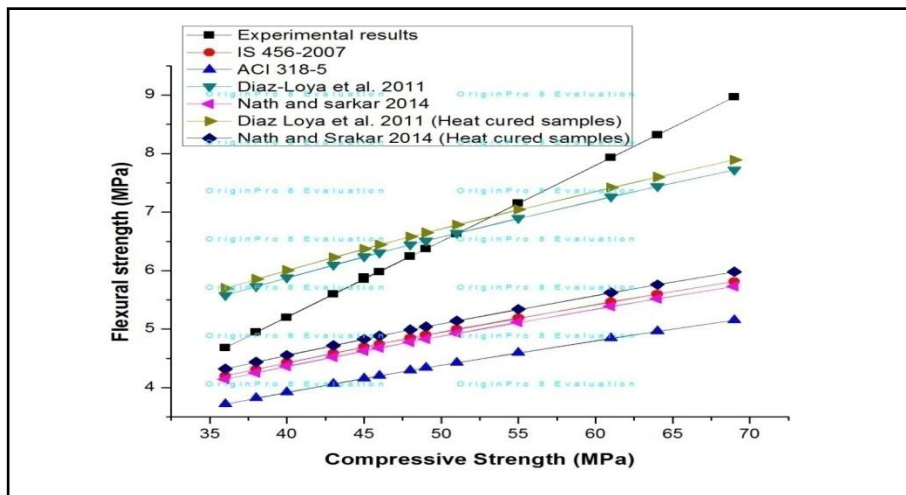

Figure 5.12 Comparison of experimental and predicted flexural strength of AASFC mixes

5.6   FATIGUE BEHAVIOR OF AASFC MIXES

The fatigue tests were performed on the prism specimens of dimension 100x100x500 mm on an MTS servo-controlled hydraulic repeated load testing machine of 5-ton capacity with a 2-ton loading cell unit. The fatigue life is represented in terms of the S-N curve shown in Figs. 5.12- 5.14. The specimens which have passed minimum flexural strength were considered for the fatigue test, i.e. (D-8, D-10, and D-14). Irrespective of the flexural failure load for all the mixes, a constant load (1125 kg) was selected to know the fatigue behavior of all the mixes.

Fatigue repetitions of AASC and AASFC mixes improves with increase in Sodium Hydroxide up to 12M which is due to internal reaction of Si, Al and Ca components caused by the increased breakage of the ionic bonds such as Ca-O and Si-O bonds in GGBFS and flyash provoked by the higher alkalinity resulting from the increasing molarity of Sodium Hydroxide. Increased FA content of 40% with SS/SH=1 showed higher fatigue life than that of control mixes. The AASFC mixes SS/SH= 2 showed higher fatigue life due to strong bonding between the mortar and aggregate matrix, preventing the early crack initiation and its propagation towards the inner structure of concrete compared to the mixes with SS/SH=1. The obtained statistical correlation is ranging from 0.991 to 0.987 for AASFC mixes, indicating a good fit.

Table 5.1 Fatigue life of AASFC mixes

Mix ID	Specimen no	Stress Ratio			
		0.85	0.80	0.75	0.60
		No of cycles to failure			
A-8	1	243	339	516	33642
	2	270	417	624	34722
	3	321	450	678	35301
A-10	1	288	384	570	33834
	2	315	462	678	34914
	3	366	495	732	35493
A-12	1	333	429	624	34026
	2	360	507	702	35106
	3	411	540	786	35685
A-14	1	303	399	576	33672

|					
	2	330	477	654	34752
	3	381	510	738	35332
A-16	1	384	480	684	34191
	2	411	558	762	35271
	3	432	591	846	35850
B-8	1	273	369	546	33696
	2	306	447	654	34776
	3	351	480	708	35361
B-10	1	318	414	603	33888
	2	345	492	708	34968
	3	396	525	762	35547
B-14	1	297	393	588	33972
	2	324	471	666	35052
	3	375	504	750	35631
C-8	1	318	414	591	33948
	2	351	492	699	34836
	3	396	525	753	35421
C-10	1	363	459	648	33948
	2	390	537	753	35028
	3	441	570	807	35607
C-14	1	411	507	698	34017
	2	438	585	801	35109
	3	489	618	855	35712
M-10	1	294	438	642	34719
	2	345	474	672	34746
	3	456	585	810	34503
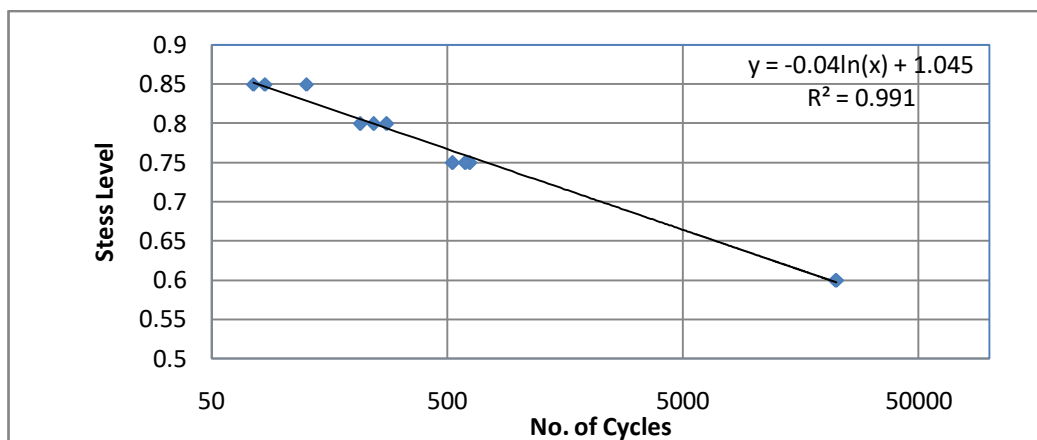
Figure 5.13 Fatigue life of AASFC specimen for D-8 mix.
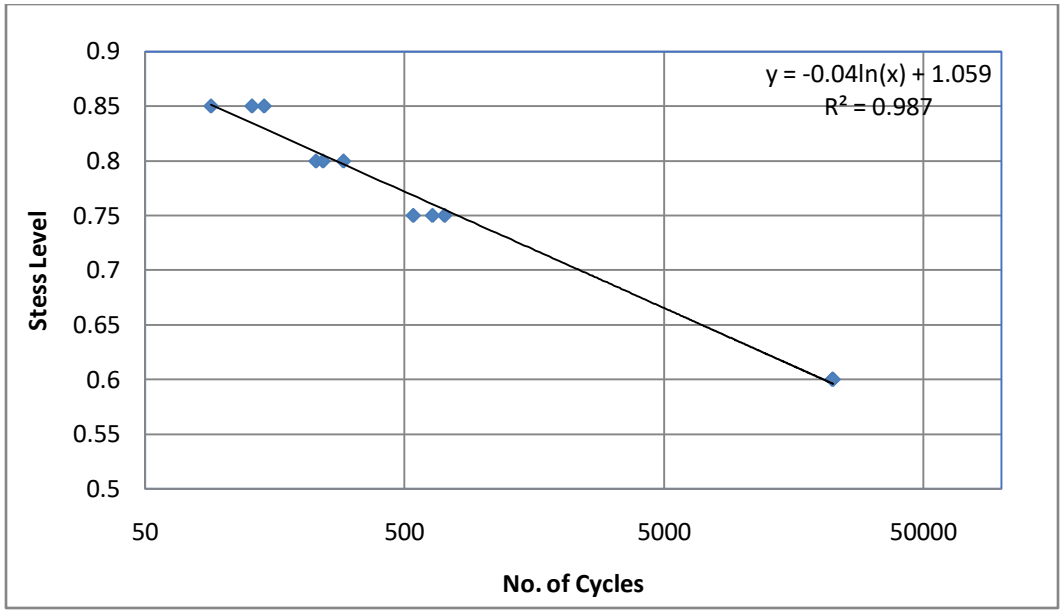
87

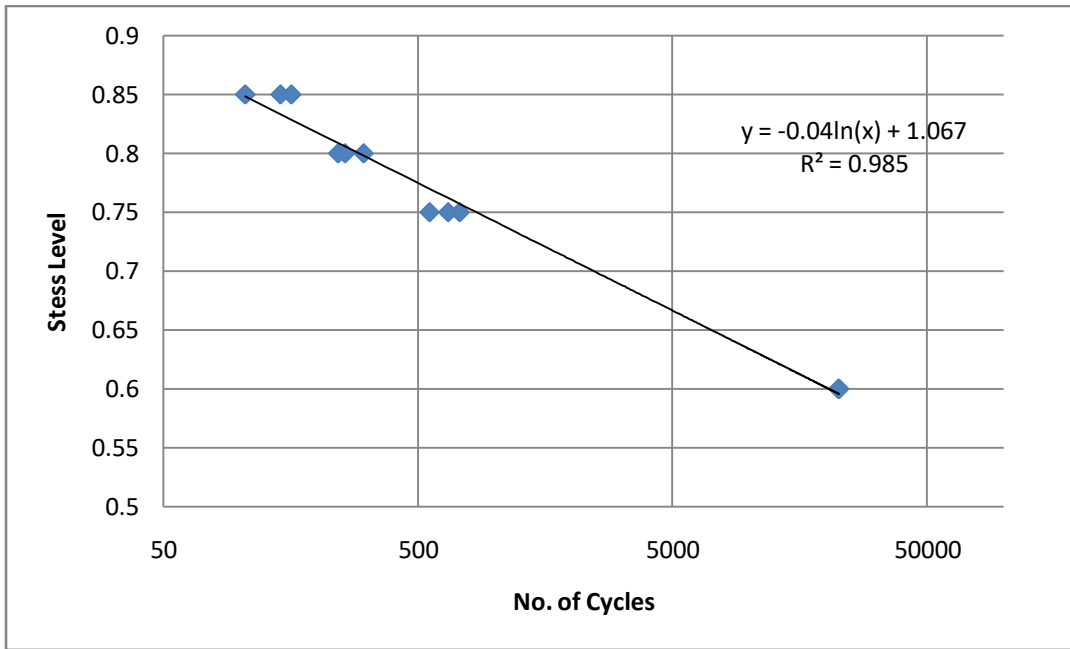**Figure 5.14**Fatigue life of AASFC specimen for D-10 mix.

Figure 5.15 Fatigue life of AASFC specimen for D-14 mix.

Table 5.2 Weibull parameters of fatigue life at different stress levels

Mix ID	Stress level	α	μ	R^2
D-8	0.6	32.41	39061	0.819
	0.75	6.92	1322.3	0.994
	0.8	4.3	1085.7	0.959
	0.85	3.9	739.4	0.962
D-10	0.6	32.63	39284	0.82
	0.75	7.31	1545.3	0.996
	0.8	4.462	1768	0.959
	0.85	4.017	1991	0.994
D-12	0.6	32.76	39553	0.82
	0.75	7.79	1814.3	0.953
	0.8	4.69	2037	0.994
	0.85	4.37	2260	0.962
M-8	0.6	29.78	33261	0.802
	0.75	6.45	1126	0.914
	0.8	3.8	928	0.926
	0.85	3.1	659	0.921
M-10	0.6	31.29	36657	0.997
	0.75	6.5	1296	0.894
	0.8	4.1	1027	0.904
	0.85	3.6	736	0.916

Table 5.3 Calculated fatigue lives corresponding to different failure probabilities
(P_f= 5%, 50%, and 95%)

Mix ID	Survival Probability, L_n= (1- P_f)	Stress Level			
		0.85	0.80	0.75	0.60
D-8	0.95	980	1401	1550	40406
	0.5	673	997	1254	38622
	0.05	345	544	861	35640
D-10	0.95	2616	2261	1795	40627
	0.5	1817	1629	1470	38845
	0.05	950	908	1029	35866
D-14	0.95	2905	2573	2089	40900
	0.5	2078	1834	1731	39113
	0.05	1145	1081	1239	36123
M-8	0.95	735	989	935	24779
	0.5	428	585	639	22995
	0.05	98	132	246	20013
M-10	0.95	888	1270	1256	27879
	0.5	581	866	960	26095
	0.05	251	413	567	23113

Analysis of fatigue data showed that the failure pattern could be convincingly explained by Weibull distribution. The estimated values of Weibull parameters using the graphical method are tabulated in Table 5.1. The estimated statistical correlation coefficient R^2, for different test series at various stress level, are in between 0.985-0.991, which indicates that the graphical method used for the estimation of Weibull parameter shows the best approximation. The Weibull parameter estimated was used to obtain the fatigue cycle of different series for various stress levels for survival probability of 5%, 50%, and 95%. The calculated fatigue lives corresponding to different failure probabilities are presented in Fig 5.16. It indicates that fatigue life is high at higher survival probability and fatigue life decreases as the survival ship decreases (or as the failure probabilities increase).

5.7 ABRASION RESISTANCE

The abrasion resistance test was performed as per IS 9284:1979, and the test results are depicted in Fig. 5.16. The percentage increase in weight loss of the specimen in case of SS/SH=1.5 and 2 are less comparable to the mixes with SS/ SH =1. It is evident from Fig 5.16 that the abrasive weight loss of AASFC mixes decreased with the increase in FA content. Since SS is the most viscous solution in the alkaline liquid, the increase of the SS/SH ratio from 1 to 2 enhances the polymerization reaction. It is evident from Fig 5.16 that the abrasive weight loss of AASFC mixes decreased with the increase in FA content. The abrasive weight loss of AASFC specimen with 10% FA (A-series) decrease by 71%, 4%, 7.4%, 9% for A-10, A-12, A-14, A-14 respectively, when compared to A-8mix. A similar trend was observed for the mixes with high FA content.
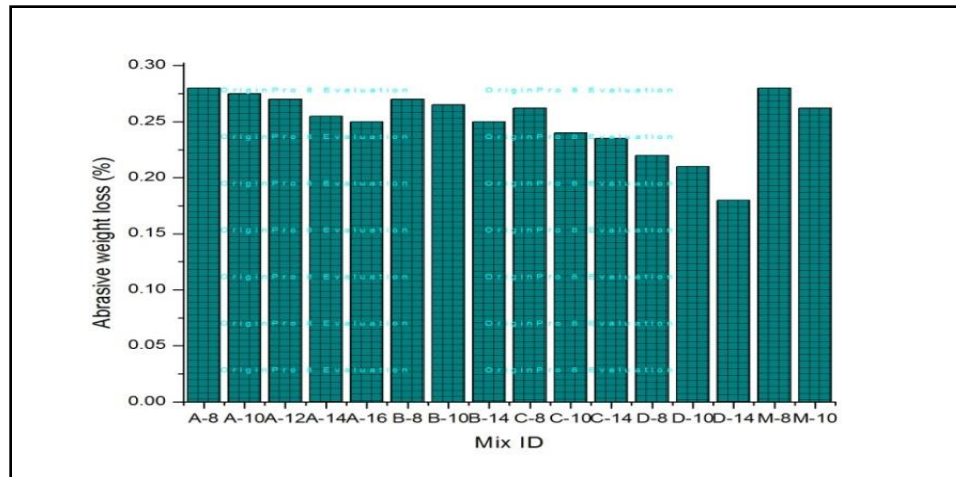
Figure 5.16 Abrasive resistance of various AASFC mixes

Summary

This chapter has provided extensive experimental results and analysis on the setting time, workability, compressive strength, flexure and fatigue behavior, and abrasive resistance of AASFC mixes consisting of PS ball as fine aggregate with slag and FA as binders. The workability of AASFC mixes was significantly affected by an increase in FA content, along with an increase in molarity of SH and SS concentration levels. A significant loss in workability was observed for the 40% FA mixes with increased SH concentration. The combined effect of SH and SS with the increase of FA has a greater influence on the setting time of AASFC mixes. The SS/SH ratio is the key parameter that affects the strength of AASFC. In the next chapter-6, the durability of alkali activated mixtures is discussed in detail.

CHAPTER 6

DURABILITY PROPERTIES

6.1   INTRODUCTION

It is also essential to study the durability properties of these mixtures against the aggressive environment. The past studies were carried out for durability for the heat-cured alkali-activated material. This chapter presents some of the durability tests conducted on air-cured alkali-activated materials. The test includes the evaluation of permeable pores, capillary sorptivity, and strength determination of alkali activated mixtures exposure to sulphuric acid, nitric acid, and hydrochloric acid.

6.2   SORPTIVITY

The sorptivity test characterizes the ability of a material to transport fluids under capillary action, which is a key factor in determining the service life of structures on exposure to acidic conditions. The relationship between water absorption and elapsed time square root for the M-8 mix is shown in Fig. 6.1. Initial/primary sorptivity (360 minutes) and secondary sorptivity (24hours) were determined, and test results of AASC and AASFC mixes are tabulated in Tables 6.1 and 6.2. The primary sorption may be due to the quick saturation of capillary pores and secondary sorption due to the gradual filling of larger air voids. The slopes of the first linear and second linear portion are primary and secondary sorptivity values, starting from 1min-360min and 24 hrs-8 day as per ASTM C-1585.
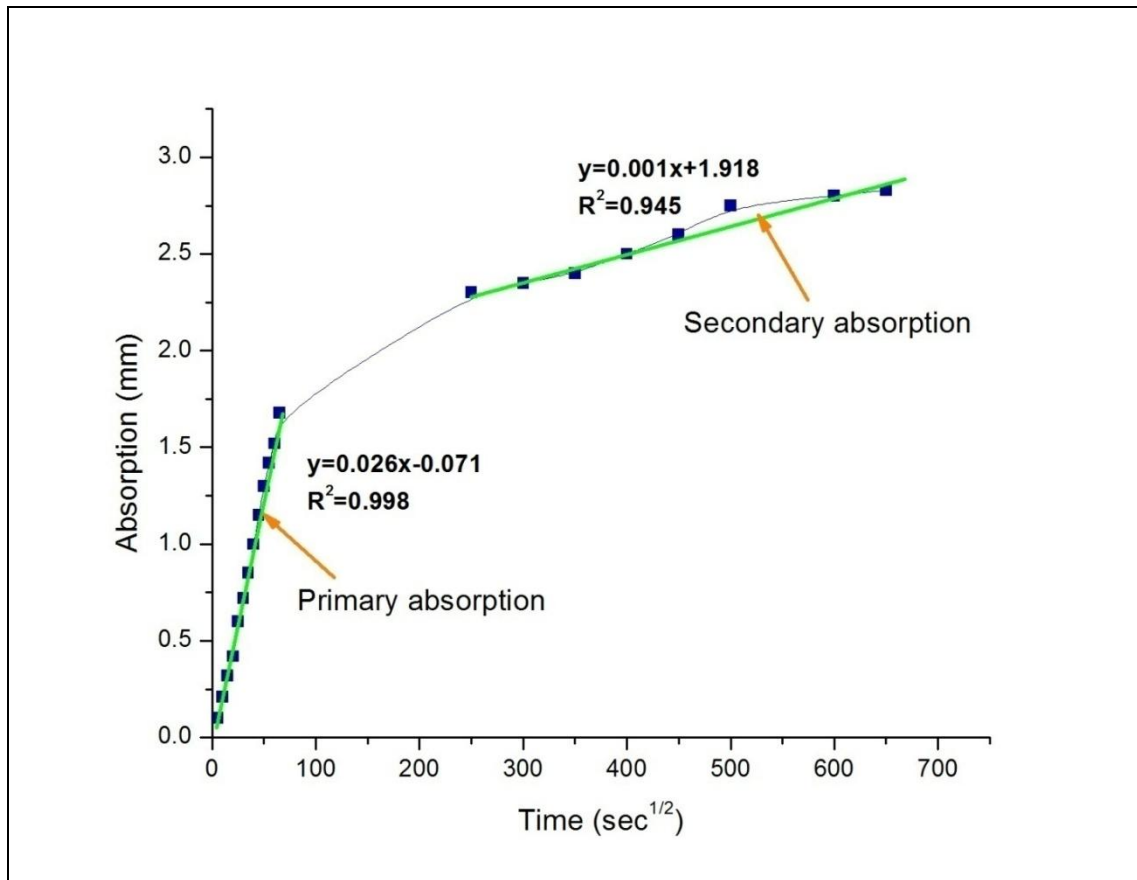
Figure 6.1 Sorptivity characteristics of alkali activated mixture for mix M-8

The sorptivity curve of alkali activated mixtures, especially with lower NaOH concentration found to be considerably linear compared to the control mix. During the initial stages of the test, the reaction mechanism is dependent on the pore structures, degree of saturation and the absorption area is significantly smaller due to the existence of the aggregate matrix. Hence, a non-linear curve was obtained as depicted in Fig. 6.1.

The primary sorptivity of alkali activated mixtures prepared with lower NaOH is about 0.0046 mm/sec$^{1/2}$. The capillary action decreases with an increase in binder content and NaOH concentration. The mixtures with lower NaOH concentration reported higher primary sorption and vice-versa, and a similar trend observed for secondary sorptivity. Secondary sorptivity exhibits better resistance towards capillary action, and the test results are tabulated in Tables 6.1 and 6.2.

94

Table 6.1 **Primary and secondary sorptivity of AASC mixes**

Mix ID	Initial Sorptivity (mm/sec$^{1/2}$)	Secondary sorptivity (mm/sec$^{1/2}$)
M8	0.026	0.001
M10	0.024	0.001
M12	0.021	0.001
N8	0.032	0.003
N10	0.029	0.003
N12	0.026	0.004
P8	0.039	0.0025
P10	0.035	0.003
P12	0.031	0.003

Table 6.2 **Primary and secondary sorptivity of AASFC mixes**

Mix ID	Initial Sorptivity (mm/sec$^{1/2}$)	Secondary sorptivity (mm/sec$^{1/2}$)
C-8	0.021	0.0021
C-10	0.025	0.0025
A-12	0.029	0.0031
B-10	0.038	0.0037
C-10	0.049	0.0043
D-10	0.06	0.0048

The reduction in sorptivity value indicates the mixtures consist of a smaller portion of air voids with minute cracks. On comparing the primary and secondary sorptivity, the primary sorptivity was more aggressive for the mixtures with lower NaOH concentration. The high rate of water absorption can be minimized by balancing the NaOH concentration. The alkali activated mixtures show a greater reduction in sorptivity with an increase in SS/SH ratio. The test results indicate that the increase in SS/SH ratio increases the silicate along in the activator solution along with flyash content; thereby reduces the porosity of alkali activated mixtures.

Alkali activated mixtures were immersed in three different acid solutions, such as Hydrochloric acid (HCL), Sulphuric acid (H_2SO_4), and Nitric acid (HNO_3) solutions. To

study the effect of these acids, nearly 30 cubes were cast for individual mix and tested at the age of 7, 28 and 56 days of immersion. Three cubes from each mix were used for determining the compressive strength. The initial weight (W_f) of all the cubes was recorded before immersion in acidic solution. A total 12-cubes from each mix immersed in a container having 5% of acid solution. The solutions are replaced at regular intervals to maintain p^H. After 7, 28, and 56 days of immersion, 3-cubes from corresponding mixtures were taken out from the acid solution and kept under room temperature to attain stable mass, and then the sample weight (W_i) and compressive strength (F_{ck}) is determined. The changes in mass and compressive strength are calculated using Equations 6.1 and 6.2.

Change in weight (%) =   x100   … (6.1)

Change in compressive strength (%) =   x100   … (6.2)

Where W_i= weight of the sample before the acid attack

   W_f=weight of the sample after acid attack

   C_i = Compressive strength of air-cured samples after 28 days

   C_f= Compressive strength of air-cured samples after acid attack

6.3 EVALUATION OF PERMEABLE PORES

Water absorption and volume of permeable pores of alkali activated mixtures were determined as per ASTM C-642, and the test results are depicted in Figs. 6.2, and 6.3. The water absorption of alkali activated mixtures prepared with 8M, 10M, 12M was 4.5%, 3.3%, 1.5%, respectively. The high NaOH concentrations have a negligible effect on the external attack. Similarly, the volumes of permeable pores were 9%, 6.5%, 4.5% for 8M, 10M, and 12M, respectively. On comparing the test results of water absorption and permeability of voids, the alkali activated mixtures with high NaOH concentration is more durable. The alkali activated mixtures with 8M has high water absorption and

permeable voids when compared to the 10M and 12M mixes. The amount of air voids and permeability is primarily dependent on the compaction and workability of mixtures. The mixes with lower workability exhibit high voids and water absorption.
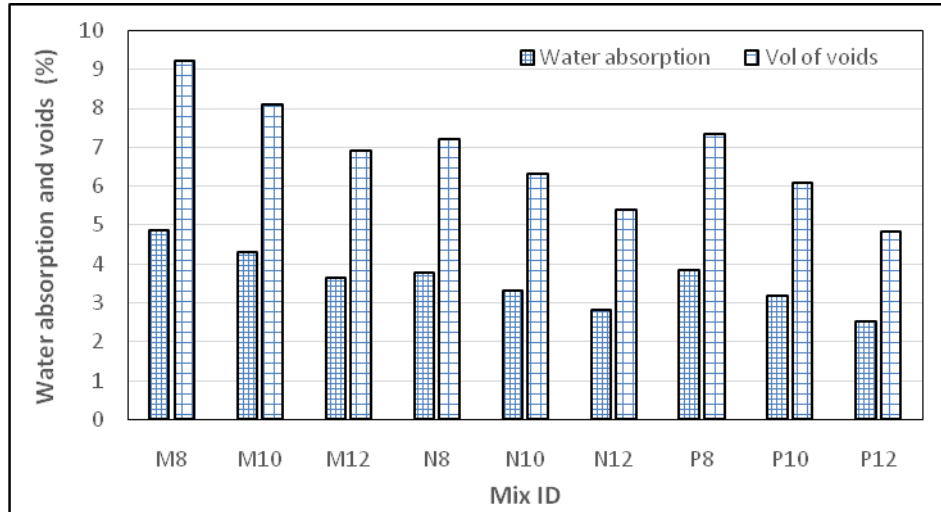

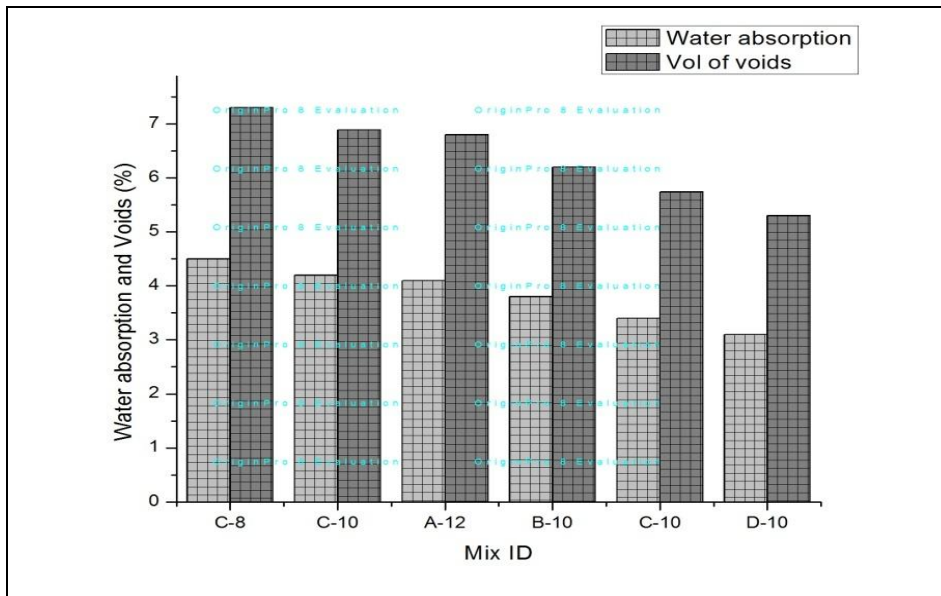**Figure 6.2** Water absorption and permeable voids for AASC mixes

Figure 6.3 Water absorption and permeable voids in for AASFC mixes

6.4   ACID ATTACK

The effect of HCL, H_2SO_4, and HNO_3 on variation in weight and compressive strength were observed. The change in weight of alkali activated mixtures subjected to acid attack for 56 days was investigated. This immersion time does not include the samples curing period. The weight of each sample is measured before and after the acid attack, and the percentage of change in weight is determined. Cubes immersed in various acid solutions are shown in Fig 6.4.

Figure. 6.4 Cubes immersed in acid solution for durability test

The percentage changes in weight calculated using the Eq 6.1. Figs. 6.7 and 6.8 show the changes in weight is very high for the samples immersed in H_2SO_4, compared to the HNO_3. The alkali activated mixtures with 8M reported higher weight loss than the 10M and 12M mixes, which is evident from Figs. 6.5 and 6.6, and it is due to lower resistance towards acid attack. The weight loss is predominantly dependent on the type of acid

98

solution and the number of days samples kept in acid solution. The weight loss can be controlled by increasing the NaOH concentration, silicate content, binder content, and alkaline liquid to binder ratio.

The mass gain is observed at the 7 days of immersion in acid solution about 2-2.5%; this may be due to the absorption of acid particles on the concrete surface. All the samples were air-dried for 1-2 days till constant weight is attained. This mass gain is due to the internal reaction between acid and constituents of concrete and results in the formation of gypsum and Calcium Hydroxide.

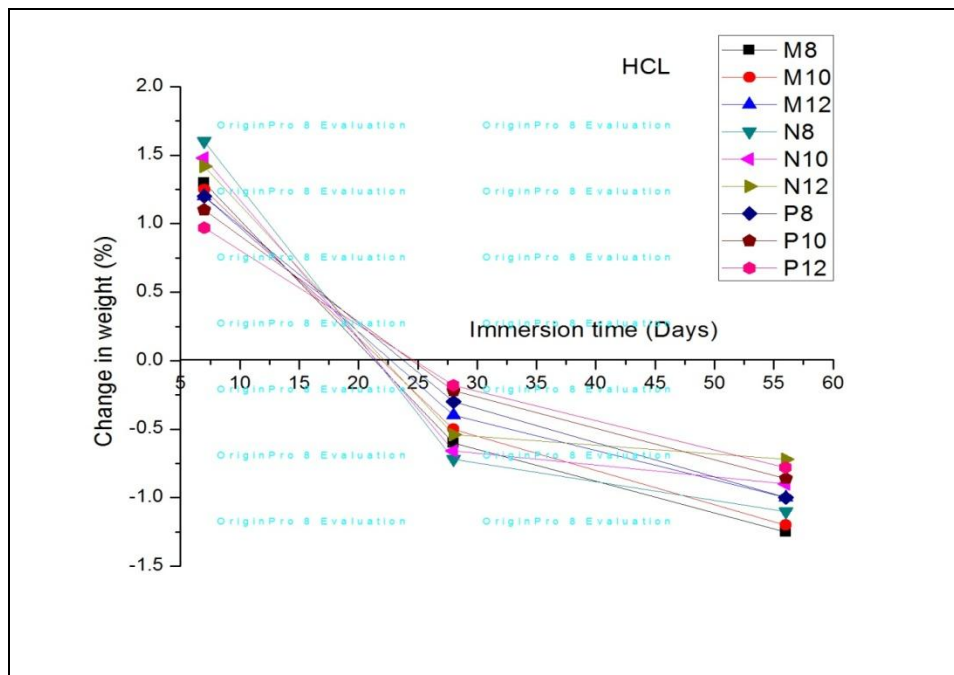

Figure 6.5 Change in weight of AASC samples immersed in HCl Solution

Figure 6.6 Change in weight of AASFC samples immersed in HCl Solution

Figure 6.7 Change in weight of AASC samples immersed in H_2SO_4 Solution

100

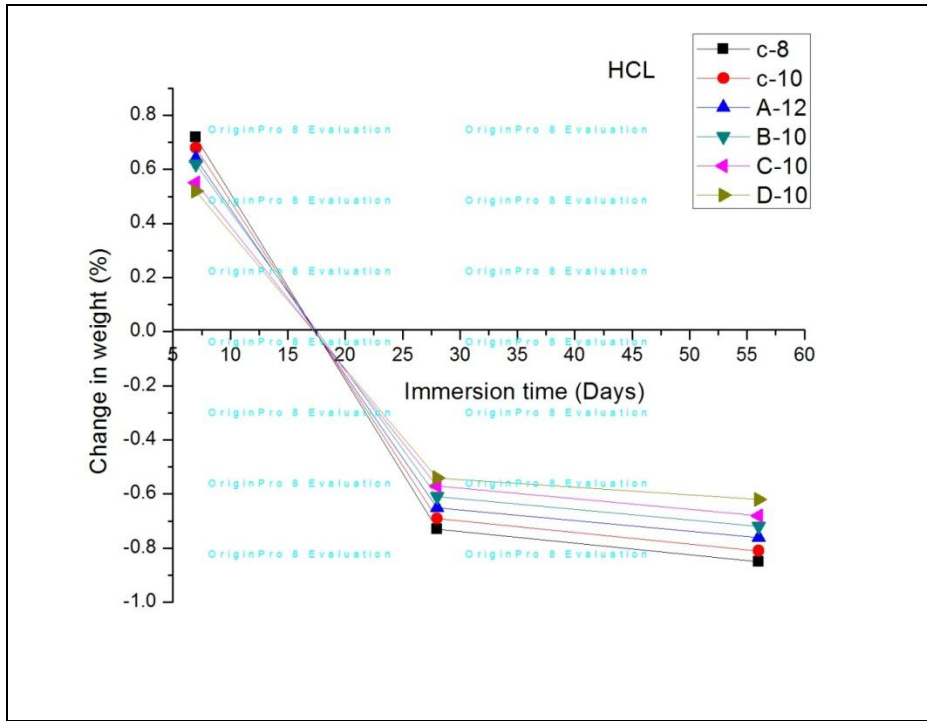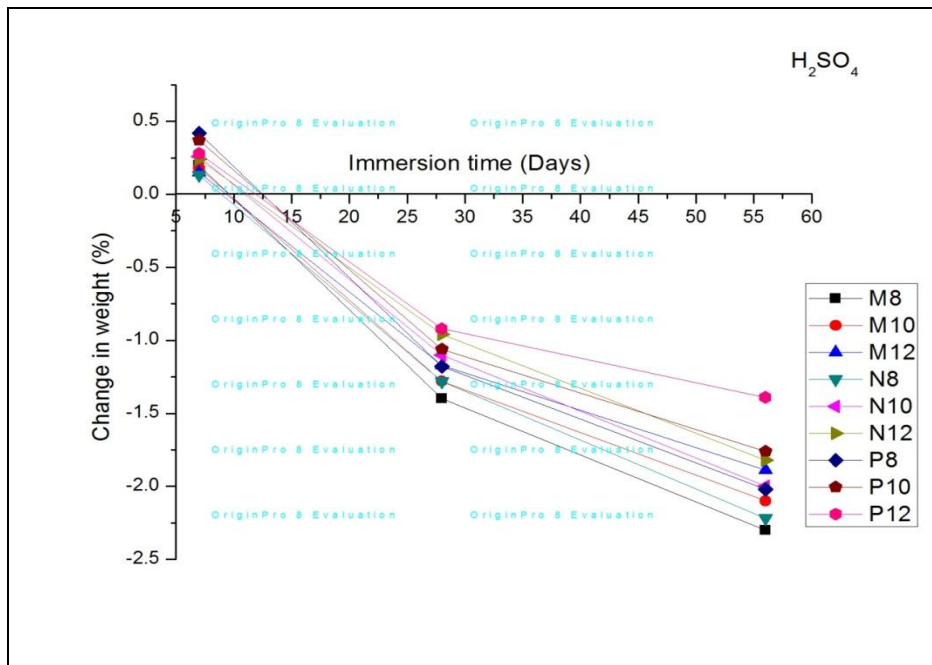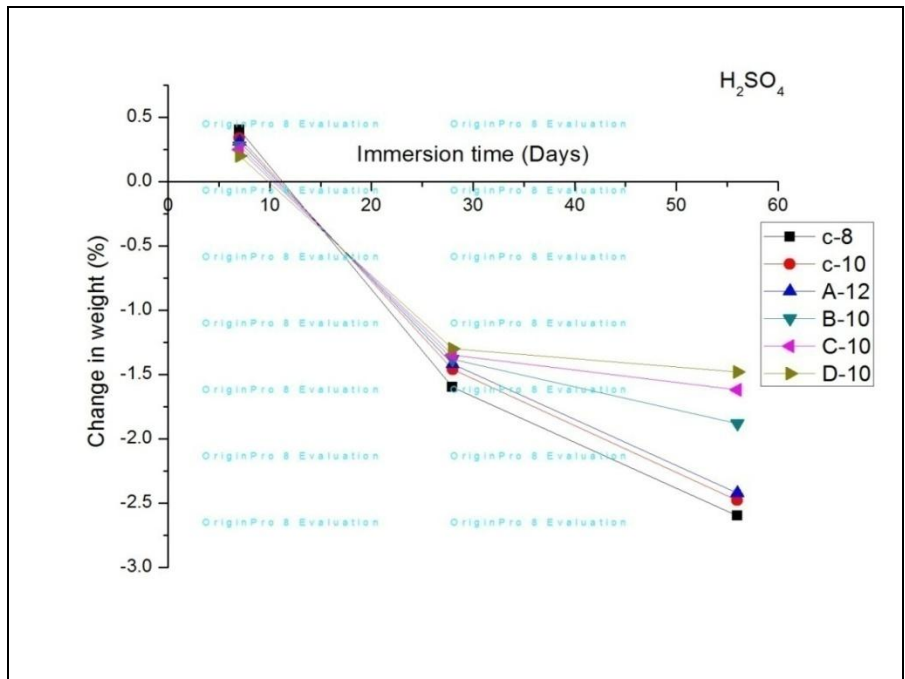**Figure 6.8** Change in weight of AASFC samples immersed in H_2SO_4 Solution
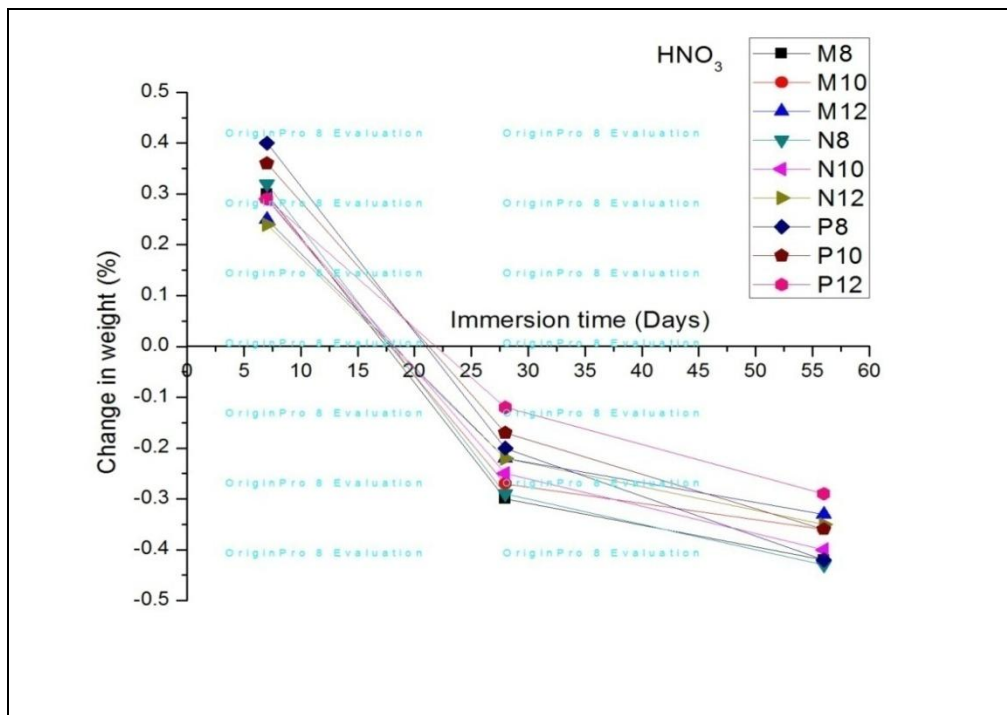
Figure 6.9 Change in weight of AASC samples immersed in HNO_3 Solution
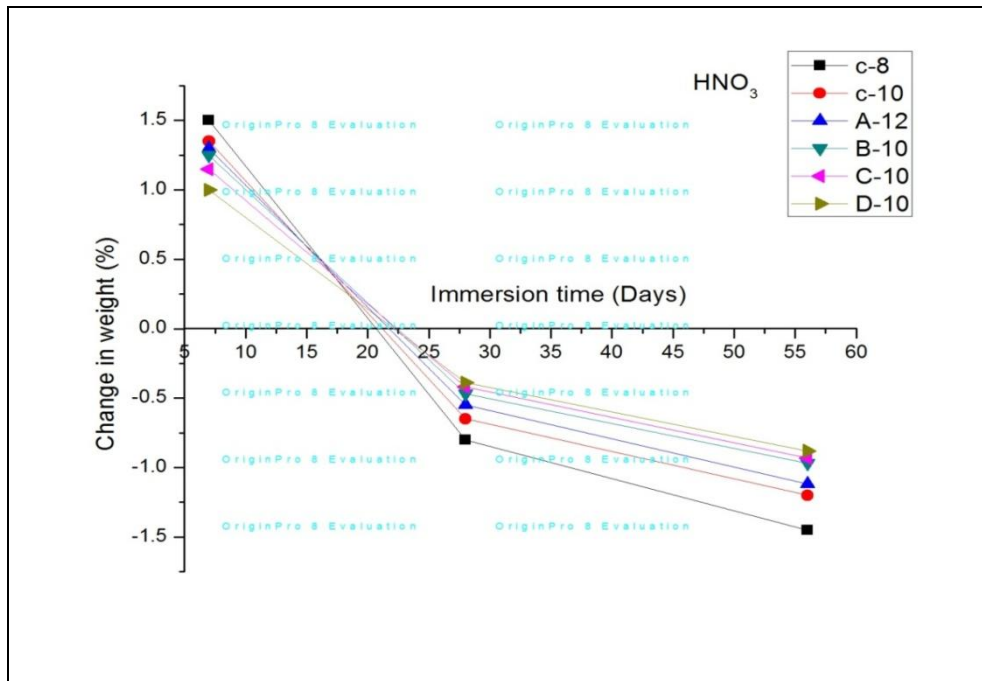
Figure 6.10 Change in weight of AASFC samples immersed in HNO₃ Solution

6.4.1 Effect of Hydrochloric acid (HCL)

The compressive strength of alkali activated mixtures subjected to HCL solution decreases with an increase in the immersion period, and the test results are depicted in Figs.6.11 and 6.12. The decrease in strength is observed for the mixes with 8M NaOH concentration due to the ingress of chloride ions. The resistance towards acid attack can be improved with an increase in NaOH concentration, binder content, and silicate content in the activator solution. The HCL acid reacts with calcium compound results in the formation of Calcium Chloride ($CaCl_2$), which will have a detrimental effect on the properties of concrete. CASH will be the final reaction product formed in alkali activated material, which on reaction with HCL, produces $CaCl_2$. It reduces the calcium content responsible for the strength development in alkali activated mixtures.

Figure 6.11 Change in compressive strength of AASC samples immersed in HCl solution
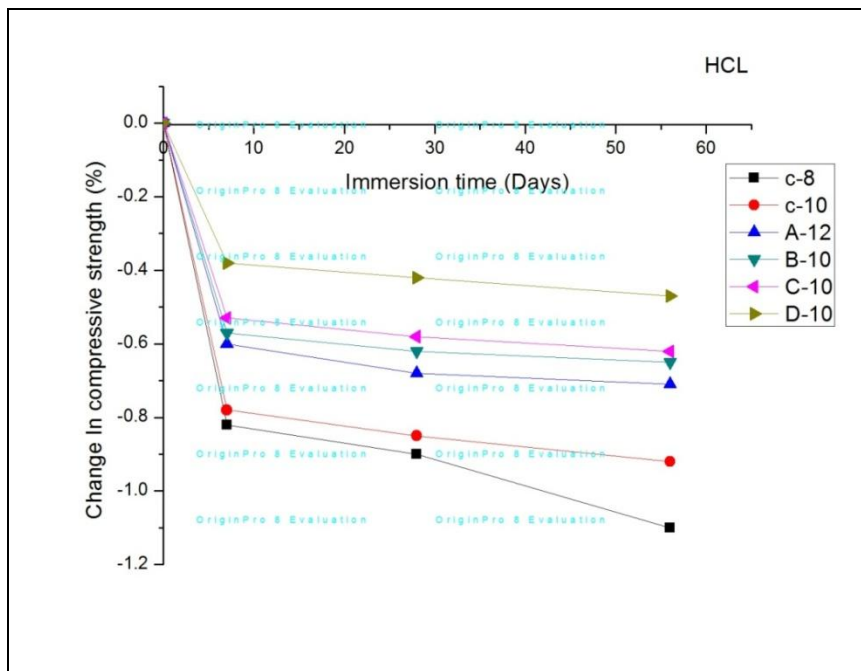
Figure 6.12 Change in compressive strength of AASFC samples immersed in HCl solution

6.4.2 Effect of Sulphuric acid (H₂SO₄)

Alkali activated mixtures exposed to H_2SO_4 solution result in higher mass loss with a reduction in compressive strength, and the test results are depicted in Figs. 6.13 and 6.14. The alkali activated mixtures of 10M and 12M with a high concentration of NaOH exhibited better resistance towards acid attack compared to the 8M mix. The sulphate ion reacts with calcium compounds to produce gypsum ($CaSO_4$) to form calcium sulfo-aluminates. The final reaction, such as CASH undergoes decalcification to form $CaSO_4$ reduces the concrete density. The effect of decalcification of the CASH compound and variation in volume caused by $CaSO_4$ tends to produce the concrete with lesser strength.

Figure 6.13 Change in compressive strength of AASC samples immersed in H_2SO_4 solution
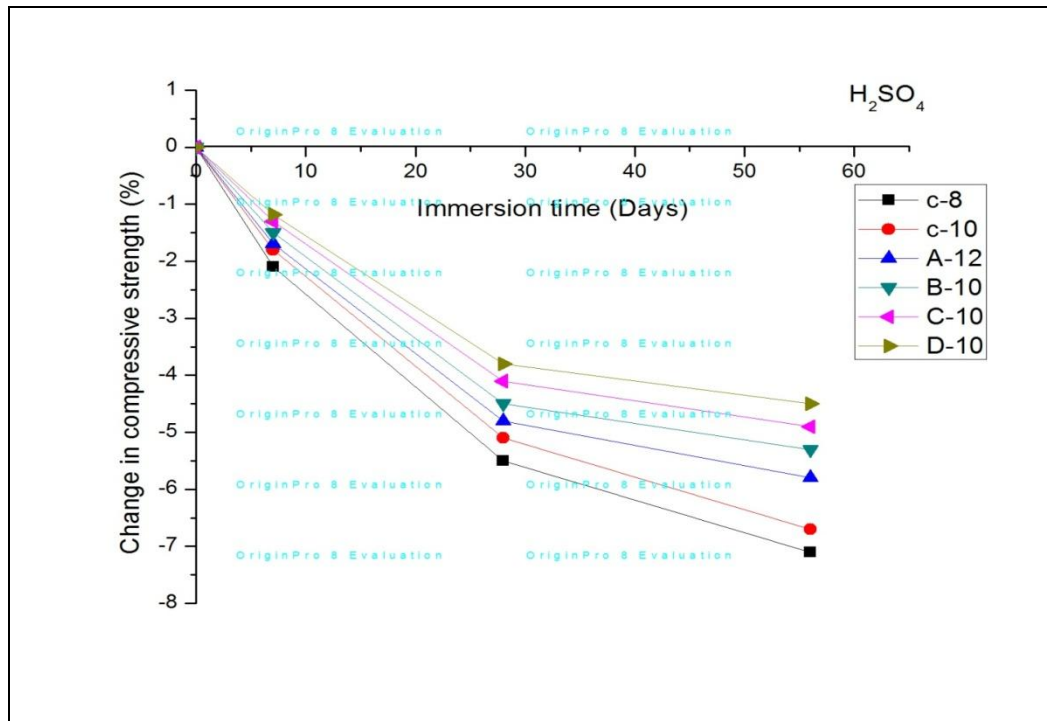
Figure 6.14 Change in compressive strength of AASFC samples immersed in H_2SO_4 solution

6.4.3 Effect of Nitric acid (HNO_3)

The compressive strength of alkali activated mixtures immersed in HNO_3 acid is negligible, and the test results are depicted in Figs. 6.15 and 6.16. Cubes dissolved in nitric acid initially observed loss in compression strength due to the ingress of nitric acid further dissolving effect of HNO_3 solution neutralizes the reaction; hence the concentration of acid content reduces. Fig. 6.15shows that alkali activated mixtures are less susceptible to nitrate attack with high resistance. The alkali activated mixes have a dense microstructure inhibiting the transport of alkalis into the concrete. This nitrate effect predominates in chemical storage units, and fertilizers go down, where the concrete deteriorates due to the formation of ammonium nitrate.
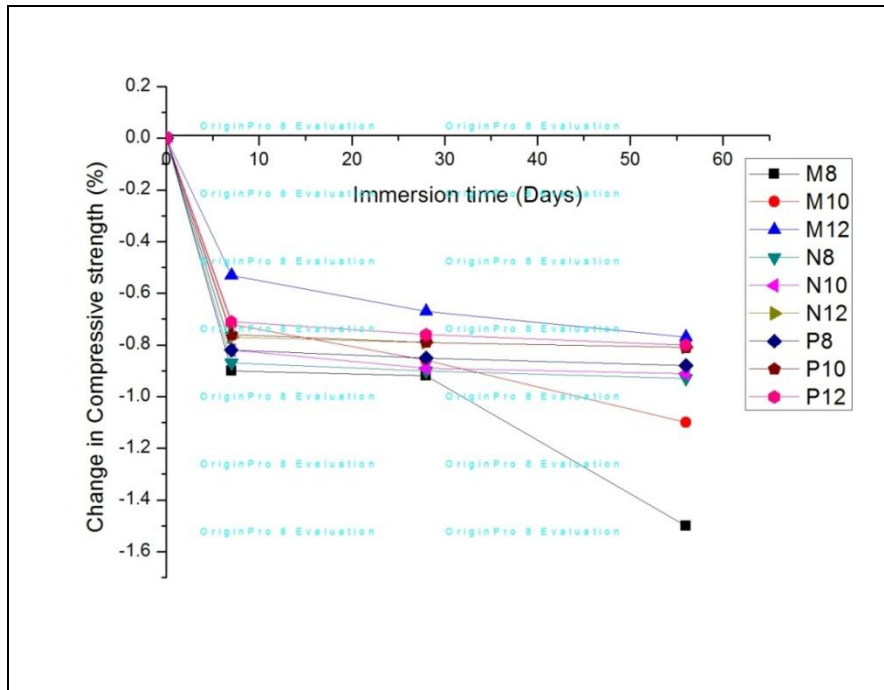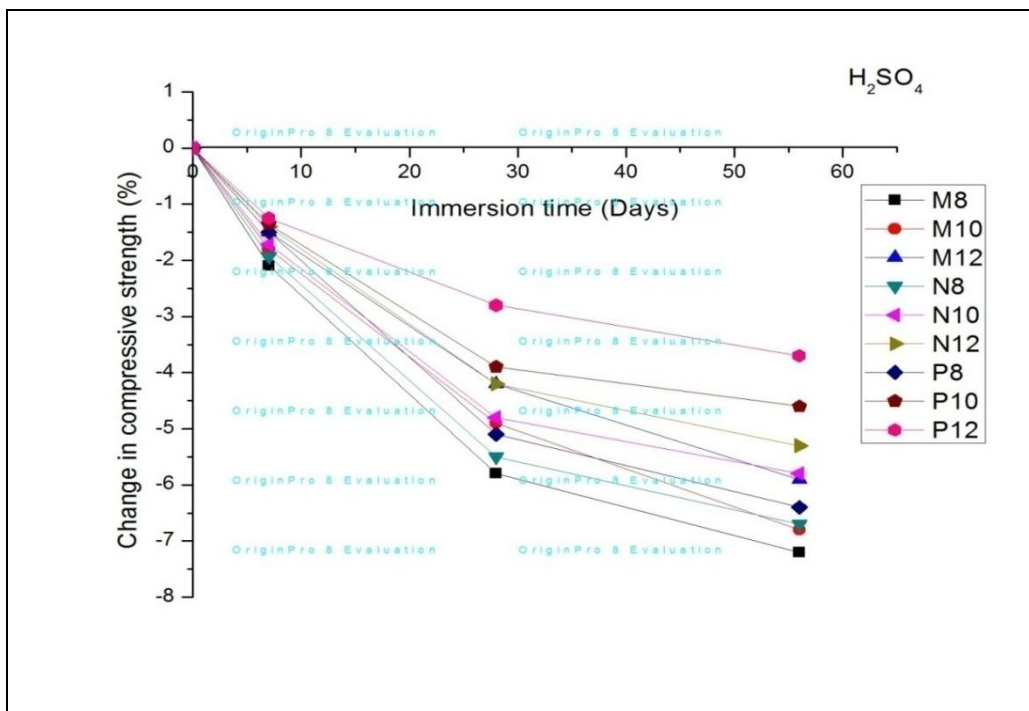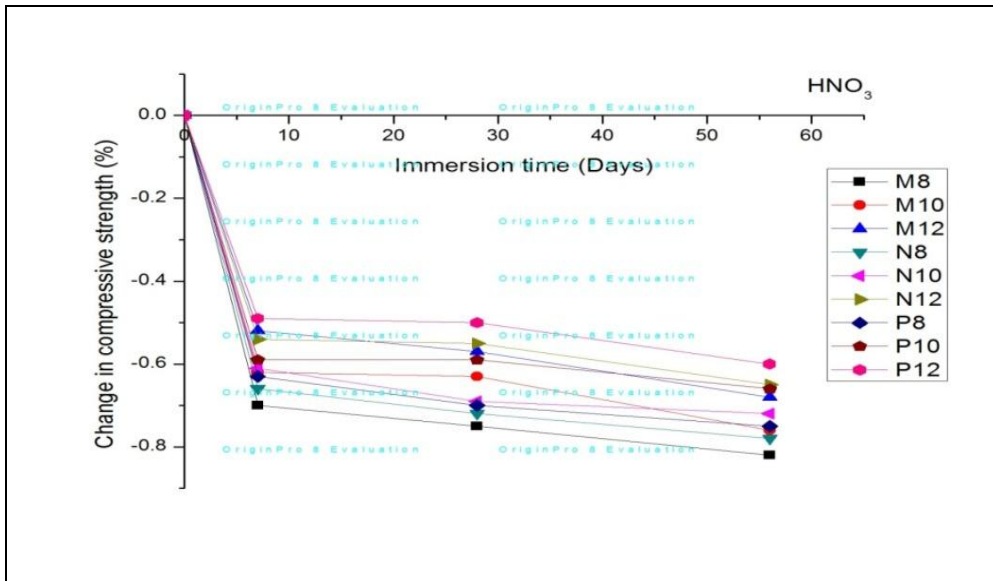
Figure 6.15 Change in compressive strength of AASC samples immersed in HNO$_3$
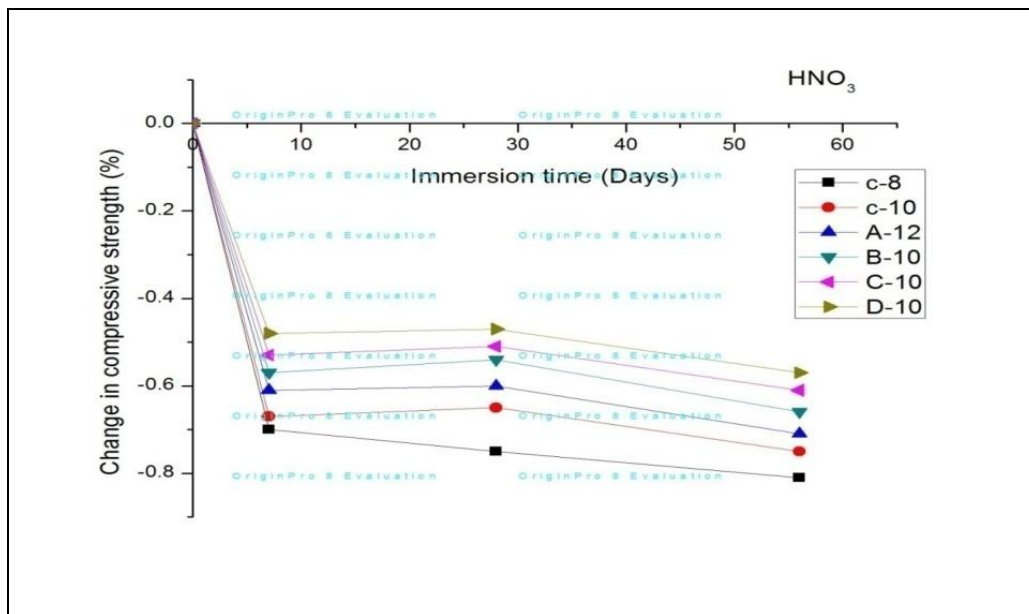
solution

Figure 6.16 Change in compressive strength of AASC samples immersed in HNO$_3$

solution

Fig. 6.17 Surface cracks and pop outs on AASC specimens immersed in sulphuric acid

Summary

The results of a sorptivity change in mass loss, permeable voids, and acid attacks such as HCl, H_2SO_4, and HNO_3 were discussed in detail. High sorptivity was reported for the mixes with 8M NaOH with gradual loss in compressive strength. The permeability property of alkali activated material depended on Na_2O content in the activator solution. The test results indicated that the alkali activated material showed better performance towards sulphate attack and good resistance towards nitrate and chloride attack. The conclusions drawn and recommendations for further work are discussed in chapter-7.

CHAPTER 7

CONCLUSIONS

7.1   General

In this study, Alkali activated concrete was developed using PS ball as fine aggregate. The physical and mechanical properties of the concrete mixes are evaluated in terms of workability, setting time, compressive, and split tensile and flexural strength, modulus of elasticity, fatigue test, and abrasion resistance. Based on the above test results, the following conclusions are drawn.

- The setting time of alkali activated mixtures decreased with the increase of NaOH concentration. The variation in the activator concentration resulted in a considerable reduction in setting time. The increase in H_2O/Na_2O and SiO_2/Al_2O_3 ratio was found to reduce setting time.

- The addition of PS ball in AASC and AASFC mixes has slightly affected the workability and the unit weight of the concrete mixes. The workability of alkali activated mixtures with PS ball varied marginally with SS/SH ratio. The AASC and AASFC mixes showed reduced workability, while the unit weight of the alkali activated mixtures increased with the PS ball.

- The strength properties of AASC and AASFC mixes are influenced by the activator solution. The AASFC mixes with 60:40 attained the highest compressive strength at a 12M NaOH. However, for the AASC mix with 12M NaOH achieved high compressive strength at SS/SH=2. The compressive strength of the AASFC and AASC mixes reduced with the NaOH concentration beyond 12M. At a constant alkaline liquid/binder ratio of 0.35, the mixes containing FA displayed higher workability.

- The alkali activated mixtures with PS ball as fine aggregate gave good tensile (flexural and split tensile) strength compared to control mixes. This is due to the

109

dense microstructure and the interfacial transition zone between the paste and aggregates in alkali activated concrete mixes.

- The AASC and AASFC mixes exhibited high early strength as compared to the control mix. Alkali activated mixtures mixes with complete replacement of river sand with PS ball attained 28 days compressive strength range between 40 to 65MPa and flexural strengths greater than 4.5 MPa. The incorporation of PS ball as fine aggregate improved the mechanical properties in both AASC and AASFC mixes.

- The modulus of elasticity of alkali activated mixtures with PS ball was higher than that of AASC, and AASFC mixes with natural aggregate. Modulus of elasticity of AASFC mixes exhibit higher values by replacing GGBFS with FA, which is due to the differences in the microstructure and binding chemistry. The modulus of elasticity of AASC and AASFC mixes increases by replacing river sand with PS ball due to a strong aggregate-paste interface.

- Alkali activated mixtures with PS ball as fine aggregate improved the fatigue life compared to the control mixes. The dense interfacial transition zone existing between the aggregate matrix and the binder resulted in higher fatigue life.

- AASC and AASFC mixes with PS ball exhibited high resistance towards abrasion compared to the control mixes. The strong bond between PS ball and the constituents of concrete results in dense microstructure and ITZ improved the abrasion resistance.

- Alkali activated concrete mixes with PS ball exhibits better resistance to hydrochloric, sulphuric, and nitric acid as compared to river sand, which is due to the properties/structure of the binders. The inclusion of higher FA in AASFC mixes improved the resistance to acid attack due to a decrease in calcium content in the binder with the addition of FA content, which tends to make the binder further resistant to acid attack. The acid resistance of alkali activated mixes increased with the replacement of river sand with PS ball.

110

- The mixtures of AASC can be suggested for pavement quality concrete with replacement of fly ash from 30% to 40%, AL/B ratio of 0.35, 12 M of SH, and SS/SH ratio 1.5 to 2.

7.2 SCOPE FOR FURTHER STUDIES

This study can be extended in the following areas:

- The results focus on the SH concentration, and SS/SH ratio in the alkali activated mixtures when the alkaline liquid to binder ratio remains almost constant; however, the effect of alkaline liquid to binder ratio requires extensive studies to validate the test results.

- Currently, there are no standard mix design guidelines available for alkali activated concrete or geopolymer concrete, which will be a considerable challenge for field application. Extensive research is required in this regard.

- The extensive microstructural analysis is required to understand the polymerization and final reaction product of the slag- fly ash blended alkali activated concrete with additives.

- The porosity of slag- fly ash blended alkali activated concrete tends to reduce with an increase in finer materials such as silica fume, quartz powder, or ultrafine fly ash as a ternary binder. However, a laboratory study is essential to explore this material.

- In this study, the durability test is limited to sorptivity, the volume of permeable voids, and acid attacks such as HCl, H_2SO_4, and HNO_3. The performance of these alkali activated mixtures against drying shrinkage, rapid chloride penetration, and carbonation test need to be investigated.

- The preparation of alkaline activator solution requires a minimum of 24 hours; it is essential to look for the material rich in sodium and silicate like feldspar mineral, which can be easily dissolved in water.

- Alkali activated material is produced with traditional coarse aggregate and PS ball as fine aggregate. For sustainable concrete, the coarse aggregate needs to be replaced by industrial byproducts or marginal material such as steel slag, construction, and demolition waste, or recycled aggregates.

- This study was limited only to short term structural application and durability properties. The long term performance of the slag- fly ash mixture needs to be investigated.

APPENDIX-I

Mix design calculation

Step-1: Density of concrete= 2400 kg/m^3

Step-2: Weight of combined aggregate= 76%= 2400x (76/100) = 1824 kg/m^3

Step-3: Weight of binder + alkaline liquid= (2400-1824) = 576 kg/m^3

Step-4: Weight of aggregates = 20mm down @ 70% = (70/100) x 1824 = 1276 kg/m^3

Fine aggregate @ 30% = (30/100-) x 1824 =548 kg/m^3

Step-5: For alkaline liquid to binder ratio 0.3

Alkaline liquid + binder =576 kg/m^3

Weight of binder = 576/ (1+0.3) = 443 kg/m^3

Step-6: For sodium silicate to sodium hydroxide ratio 2.5

Weight of alkaline liquid = 576- weight of binder = 576-443= 133 kg/m^3

Weight of sodium hydroxide = 133/ (1+2.5) = 38 kg/m^3

Weight of sodium silicate = 133- 38 = 95 kg/m^3

Molarity calculation

NaOH solution with concentration of 8M consists of 8x40 = 320 grams

NaOH solids per litre of water, where 40 is the molecular weight of NaOH

Therefore, 0.32 kg of NaOH flakes in 1 kg of water

1.32 kg of NaOH solution contains 0.32 kg of flakes

1 kg NaOH solution contains = 1x 0.32/1.32=0.2424 kg NaOH flakes

REFERENCES

Albitar, M., Mohamed Ali., M. S., Vistin, P. and Drenchsler, B. M. (2015), "Effect of Granulated lead smelter slag on strength of flyash based Geopolymer concrete", Construction and Building materials, 83, 128-135

Allahverdi, A., Bakhtiyari, A., Rais-Ghasemi, A. and Zarrabi, B. A. (2011). "Self compacting concrete containing different powders at elevated temperatures- mechanical properties and changes in phase composition." Thermochimica Acta, 514 (2), 74-81.

Alonso, S. and Palomo, A. (2001). "Alkaline activation of metakaolin and calcium hydroxide mixtures: Influence of temperature, activator concentration and solid ratio." *Material Letters*, 47(1-2), 55-62.

Altan, E. and Erdogan, S. T. (2012). "Alkali activation of slag at ambient and elevated temperatures." Cement and concrete Research, 34 (2), 131-139.

Amjad, A. S. (2019). "The Efficiency of Steel Slag and Recycled Concrete Aggregate on the Strength Properties of Concrete." KSCE journal of civil engineering, 23, 4846-4851

Atis, C. D., Bilim, C., Celik, O. and Karahan, O. (2009). "Influence of activator on the strength and drying shrinkage of alklai activated slag mortar." Constructon and Building Materials, 23, 548-555.

Aydin, S. and Baradan, B. (2012). "Mechanical and microstructural properties of heat cured alkali activated slag mortars." Materials and Design, 35, 374-383.

Bakharev, T. (2003). "Geopolymeric materials prepared using Class F fly ash and elevated temperature curing." *Cement and Concrete Research*, *35*(6), 1224-1232.

Bakharev, T. (2005). "Geopolymeric materials prepared using class-F flyash and elevated temperature curing." Cement and concrete research, 35, 1224-32

Bakharev, T., Sanjayan, J. G. and Cheng, Y. B. (1999). "Effect of elevated temperature curing regime on properties of alkali activated slag concrete." Cement and Concrete Research, 29 (10), 1619-1625.

Bakharev, T., Sanjayan, J. G. and Cheng, Y. B. (2000). "Effect of admixtures on properties of alkali activated slag concrete." Cement and Concrete Research, 30, 1367-1374.

Bernal, S. A., Provis, J. L., Rose, V. and De-Gutierrez, R. M. (2011). "Evolution of binder structure in sodium silicate activated slag-metakaolin blends." Cement and Concrete Composites, 33, 46-54.

Bernal, S., De-Gutierrez, M. R. and Provis, L. P. (2012). "Durability and engineering properties of AASC mixes." Construction and Building Materials, 33, 99-108.

Bilim, C., Atis, C. D., Gorur, E. B. and Luga, B. (2015). "Very high strength (120 MPa) class F fly ash geopolymer mortar activated at different NaOH amount, heat curing temperature and heat curing duration." Construction and Building Material, 96, 673-678.

Brough, A. R., Holloway, M., Sykes, J. and Atkinson, K. (2000). "Sodium silicate-based alkali activated slag mortars part II; Sodium chloride or malic acid as a retarder." Cement and Concrete Research, 30, 1375-1379.

Chang, J. J. (2003). "A study on the setting characteristics of sodium silicate-activated slag pastes." Cem. Concr. Res., 33 (7), 1005–1011.

Chareerat, T., Chindaprasirt, P., Hatanaka, S. and Cao, T. (2016). "High strength geopolymer using fine high calcium flyash." Journal of materials in Civil Engineering, 23 (3), 264-270.

Chi, M. (2012). "Effect of dosage of alkali-activated solution and curing conditions on the properties and durability of alkali-activated slag concrete." Constr. Build. Mater., 35 (10), 240–245.

Chi, M. and Huang. R. (2013). "Binding mechanism and properties of alkali activated flyash/slag mortars." Construction and Building Materials, 40, 291-298.

Chindaprasirt, P., Chai, J. and Theerawat, S. (2007). "Effect of flyash fineness on microstructure of blended cement paste." Construction and Building Materials, 21 (7), 1534-1541.

Chindaprasirt, P., Chareerat, T. and Sirivivatnanon, V. J. (2009). "Workability and strength of high calcium fly ash geopolymer." *Cement and Concrete Composites*, *29*(3), 224-229.

Chindaprasirt, P., De-Silva, P., Sagoe-Crentsil, K. and Hanjitsuwan, S. (2012). "Effect of SiO_2 and Al_2O_3 on the setting and hardening of high calcium fly ash-based geopolymer systems." *Journal of Materials Science*, *47*(12), 4876-4883.

Collins, F. and Sanjayan, J. G. (2000). "Effect of pore size distribution on drying shrinking of alkali activated slag concrete. Cem. Concr. Res., 30 (9), 1401–1406.

Collins, F. G. and Sanjayan, J. G. (1999). "The study on the workability and strength of AASC using ultra-fine materials and slag as the binder." Cement and Concrete Research, 29, 459-462.

Criado, M., Fernández-Jiménez, A. and Palomo, A. (2007). "Alkali activation of fly ash: Effect of the SiO2/Na2O ratio." *Microporous and Mesoporous Materials*, *106*(1-3), 180-191.

Davidovits, J. (1999). "Chemistry ofgeopolymeric systems, terminology." *Proceeding of Geopolymer '99 International Conference,* Saint-Quentin, France.

Deb, P. S., Pradip, N. and Prabir, K. S. (2014). "Effect of GGBS blending with flyash and activator content on the workability and strength properties of geopolymer concrete cured at ambient temperature." Materials and Design, 62, 32-39.

Delatte, H. (2009). "Failure, distress and repair of concrete structures." Woodhead publishing series in civil and structural engineering, 1, 13-15.

Diaz-Loya, E, I., Allouche, E.N. and Vaidya, S. (2011). "Mechanical properties of fly-ash based polymer concrete." Journal of ACI materials, 108, 300-306.

Ding, Yao., Jian-Guo, Dai. and Cai-jun, Shi. (2016). "Mechanical properties of alkali activated concrete: a state of art review." Construction and building materials, 127, 68-79.

Douglas, E., Bilodeau, A., Brandstetr, J. and Malhotra, L. (1991). "Alkali activated ground granulated blast furnace slag concrete; preliminary investigation." Cement and Concrete Research, 21, 101-108.

Duxson, P., Fernández-Jiménez, A., Provis, J. L., Lukey, G. C., Palomo, A. and Van Deventer, J. S. J. (2007). "Geopolymer technology: the current state of the art." *Journal of Materials Science*, *42*(9), 2917-2933.

Fang, Guohao., Wing, Kei., Wenlin, Ho., Mingzhong, Tu. and Zhang. (2018). "The mechanical properties and workability of fly ash- slag concrete cured under ambient temperature." Construction and Building Material, 172, 476-487.

Feng, D., Tan, H. and van Deventer, J. S. J. (2004). "Ultrasound enhanced geopolymerisation." *Journal of Materials Science*, *39*(2), 571-580.

Fernández-Jiménez, A. and Palomo, A. (2003). "Characterisation of fly ashes. Potential reactivity as alkaline cements." *Fuel*, *82*(18), 2259-2265.

Fernandez-Jimenez, A. and Palomo, A. (2005). "Mid infrared spectroscopic studies of alkali activated flyash structure." Microporous and Mesoporous Materials, 86 (3), 207-214.

Fernandez-Jimenez, A., Palomo, J. and Puertas, G. (1999). "Alkali-activated slag mortars mechanical strength behaviour." Cement and Concrete Research, 29(8), 1313-21.

Fernandez-Jimenez, F., García-Lodeiro, A. and Palomo. A. I. (2007). "Durability of alkali activated fly ash cementitious materials." J. Mater. Sci., 42 (9), 3055– 3065.

Fernández-Jiménez, F., Puertas, I., Sobrados. and Sanz. (2003). "Structure of calcium silicate hydrates formed in alkaline activated slag; influence of the type of alkaline activator." J. Am. Ceram. Soc., 86, 1389–1394.

118

FHWA, (2012). "User guidelines for byproducts and secondary use materials in pavement construction." Publication Number: FHWA-RD-97-148.

Gao, K., Lin, K., Wang, D., Hwang, C., Shiu, H., Chang, Y. and Cheng, T. (2014). "Effect of molar ratio on the microstructure and mechanical properties of meatkolin based geoplymer." Construction and Building Material, 53, 503-510.

Gao, X., Yuan, B., Yu, Q. L. and Brouwers, H. J (2016). "Characterization and application of municipal solid waste incineration bottom ash and waste granite powder in alkali activated slag." Journal of Cleaner Production, 164, 410-419.

Glukhovsky, V.D. (1994). "Ancient, Modern and Future Concretes." In Krivenko, P. V. (Ed.), *Proceedings of the First International Conference on Alkaline Cements and Concretes*, VIPOL Stock Company, Kiev, Ukraine, (pp. 1–9).

Graeff, A. G., Pilakoutas, K., Neocleous, K. and Vania, N. (2012), "Fatigue resistance and cracking mechanism of concrete pavements reinforced with recycled steel fibres recovered from post-consumer tyres." Engineering Structures, 45(7), 385–395.

Hamed, M., Farshad, R., Carlo, G. P. and William, D. Burgos. (2016). " Effect of calcium on dissolution and precipitation reactions of amorphoys silica at high alkalinity." Cement and concrete research, 87, 1-13.

Hanjitsuwan, S., Hunpratub. P., Thongbai, S., Maensiri, V., Sata. S. and Chindaprasirt, P. (2014). "Effects of higher concentration of NaOH on the physical and electrical conductivity properties of fly ash-based geopolymer paste." Cement and Concrete Composites, 45: 9-14.

Hardjito, D., Antoni. K. and Chandra. L. (2015). "The impact of flyash, silica fume and calcium carbonate on the workability and compressive strength of mortar." Procedia Engineering, 125, 773-779.

119

Hoderio, M. I., Garcia. M., Ana. F., Angel, P and Donald, M. (2011). "Compatibility studies between N-A-S-H and C-A-S-H gels; Study in the ternary diagram Na2O–CaO–Al2O3–SiO2–H2O." Cement and Concrete Research, 41 (9), 923-931.

Hyeongi, Lee., Asad, Hanif., Muhammad, Usman., Younghwan, Kim., Hongseob, Oh. and Seong, K. Kim. (2020). "Interfacial characteristics of cement mortars containing aggregate derived from industrial slag waste." Journal of structural integrity and maintenance, 5, 236-243.

Idawati, I., Susan, A., Bernal, A., John, L. P., Rackel, S. N., David, G. B., Adam, R. K., Sinin, H. and Jannie, S. D. (2013). "Influence of flyash on the water and chloride permeability of alkali activated slag mortars and concretes." Construction and Building Materials. 48, 1187-1201.

IS 456-2007, Code for practice- Plain and reinforced concrete. Bureau of Indian standard.

Ismail, S., Bernal, A., John, L. P., Rackel, S. N., Sinin, H. and Jannie, S. D. (2014) "Modification of phse evolution in alkali activated blast furnace slag by the incorporation of flyash." Construction and Building Material, 45, 125-135

Jagadish, Mallick., Shakti, Soumya. and Pratap, K. P. (2020). "Strength and durability study of concrete using precious slag balls." Materials today: proceedings, https://doi.org/10.1016/j.matpr.2020.02.923

Joy, S. J. and Mini, Mathew.(2015), "Experimental study on Geopolymer concrete with partial replacement of fine aggregate with foundry sand", IJATES, volume no.3, special issue no.01, September (2015), 559-569.

Junaid, T. M., Obada, K., Amar, K. and Jarvis. B. (2015). "A mix design procedure for low calcium alkali activated flyash based concrete." Construction and Building Materials, 79, 301-310.

Khale, D. and Chaudary, R. (2007). "Mechanism of geopolymerization and factors influencing its development a review." Journal of material science, 42 (3), 729-746.

Kong, D. L., Sanjayan, J. G. and Sagoe-Crentsil, K. (2007). "Comparative performance of geopolymers made with metakaolin and flyash exposed to elevated temperature." Cement and Concrete Research, 37(12), 1583-1589.

Krivenko, P. (1994). "Progress in alkaline cements." Proceedings of the 1st Inter. Conf. Alkaline Cements and Concrete, 11-29.

Krizan, D. and Zivanovic, B. (2002). "Effects of dosage and modulus of water glass on early hydration of alkali-slag cement." Cem. Concr. Res., 32, 1181–1188.

Lee, M. K. and Baar B. I. (2004). "An overview of the fatigue behavior of plain and reinforced concrete." Cement and Concrete Composites, 26, 299-305.

Lee, N. K. and Lee, H. K. (2013). "Development of alkali activated fly ash/ slag concrete for setting and mechanical properties at room temperature." Construction and Building Material. 47:1201-1209.

Lee, W. K. and Van Deventer, J. S. J. (2002). "The effect of ionic contaminants on the early-age properties of alkali-activated fly ash-based cements." *Cement and Concrete Research*, *32*(4), 577-584.

Ma, Y., Hu, J. and Ye, G. (2013). "The pore structure and permeability of alkali activated fly ash." *Fuel*, *104*, 771-780.

Miranda, J. M., Fernandez, J. A., Gonzalez, J. A. and Palomo, A. (2005). "Corrosion resistance in activated flyash mortars." Cement and Concrete Research, 35 (6), 1210-1217.

Mithun, B. M. and Narasimhan, M. C. (2016). "Performance of alkali activated slag concrete mixes incorporating copper slag as fine aggregate." Journal of cleaner production, 112, 837-844.

Moruf, O. Y., Megat, A. M. J., Zainal, A. and Mohammad. M. (2014). "Evoluton of alkaline activated ground granulated blast furnace slag-ultrafine palm oil fuel ash based concrete." Materials and Design, 55, 387-393.

Mustafa, A. B., Kamarudin, A., Banhussain, H., Rafiza, A. and Zarina, Y. (2012). "Effect of SS/SH ratios and NaOH molarities on compressive strength of flyash based geopolymer." ACI Material Journal, 109(5), 503-508.

Nath, P. and Sarker. (2014). "The setting, workability and early strength properties of slag and FA based geopolymer under ambient temperature". Construction and Building Material, 66, 163-171.

Olivia, M., Sarker, P. and Nikraz, H. (2008). "Water Penetrability of Low Calcium Fly Ash Geopolymer Concrete." In *proceedings of The International Conference on Construction and Building Technology 2008 (ICCBT 2008)*, 16 – 20 June, KualaLumpur.

Pacheco-Torgal, F., Joao, C. and Said, J. (2007). "Investigations about the effect of aggregates on strength and microstructure of geopolymeric mine wste mud binders." Cement and Concrete Research, 37(6), 933-941.

Palacio, M. and Puertas, F. (2005). "Effect of superplasticizer and shrinkage reducing admixtures on alkali activated slag pastes and mortars." Cement and Concrete Research, 35(7), 1358-1367.

Palomo, A., Blanco-Varela, M. T., Granizo, M. L., Puertas, F., Vazquez, T. and Grutzeck, M. W. (1999). "Chemical stability of cementitious materials based on metakaolin." Cement and Concrete Research, 29(7), 997-1004.

Palomo, A., Grutzeck, M. W. and Blanco, M. T. (1999). "Alkali-activated fly ashes." *Cement and Concrete Research*, *29*(8), 1323-1329.

Palomo, A., Krivenko, P., Garcia-Lodeiro, I., Kavalerova, E., Maltseva, O. and Fernández- Jiménez, A. (2014). "A review on alkaline activation: new analytical perspectives." *Materiales de Construcción, 64*(315), e022. doi:10.3989/mc.2014.00314

Perdikaris, P., Calomino, A. M. and Chudnovsky, A. (1986). "Effect of fatigue on fracture toughness of concrete." Journal of Engineering Mechanics, 8, 112

Priyadarshini, P., Ramamurty, K. and Retnamony, G. R. (2017). "Excavated soil waste as fine aggregate in fly ash based geopolymer mortar." Applied clay science, 146, 81-91.

Puertas, F., Martínez-Ramírez, S., Alonso, S. and Vázquez, T. (2000). "Alkali-activated fly ash/slag cements; Strength Behaviour and Hydration Products." *Cement and Concrete Research*, *30*(10), 1625-1632.

Puertas, F., Palacios, M., Manzano, H., Dolado, J.S., Rico, A. and Rodríguez. J. (2011). "A model for the C-A-S-H gel formed in alkali-activated slag cements." J. Euro Cera Soc., 31 (12), 2043–2056.

Qureshi, M. N. and Ghosh, S. (2014). "Effect of silicate content on the properties of alkali-activated blast furnace slag paste." Arab. J. Sci. Eng., 39 (8), 5905–5916.

Rangan, B. V., Hardjito, D., Wallah, S. E. and Sumajouw, D. M. J. (2005). "Flyash based geopolymer concrete: a construction material for sustainable development." Concrete in Australia, 31, 25-30.

Rashad, A. (2013). "A comprehensive overview about the influence of different admixtures and additives on the properties of alkali-activated fly ash." J. *Materials & Design.*, *53*, 1005-1025.

Rattanasak, U. and Chindaprasirt, P. (2009). "The study on NaOH influences on a synthesis of FA based geopolymer." Mineral Engineering, 22(12), 1073-78.

Roy, D. (2000). "Alkali activated cements- opportunites and challenges." Cement and concrete Research, 29 (2), 249-254.

Ryu, G. S., Lee, Y. B., Koh, K. T. and Chung. Y. S. (2013). "The mechanical properties of fly ash-based geopolymer concrete with alkaline activators." Constr. Build. Mater., 47,409–418.

Ryu, G. S., Young, B. L., Kyung, T. K. and Young, S. C. (2008). "The mechanical properties of fly ash-based geopolymer concrete with alkaline activators." Construction and Building Material, 47, 409-418.

Sharath, S., Gayana, B., Krishna, Reddy. and Ramachandra, K. (2019). "Experimental investigations on performance of concrete incorporating PS ball as fine aggregate." Advances in concrete construction." 8 (3), 239-246

Shekhovtsova, J., Zehernovsky, I., Kovtun, M., Kozhukhova, N. and Kearsley, E. (2014). "Estimation of fly ash reactivity for use in alkali-activated cements - A step towards sustainable building material and waste utilization." Journal of cleaner production, 178, 22-23.

Shi, C. and Xie, P. (1998). "Interface between cement paste and quartz sand in alkali activated slag mortars." Cement and Concrete Research, 28(6), 887-896.

Shi, C., Krivenko, P. V. and Roy, D. (2006). "Alkali activated cement and concretes". Taylor Francis, Abington, UK.

Silva, P., Sagoe-Crenstil, K. and Sirivivatnanon, V. (2007). "Kinetics of geopolymerization: Role of Al2O3 and SiO2." *Cement and Concrete Research*, *37*(4), 512-518.

Sindhunata, (2006a). "*A Conceptual Model of Geopolymerisation.*" The University of Melbourne, Melbourne.

Sing, N. and Singh, S. P. (2017). "Carbonation resistance and microstrucral analysis of low and high volume flyashself compacting concrete containing recycled aggregates." Construction and Building material, 127, 824-842.

Siyal, A., Khairun, A. A. and Zakaria, M. (2016). Effects of parameters on setting time of flyash based geopolymers using taguchi method." Procedia Engineering, 148, 302-307.

Sofi, M. (2007). "Determining the mechanical properties of polymer concretes of inorganic type." Cement and Concrete Research, 37, 251-257.

Somna, K., Jaturapitakkul, C., Kajitvichyanukul, P. and Chindaprasirt, P. (2011). "NaOH activated ground fly ash geopolymer cured at ambient temperature." *Fuel*, *90*(6), 2118-2124.

Song, S. and Jennings, H. M. (1999). "Pore solution chemistry of alkali-activated ground granulated blast-furnace slag." *Cement and Concrete Research, 29*(2), 159-170.

Song, X., Munn, R., Marosszeky, M. and Brungs, M. (2005). "Durability of fly ash based geopolymer concrete against sulphuric acid attack." In *Proceedings of 10DBMC international conference on durability of building materials and components*, Lyon France, 17-20 April.

Song-piriyakil, S., Kubprasit, T., Jaturapitakkul, C. and Chindaprasirt P. (2010). "Compressive strength and degree of reaction of biomass- and fly ash-based Geopolymer." Construction and Building Materials, 24, 236–240.

Swanepoel, J. C. and Strydom, C. A. (2002). "Utilization of flyash in geopolymeric material." Applied Geochemistry. 17(8), 1143-1148.

Tan, Lie., Ronald, Simatupang. and Deni, Setiawan. (2015). "Comprehensive study effect of steel waste into mechanical properties of concrete." International journal of advances in mechanical and civil engineering, 2(6), 14-19

Taylor. (1997). HFW. Cement Chemistry. 2nd London: Thomas Teford press, Newyork.

Tekin, I. (2016). "Properties of NaOH activated geopolymer with marble, travertine and volcanic tuff wastes." Construction and Building Materials, 127, 607-617.

Wallah, S. E and Rangan, B. V. (2005). "Low calcium flyash based geopolymer concrete: long term properties." Research report, Curtin University of Technology, Perth.

Wang, H., Li, H. and Yan, F. (2005). "Reduction wear of metakolinite based geopolymer composite through filling of PTFE." Wear, 258 (10), 156-1566.

Wang, S. D., Pu, X., Scrivener, K. L. and Pratt, P. L. (1995) "Alkali-Activated Slag Cement and Concrete: a review of properties and problems." Advances in Cement Research, No. 27, pp. 93-102.

Wang, S. D., Scrivener, K. L. and Pratt, P. L. (1994). "Factors Affecting the Strength of Alkali-Activated Slag." Cement and Concrete Research, 24 (6), 1033-1043.

Wang, Y. S., Provis, J. L. and Dai, J. G. (2018b). "Role of soluble aluminum species in the activating solution for synthesis of silico-alumino phosphate geopolymers." *Cement Concrete Compos.*, 93, 186–195.

Wongpa, J., Kiattikomol, K., Jaturapitakkul, C. and Chindaprasirt, P. (2010). ''Compressive strength, modulus of elasticity, and water permeability of inorganic polymer concrete.'', Mater. Des., 31(10), 4748–4754.

Xu, H. and Van Deventer, J. S. J. (2002). "The effect of alkali metals on the formation of geopolymeric gels from alkali-feldspars." *Colloids and Surfaces A: Physicochemicaland Engineering Aspects*, *216*(1-3), 27-44.

Yaseer, M. M., Taha, M. J., Kow, K. and Jason, Y. (2019). "Novel cement curing technique by using controlled release of carbon dioxide coupled with nanosilica." Construction and Building Material, 223, 692-704.

Zaharieva, R., Buyle-Bodin. F., Skoczylas, F. and Wirquin, E. (2009). "Assessment of the surface permeation properties of recycled aggregate concrete."Cem. Concr. Composit., 25 (2), 223-232

Zuhua, Z., Xiao, Y., Huajun, Zhu. and Yue. C. (2009). "Geopolymerization process of alkali metakaolinite characterized by isothermal calorimetry." Thermochemica Acta. 493 (1), 49-54.

PUBLICATIONS

International Journals

Avinash.H.T and A.U. Ravi Shankar. "Alkali Activated Slag-Fly Ash Concrete Incorporating PS Ball as Fine Aggregate for Rigid Pavements."**Journal of Traffic and Transportation Engineering, Elsevier Publications**., Article in press, 2019.

Avinash.H.T and A.U. Ravi Shankar. "A study on initial setting time and the mechanical properties using the PS ball as fine aggregate." **International Journal of Pavement Research and Technology, Springer nature publication,DOI: https://doi.org/10.1007/s42947-019-0078-0**

Avinash.H.T and A.U. Ravi Shankar. "Experimental study on AASC using PS ball as fine aggregate at the higher concentration of sodium silicate."**International Journal of Research in Engineering and Technologyhttps://www.ijret.org/Archive?VI=20180713**.

Avinash.H.T and A.U. Ravi Shankar. "Laboratory investigation on alkali activated slag-fly ash concrete for rigid pavement." **International Journal of Pavement Research and Technology, springer nature publication (under review)**

International/National Conference

Avinash.H.T and A.U. Ravi Shankar. "A study on initial setting time and the mechanical properties using the PS ball as fine aggregate." **WCTR-2019, IIT Bombay, 26-31May 2019**.

Avinash.H.T and A.U. Ravi Shankar. "Experimental study on AASC using PS ball as fine aggregate at the higher concentration of sodium silicate."**Indian Concrete Institute IWC-2018, Bengaluru, Nimhans Convention Center, 20-23 Oct 2018**.

Avinash.H.T and A.U. Ravi Shankar. "Effective utilization of fly ash as binder in alkali enacted slag-fly ash concrete incorporating precious slag as fine aggregate" **Next frontiers in civil engineering-2018, IIT Bombay. (Best paper award)**

CURRICULUM VITAE

Name: AVINASH H TALKERI

Contact No.: +91-9481643343

E-mail ID:avinashmng@gmail.com

Date of Birth: 30-08-1990

Permanent Address: H No 8/60, Plot no-81,

Prashant Nagar 'A'

Gulbarga- 585105

Educational Qualifications:

Degree	Subject	University	Year	Division
Ph.D	Transportation Engineering (Civil Engineering)	National Institute of Technology Karnataka, Surathkal	2016-2020	---
M. Tech	Transportation Engineering and Management	VTU Belgaum	2012-2014	Distinction
B. Tech	Civil Engineering	VTU Belgaum	2008-2012	First Class

Teaching Experience:

Name of Institute	Post held	Period
National Institute of Technology Karnataka Surathkal	Assistant Lecturer	29-12-2014 to 10-07-2015 & 27-12-2015 to 16-05-2016

Subject studied in M. Tech Degree

- Traffic Engineering-I
- Transport Planning
- Applied Statistics
- Pavement Materials and Construction
- Applied Soil Mechanics
- Traffic Engineering-II
- Analysis, Design and Evaluation of Pavements
- Road Safety and Management
- Urban Public Transport
- Rural Roads
- Geometric design of Transportation Facilities
- Infrastructure Management

Software Known

- SPSS
- IIT Pave
- X-Pert High Score
- Minitab-16

Awards

- ***Best Paper Award for the research paper entitled*** *"Effective utilization of fly ash as binder in alkali enacted slag-fly ash concrete incorporating precious slag as fine aggregate"* ***Next frontiers in civil engineering -2018, IIT Bombay.***

International Conference

Avinash, H. T., A, U. Ravi Shankar., Chethan, B. A. and Raghuram, K. C. (2020). "Development of alkali activated slag concrete by partial replacement of sand with granulated blast sand." ***Challenges of Resilient and Sustainable Infrastructure Development in Emerging Economies. ASCE India 2020 Conference.***

Raghuram, K. C., A, U. Ravi Shankar., Avinash, H. T. and Chethan, B. A. (2020). "Comparison of performance of Stone Matrix Asphalt (SMA) using ViaTop pellets and

Sisal Fibers."***Challenges of Resilient and Sustainable Infrastructure Development in Emerging Economies. ASCE India 2020 Conference.***

Chethan, B. A., Ravi Shankar, A, U Avinash, H. T. and Raghuram, K. C. (2020). *"Strength and Durability Characteristics of Fly Ash Admixed Black Cotton Soil." **Challenges of Resilient and Sustainable Infrastructure Development in Emerging Economies. ASCE India 2020 Conference.***

<u>Webinar</u>

Recent Advancements in Concrete Technology *(RACT-2020) 22nd to 26th June 2020 organized by B.M.S. College of Engineering, Bangalore-560019.*

1st Indo-Japan webinar series on "Geotechnics for Disaster Mitigation"*8th to 13th June 2020 organized by NITK Surathkal, IGS Surathkal Chapter, IIT Tirupati, Kyushu University Fukuoka 819 0395 Japan.*

Recycling of Asphalt pavements for sustainable road construction *29th May 2020 organized by MIT-ADT University, Pune Maharashtra.*

Application of Intelligent Transportation System (ITS) in road safety *30th May 2020 organized by MIT-ADT University, Pune Maharashtra.*

The secret of publishing your research in High Impact Journal *17th June 2020 organized by Rasayanika Biotechnologies India Pvt Ltd.*

Plumbing for High-Rise Buildings, *16th June 2020 organized by B.V. Raju Institute of Technology, Narsapur, Hyderabad.*